

ผลของสารลดแรงตึงผิวและปริมาณของดินเหนียวปรับสภาพต่อสมบัติของโฟมพอลิยูรีเทน/
ดินเหนียวนาโนคอมพอสิต



นางสาว เสวิตา อินทพิชัย

ศูนย์วิทยทรัพยากร จุฬาลงกรณ์มหาวิทยาลัย

วิทยานิพนธ์นี้เป็นส่วนหนึ่งของการศึกษาตามหลักสูตรปริญญาวิศวกรรมศาสตรมหาบัณฑิต

สาขาวิชาวิศวกรรมเคมี ภาควิชาวิศวกรรมเคมี

คณะวิศวกรรมศาสตร์ จุฬาลงกรณ์มหาวิทยาลัย

ปีการศึกษา 2552

ลิขสิทธิ์ของจุฬาลงกรณ์มหาวิทยาลัย

EFFECT OF SURFACTANTS AND ORGANOCCLAY LOADING ON PROPERTIES
OF POLYURETHANE/CLAY NANOCOMPOSITE FOAMS



Ms. Sevita Inthapichai

ศูนย์วิทยทรัพยากร
จุฬาลงกรณ์มหาวิทยาลัย
A Thesis Submitted in Partial Fulfillment of the Requirements
for the Degree of Master of Engineering Program in Chemical Engineering

Department of Chemical Engineering

Faculty of Engineering

Chulalongkorn University

Academic Year 2009

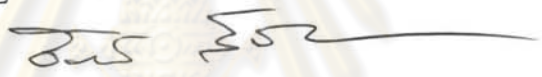
Copyright of Chulalongkorn University

Thesis Title EFFECT OF SURFACTANTS AND ORGANOCCLAY LOADING ON
PROPERTIES OF POLYURETHANE/CLAY NANOCOMPOSITE
FOAMS
By Ms. Sevita Inthapichai
Field of Study Chemical Engineering
Thesis Advisor Assistant Professor Anongnat Somwangthanaroj, Ph.D.

Accepted by the Faculty of Engineering, Chulalongkorn University in
Partial Fulfillment of the Requirements for the Master's Degree


.....Dean of the Faculty of
Engineering
(Associate Professor Boonsom Lerdkhironwong, Dr. Ing.)

THESIS COMMITTEE


..... Chairman
(Associate Professor Chairit Satayaprasert , Ph.D.)


..... Thesis Advisor
(Assistant Professor Anongnat Somwangthanaroj, Ph.D.)


.....Examiner
(Sarintorn Limpanart, Ph.D.)


.....External Examiner
(Sawitree Petchuay, Ph.D.)

เสวิตา อินทพิชัย : ผลของสารลดแรงตึงผิวและปริมาณของดินเหนียวปรับสภาพต่อสมบัติของ โฟมพอลิยูรีเทน/ดินเหนียวนาโนคอมโพสิต (EFFECT OF SURFACTANTS AND ORGANOCLAY LOADING ON PROPERTIES OF POLYURETHANE/CLAY NANOCOMPOSITE FOAMS) อ. ที่ปรึกษา วิทยานิพนธ์หลัก : ศศ.ดร.อนงค์นาฏ สมหวังธนโรจน์, 129 หน้า.

งานวิจัยนี้มีจุดประสงค์เพื่อศึกษาการนำดินเหนียวที่ปรับสภาพแล้ว มาใช้เป็นสารเสริมแรงในโฟม พอลิยูรีเทนชนิดยืดหยุ่น เพื่อลดปริมาณการใช้วัตถุดิบที่ส่งผลกระทบต่อสิ่งแวดล้อม เช่น ไอโซไซยานเนต โดย ดินเหนียวทั้งสองชนิดที่นำมาศึกษามีขนาดอนุภาคอยู่ในระดับนาโนเมตร แต่ต่างกันที่ความสามารถในการ แลกเปลี่ยนประจุบวกและปริมาณซิลิกาอิสระภายในดินเหนียว นอกจากนี้อิทธิพลของโครงสร้างทางเคมีของ สารลดแรงตึงผิว ลำดับในการผสมดินเหนียวลงในมอนอเมอร์ และปริมาณของดินเหนียวที่เหมาะสมต่อการ กระจายตัวของดินเหนียวในโฟมพอลิยูรีเทนนาโนคอมโพสิตชนิดยืดหยุ่นก็ได้ถูกนำมาศึกษาในงานวิจัยนี้ด้วย จากการวิจัยพบว่า สารลดแรงตึงผิวที่มีหมู่ไฮดรอกซิลอยู่ในองค์ประกอบทำให้ระยะห่างระหว่างชั้นของ ดินเหนียวขยายออกมากที่สุด และจากการทดสอบด้วยเครื่องฟูรีเออร์ทรานสฟอร์มอินฟราเรดสเปกโตรมิเตอร์ พบว่า ดินเหนียวที่ใส่ลงในโฟมพอลิยูรีเทนไม่ได้เข้าไปขัดขวางการเกิดพันธะไฮโดรเจนที่เกิดภายในส่วนแข็ง ของพอลิยูรีเทน นอกจากนี้เมื่อนำพอลิยูรีเทนคอมโพสิตไปทดสอบสมบัติทางกล เช่น ความแข็ง การกระดอน กลับ และการกดทับด้วยเวลานาน พบว่าค่าความแข็ง ของโฟมพอลิยูรีเทนนาโนคอมโพสิตมีค่าสูงขึ้นเมื่อเทียบกับ โฟมพอลิยูรีเทนที่ไม่ได้ใส่ดินเหนียวปรับสภาพ แต่สมบัติการกระดอนกลับและการกดทับเป็นเวลานานของ โฟมพอลิยูรีเทนนาโนคอมโพสิตมีค่าลดลง อย่างไรก็ตามอุณหภูมิการสลายตัวของโฟมพอลิยูรีเทนนาโน คอมโพสิตมีค่าสูงขึ้น เนื่องจากดินเหนียวเข้าไปทำให้ส่วนแข็งในพอลิยูรีเทนสลายตัวช้าลง ทั้งนี้สมบัติที่ดีขึ้นอยู่กับ ความสามารถในการกระจายตัวของดินเหนียวในโฟมพอลิยูรีเทน ซึ่งจากการทดลองพบว่า ดินเหนียวจะ กระจายตัวได้ดีเมื่อมีปริมาณเพียงเล็กน้อย

ภาควิชา.....วิศวกรรมเคมี.....ลายมือชื่อนิติ.....เสวิตา อินทพิชัย.....

สาขาวิชา.....วิศวกรรมเคมี.....ลายมือชื่อ อ.ที่ปรึกษาวิทยานิพนธ์หลัก.....

ปีการศึกษา.....2552.....

4970665821: MAJOR CHEMICAL ENGINEERING

KEYWORDS: FLEXIBLE POLYURETHANE FOAM / NANOCOMPOSITE /
ORGANOCLAY / CLAY DISPERSION

SEVITA INTHAPICHAJ: EFFECT OF SURFACTANTS AND
ORGANOCLAY LOADING ON PROPERTIES OF
POLYURETHANE/CLAY NANOCOMPOSITE FOAMS. THESIS
ADVISOR: ANONGNAT SOMWANGTHANAROJ, Ph.D. 129 pp.

The present study emphasized on adding organoclay as filler in flexible polyurethane foams to reduce the usage of raw materials which affect the environment such as isocyanate. Two types of clay that were used in this study were in nanometer range. However the difference of ability to exchange cation and the amount of free silica within the clay are observed. Furthermore, the effect of chemical structure of surfactant and the effect of mixing sequence between nanoclay and monomer as well as organoclay loading on the degree of clay dispersion in polyurethane/clay nanocomposite foams are investigated. The results show that the organoclay which was treated by hydroxyl group surfactant shows the highest d-spacing of layered silicates and clay particles did not interfere with hydrogen bond formation as evidenced by fourier transform infrared spectroscopy. The investigation of mechanical properties such as hardness test, resilience test and compression set test show that hardness of polyurethane/clay nanocomposite foams is higher than that of pure polyurethane foam but resilience and compression set properties show lower value compared with those of pure polyurethane foam. Furthermore, the investigation of thermogravimetric analysis of polyurethane/clay nanocomposite foams showed that the nanocomposite foams is higher thermal degradation temperature because the silicates served as a thermal barrier for delaying the hard segments from degradation during heating. Nevertheless, the improvement of the properties depends on clay dispersion ability in the polyurethane matrix. Good dispersion of clay is observed at low organoclay content.

Department :..Chemical Engineering...Student's Signature.....*Sevita Inthapichai*.....

Field of Study :..Chemical Engineering...Advisor's Signature.....*A. N. Somwangthanaroj*.....

Academic Year :.....2009.....

ACKNOWLEDGEMENTS

I would like to express my sincerest gratitude and deep appreciation to my advisor, Assistance Professor Dr. Anongnat Somwangthanaroj, for her kindness, invaluable supervision, invaluable guidance, advices, and encouragement throughout the course of this study.

I am very grateful to my chairman, Associate Professor Dr. Chairit Satayaprasert and my committee members, Associate Professor Dr. Sarawut Rimdusit, Dr. Sarintorn Limpanart and Dr. Sawitree Petchuay for giving substantial advice that is useful for my research. I would like to thank Miss Wirongrong Sri-ngo from Summit Auto Seats Industry Co., Ltd. for giving tremendous advice.

I gratefully thank to Mr. Surapong Tanawan from BASF Polyurethanes (Thailand) Limited. His invaluable discussion and suggestion are greatly appreciated. Furthermore they also provide materials including polyol and toluene diisocyanate and kindly supporting equipments. Without these supports from BASF Polyurethanes (Thailand) Limited., this work will not probably complete. I also gratefully thank to the staffs at Thai Nippon Chemical Industrial Co., Ltd. for their kindly MMT nanoclay support and for their help in the treatment of nanoclay. Thankful to Akzo Nobel, Arnhem, Kunimine Industrial Co., Ltd., Japan for their raw materials support. They support surfactant and MMJ nanoclay respectively. In addition, I am grateful for the partial research grant provided by Thailand Research Fund (TRF).

Additionally, I am grateful to everyone in the Polymer Engineering Laboratory, Chulalongkorn University, especially Mr. Jakkid Sanetuntikul for their discussion and friendly encouragement. Moreover, I would like to thank everyone. I feel so fortunate having a chance to study here.

Finally, my deepest regard to my family and parents who have always been the source of my unconditional love, understanding and generous encouragement throughout my entire study.

CONTENTS

	PAGE
ABSTRACT (THAI)	iv
ABSTRACT (ENGLISH)	v
ACKNOWLEDGEMENTS	vi
CONTENTS	vii
LIST OF TABLES	xii
LIST OF FIGURES	xiii
CHAPTER I INTRODUCTION	1
1.1 General Introduction	1
1.2 Objectives of the Present Study	3
1.3 Scopes of the Research	3
CHAPTER II THEORY	5
2.1 Polyurethane Foams.....	5
2.2 Types of Polyurethane Foams.....	5
2.2.1 Low-density flexible foams	5
2.2.2 Low-density rigid foams	6
2.2.3 High-density flexible foams.....	7
2.3 Raw Materials Used in Polyurethanes	7
2.3.1 Isocyanates	8
2.3.1.1 Toluene diisocyanate	8
2.3.1.2 4,4' Diphenylmethane diisocyanate.....	8
2.3.2 Polyols.....	9
2.3.2.1 Polyether polyols	9
2.3.2.2 Polyester polyols.....	10
2.3.3 Catalysts.....	11
2.3.4 Blowing agents.....	11
2.3.5 Surfactants.....	12
2.3.6 Additives	12

	PAGE
2.3.6.1 Flame retardants.....	12
2.3.6.2 Fillers	13
2.3.6.3 Colouring materials.....	13
2.3.6.4 Chain extenders/crosslinking agents.....	13
2.4 Basic Flexible Foam Chemistry.....	14
2.4.1 Isocyanate reactions with hydroxyl	14
2.4.2 Isocyanate reactions with water	15
2.4.3 Isocyanate reactions with amines.....	16
2.4.4 Isocyanate reactions with urethanes.....	17
2.5 Flexible Foam Processing.....	19
2.5.1 Moulded flexible foam.....	19
2.5.2 Slabstock flexible foam.....	20
2.6 Clay and Organoclay.....	21
2.6.1 Clay	21
2.6.2 Organoclay	24
2.7 Polymer/Clay Nanocomposites.....	25
2.8 Polymer Characterizations	27
2.8.1 The composition of pristine clay.....	27
2.8.1.1 X-ray fluorescence	27
2.8.2 Degree of clay dispersion.....	29
2.8.2.1 X-ray diffraction	29
2.8.3 Morphology characterization.....	31
2.8.3.1 Scanning electron microscope	31
2.8.4 The chemical reactivity between nanoclay and polyurethane	31
2.8.4.1 Fourier transform infrared spectroscopy.....	31
2.8.5 Physical characterization	33
2.8.5.1 Apparent density	33
2.8.6 Mechanical characterizations.....	34
2.8.6.1 Hardness.....	34
2.8.6.2 Indentation force deflection	34
2.8.6.2.1 Support factor (Sag factor).....	34

	PAGE
2.8.6.2.2 Guide factor	35
2.8.6.3 Constant deflection compression set.....	35
2.8.6.4 Resilience (ball rebound)	36
2.8.7 Thermal characterization	36
2.8.7.1 Thermogravimetric analysis.....	36
CHAPTER III LITERATURE REVIEWS	37
CHAPTER IV EXPERIMENTS	43
4.1 Materials	43
4.2 Preparation of Polyurethane/Clay Nanocomposite Foams	44
4.2.1 Determination of cation exchange capacity value of clay	44
4.2.2 Preparation of organoclay	45
4.2.3 Preparation of polyurethane/clay nanocomposite foams	47
4.3 Specimen Characterizations.....	50
4.3.1 The composition of pristine clay.....	50
4.3.2 Inorganic content in clay and organoclay	51
4.3.3 Degree of clay dispersion.....	52
4.3.4 Microscopic observation.....	53
4.3.5 The chemical reactivity between nanoclay and polyurethane	54
4.3.6 Physical property	55
4.3.6.1 Apparent density	55
4.3.7 Mechanical properties.....	56
4.3.7.1 Hardness.....	56
4.3.7.2 Indentation force deflection	57
4.3.7.3 Constant deflection compression set.....	58
4.3.7.4 Resilience (ball rebound)	59
4.3.8 Thermal property	60
4.3.8.1 Degradation temperature.....	60

CHAPTER V RESULTS AND DISCUSSION	61
5.1 The Composition of Pristine Clay.....	61
5.2 Inorganic Content in Pristine Clay and Organoclay	62
5.3 Degree of Clay Dispersion.....	63
5.3.1 Effect of clay composition and chemical structure of surfactant on d-spacing of layered silicates	63
5.3.2 Effect of chemical structure of surfactant and mixing sequence between nanoclay and monomer on degree of clay dispersion	68
5.3.3 Effect of clay composition and organoclay loading on degree of clay dispersion	72
5.4 Morphological Characterization	75
5.5 The Chemical Reactivity between Nanoclay and Polyurethane.....	78
5.5.1 Effect of chemical structure of surfactant and mixing sequence between nanoclay and monomer	78
5.5.2 Effect of clay composition and organoclay loading	82
5.6 Physical Property	86
5.6.1 Apparent density	86
5.7 Mechanical Properties.....	87
5.7.1 Hardness.....	87
5.7.1.1 Effect of chemical structure of surfactant and mixing sequence between nanoclay and monomer	87
5.7.1.2 Effect of organoclay loading and clay composition	89
5.7.2 Indentation force deflection.....	91
5.7.2.1 Support factor (Sag factor).....	91
5.7.2.1.1 Effect of chemical structure of surfactant and mixing sequence between nanoclay and monomer	91
5.7.2.1.2 Effect of clay composition and organoclay loading	93
5.7.2.2 Guide factor	95

	PAGE
5.7.2.2.1 Effect of chemical structure of surfactant and mixing sequence between nanoclay and monomer	95
5.7.2.2.2 Effect of clay composition and organoclay loading	96
5.7.3 Constant deflection compression set.....	98
5.7.3.1 Effect of chemical structure of surfactant and mixing sequence between nanoclay and monomer	98
5.7.3.2 Effect of clay composition and organoclay loading	99
5.7.4 Resilience (ball rebound)	101
5.7.4.1 Effect of chemical structure of surfactant and mixing sequence between nanoclay and monomer	101
5.7.4.2 Effect of clay composition and organoclay loading	102
5.8 Thermal Property	104
5.8.1 Degradation temperature.....	104
5.8.1.1 Effect of clay composition and chemical structure of surfactant.....	104
5.8.1.2 Effect of mixing sequence between nanoclay and monomer	107
5.8.1.3 Effect of clay composition and organoclay loading	109
CHAPTER VI CONCLUSIONS	112
6.1 Conclusions.....	112
6.2 Recommendations for Further Studies.....	112
REFERENCES	113
APPENDICES	116
VITA	129

LIST OF TABLES

TABLE	PAGE
2.1 Summary of foam polyol properties	11
2.2 Timeline of foam development.....	18
2.3 Classification scheme and ideal chemical composition of clay minerals in soils and sediments	23
2.4 Infrared absorption band assignments of polyurethane foams	33
4.1 The abbreviations of clay and organoclay samples	47
4.2 Reaction test of neat flexible polyurethane foams system.....	47
4.3 The abbreviations of polyurethane/clay nanocomposite foams.....	49
5.1 The composition of two sources of clay	61
5.2 Percentage of inorganic content of clay and organoclay	63
5.3 Ratio of the area under the peak of hydrogen bond –NH ($A_{[NH]}$), C=O ($A_{[CO]}$) and –CH stretching ($A_{[CH]}$) of FTIR spectra (part I).....	82
5.4 Ratio of the area under the peak of hydrogen bond –NH ($A_{[NH]}$), C=O ($A_{[CO]}$) and –CH stretching ($A_{[CH]}$) of FTIR spectra (part II).....	85
5.5 Weight and density of neat polyurethane and polyurethane/clay nanocomposite foams.....	86

ศูนย์วิทยทรัพยากร
 จุฬาลงกรณ์มหาวิทยาลัย

LIST OF FIGURES

FIGURE	PAGE
2.1 Scanning electron micrograph showing the open cells of flexible foam.....	6
2.2 Scanning electron micrograph showing the closed cells of rigid foam	7
2.3 Toluene diisocyanate isomers used for PURFs manufacture	8
2.4 Molecular structure of MDI	9
2.5 Example of aliphatic and aromatic dicarboxylic acids used in the production of polyester polyols.....	10
2.6 Urethane reaction	15
2.7 Water reaction	16
2.8 Urea formation	17
2.9 Allophonate formation	18
2.10 Silicon – oxygen tetrahedron, (SiO ₄)	21
2.11 The tetrahedral sheet, [Si ₄ O ₁₀] ⁴⁻	22
2.12 Aluminum octahedron, Al(OH) ₆ ³⁻	22
2.13 Structural scheme of the montmorillonite.....	24
2.14 Illustration of the three different types of polymer/clay nanocomposites	26
2.15 The principal of XRF and the typical XRF detection arrangement	28
2.16 The composition of X-ray diffractometer	29
2.17 Diagram of X-ray diffraction analysis	30
2.18 A multiple reflection ATR system.....	32
3.1 Molecular structure of the amine used to form organoclay	38
3.2 XRD of 5 wt% MMT-OH/PU nanocomposite prepared by different mixing procedures.....	40
3.3 Different nanoparticle	42
4.1 Molecular structure of amine salts	44
4.2 (a) Mixing of polyol and isocyanate (with or without nanoclay) (b) Flexible polyurethane mould foam process	49
4.3 X-ray fluorescence spectrometer	50
4.4 Furnace	51
4.5 X-ray diffractometer	52

FIGURE	PAGE
4.6 Scanning electron microscope	53
4.7 Fourier transform infrared spectrometer.....	54
4.8 Auto urethane H/N tester	56
4.9 Indentation force deflection test	57
4.10 Constant deflection compression set test	58
4.11 Resilience (ball rebound) test.....	59
4.12 Thermogravimetric analyzer.....	60
5.1 XRD patterns of pristine clay (MMT) and modified clay at $2\theta = 1-10^\circ$	65
5.2 XRD patterns of pristine clay (MMJ) and modified clay at $2\theta = 1-10^\circ$	66
5.3 XRD patterns of modified clay, MJ2TOH and MT2TOH at $2\theta = 1-10^\circ$	67
5.4 XRD patterns of polyurethane/clay nanocomposite foams by using 3 wt% of modified clay premixed with polyol at $2\theta = 1-10^\circ$	69
5.5 XRD patterns of polyurethane/clay nanocomposite foams by using 3 wt% of modified clay premixed with isocyanate at $2\theta = 1-10^\circ$	70
5.6 XRD patterns of polyurethane/clay nanocomposite foams compared between using 3 wt% of modified clay premixed with isocyanate, PU_3%IMT-2TOH and 3 wt% of modified clay premixed with polyol, PU_3%PMT-2TOH at $2\theta = 1-10^\circ$	71
5.7 XRD patterns of polyurethane/clay nanocomposite foams containing 0, 1, 3, 5, 7 and 10 wt% of MMT-2TOH modified clay premixed with isocyanate at $2\theta = 1-10^\circ$	73
5.8 XRD patterns of polyurethane/clay nanocomposite foams containing 0, 1, 3, 5, 7 and 10 wt% of MMJ-2TOH modified clay premixed with isocyanate at $2\theta = 1-10^\circ$	74
5.9 SEM micrographs of pristine clay	76
5.10 SEM micrographs of Neat PU foam	76
5.11 SEM micrographs of polyurethane/clay nanocomposite foams containing 1 and 5 wt% of MMT-2TOH and MMJ-2TOH modified clay premixed with isocyanate	77
5.12 FTIR spectra of composites of polyether polyol.....	79

FIGURE	PAGE
5.13 FT-IR spectra of polyurethane/clay nanocomposite foams by using 3 wt% of modified clay premixed with polyol.....	80
5.14 FT-IR spectra of polyurethane/clay nanocomposite foams by using 3 wt% of modified clay premixed with isocyanate.....	81
5.15 FT-IR spectra of polyurethane/clay nanocomposite foams containing 0, 1, 3, 5, 7 and 10 wt% of MMT-2TOH modified clay premixed with isocyanate.....	83
5.16 FT-IR spectra of polyurethane/clay nanocomposite foams containing 0, 1, 3, 5, 7 and 10 wt% of MMJ-2TOH modified clay premixed with isocyanate.....	84
5.17 Hardness of polyurethane/clay nanocomposite foams by using 3 wt% of modified clay premixed with isocyanate and 3 wt% of modified clay premixed with polyol at different types of surfactant.....	88
5.18 Hardness of polyurethane/clay nanocomposite foams containing 0, 1, 3, 5, 7 and 10 wt% of modified clay, MMT-2TOH and MMJ-2TOH premixed with isocyanate	90
5.19 Support factor of polyurethane/clay nanocomposite foams by using 3 wt% of modified clay premixed with isocyanate and 3 wt% of modified clay premixed with polyol at different types of surfactant.....	92
5.20 Support factor of polyurethane/clay nanocomposite foams containing 0, 1, 3, 5, 7 and 10 wt% of modified clay, MMT-2TOH and MMJ-2TOH premixed with isocyanate	94
5.21 Guide factor of polyurethane/clay nanocomposite foams by using 3 wt% of modified clay premixed with isocyanate and 3 wt% of modified clay premixed with polyol at different types of surfactant.....	96
5.22 Guide factor of polyurethane/clay nanocomposite foams containing 0, 1, 3, 5, 7 and 10 wt% of modified clay, MMT-2TOH and MMJ-2TOH premixed with isocyanate	97
5.23 Compression set value of polyurethane/clay nanocomposite foams by using 3 wt% of modified clay premixed with isocyanate and 3 wt% of modified clay premixed with polyol at different types of surfactant.....	99

FIGURE	PAGE
5.24 Compression set value of polyurethane/clay nanocomposite foams containing 0, 1, 3, 5, 7 and 10 wt% of modified clay, MMT-2TOH and MMJ-2TOH premixed with isocyanate	100
5.25 Resilience value of polyurethane/clay nanocomposite foams by using 3 wt% of modified clay premixed with isocyanate and 3 wt% of modified clay premixed with polyol at different types of surfactant.....	102
5.26 Resilience value of polyurethane/clay nanocomposite foams containing 0, 1, 3, 5, 7 and 10 wt% of modified clay, MMT-2TOH and MMJ-2TOH premixed with isocyanate	103
5.27 Thermal degradation of pristine clay (MMT) and modified clay	105
5.28 Thermal degradation of pristine clay (MMJ) and modified clay.....	106
5.29 Thermal degradation of polyurethane/clay nanocomposite foams compared between using 3 wt% of modified clay premixed with isocyanate, PU_3%IMT-2TOH and 3 wt% of modified clay premixed with polyol, PU_3%PMT-2TOH.....	108
5.30 Thermal degradation of polyurethane/clay nanocomposite foams containing 0, 1, 3, 5, 7 and 10 wt% of MMT-2TOH modified clay premixed with isocyanate	110
5.31 Thermal degradation of polyurethane/clay nanocomposite foams containing 0, 1, 3, 5, 7 and 10 wt% of MMJ-2TOH modified clay premixed with isocyanate	111

CHAPTER I

INTRODUCTION

1.1 General Introduction

In recent years, the investigation of polymer/clay nanocomposites received widely attention because of the ability to enhance mechanical properties, thermal stability, gas barrier, flame retardancy and other properties at low content of clay compared to neat polymer. All mentioned properties make these composites more interesting for widespread use of application, e.g., automotive, food packaging, and others. [14]

Polyurethanes (PUs) are interesting polymer materials with highly versatile properties and wide range of commercial applications such as coatings, adhesives, fibers, thermoplastic elastomers, and foams. The largest use for polyurethanes is as foams in automotive industry such as car seat manufacture. [5] Adding small amount of clay as filler in polyurethanes has been found to reduce the amount of polyurethanes, thereby lowering cost of polyurethanes used in automotive industry and overcome some disadvantages properties of polyurethanes concerning with low thermal stability, low mechanical strength and poor barrier properties which limit their application. Plate-like nanoparticles can also reduce gas diffusivity in the polymer matrix. Due to higher surface energy of clay, it tends to agglomerate and in most case it is very difficult to disperse these nanoparticles into polymer matrix. Agglomerated nanoparticles act as defects and can have detrimental effect on polymer performances. Thus, the improvement of the properties as mentioned above will depend on clay dispersion ability in the polyurethane matrix. Since sodium montmorillonite (subgroup of smectite or bentonite clay) is hydrophilic inorganic material so it is necessary to exchange cations of the native clay with more organophilic or hydrophobic materials such as quaternary alkyl ammonium surfactants then the extents of clay dispersion in polyurethane matrix is reached and thus improve the compatibility between nanoclay and polymer. [6,7] Depending on the structure of dispersed clay platelets in the polymer matrix, the composites can be classified as intercalated or exfoliated nanocomposites. Intercalated structures are self-assembled, well ordered multilayered structures where

the extended polymer chains are inserted into the gallery space of the clay. This leads to an expansion of the interlayer spacing. In an exfoliated structure, individual silicate sheets lose their layered geometry as a result of delamination, and dispersed as nanoscale platelets in a polymer matrix. The presence of exfoliated polyurethane nanocomposite produce finer cell size and higher cell density compare to pristine polyurethane foams which results in improved thermal and mechanical properties for polyurethane foams. [8]

The previous studies have shown that a polar polymer such as nylon 6 exhibits a better dispersion of layered silicates based on a surfactant with one alkyl tail, while nanocomposites made from non-polar polymers such as polypropylene, polyethylene, and various copolymer show completely opposite trends, these results suggest that nylon 6 has a higher affinity for the polar surface of the clay than for the largely non-polar surfactant, while the opposite is true for non-polar matrices. [9]

Polyurethanes have similar functional group as nylon 6 but rather different repeating unit structures. Good dispersion of clay in the polyurethane matrix has been achieved through the modification of clay surface with active surfactants containing more than two hydroxyl groups. The presence of hydroxyl groups enhanced intra-gallery polymerization, which in turn led to better clay dispersion. [8]

Flexible foams can be easily produced in a variety of shapes by cutting or moulding. They are used in most upholstered furniture and mattresses. Flexible foam moulding processes are used to make comfortable and durable seating cushions for many types of seats and chairs. Most flexible polyurethane foams are based upon the reaction of diisocyanates with polyether or polyester diols or triols, but over 90% of all flexible polyurethane foam production is now based upon polyether polyol and the mixture of 80:20 by weight of the 2,4 and 2,6 isomers of toluene diisocyanate.

The purpose of this research is to study the effect of chemical structure of surfactant on the ability to disperse clay in polyurethane matrix, the effect of mixing sequence between nanoclay and monomer, clay types, as well as organoclay loading on mechanical and thermal properties of polyurethane nanocomposite foams. Finally the relationship between the degree of clay dispersion and polyurethane nanocomposite foams' properties will be evaluated.

1.2 Objectives of the Present Study

1. To study the effect of chemical structure of surfactant on the degree of clay dispersion in polyurethane/clay nanocomposite foams
2. To investigate the synthesis routes of polyurethane/clay nanocomposite foams
3. To examine the efficiency of two types of clay which have different composition and cation exchange capacity
4. To explore the effect of organoclay loading on mechanical and thermal properties of polyurethane nanocomposite foams
5. To investigate the relationship between the degree of clay dispersion and polyurethane nanocomposite foams' properties especially mechanical properties for application in automotive industry

1.3 Scopes of the Research

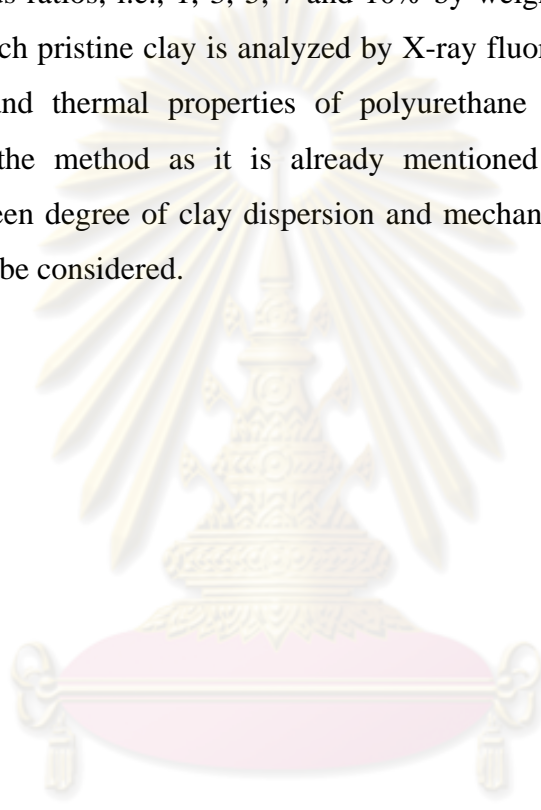
The current study consists of two parts as follow.

Part I: Effect of chemical structure of surfactant and the mixing sequence between nanoclay and monomer on properties of polyurethane/clay nanocomposite foams.

This part concentrates on the affect of chemical structure of surfactant and the mixing sequence between nanoclay and monomer on degree of clay dispersion. In this study three types of surfactant are used, i.e., octadecyl methyl [polyethylene(15)] ammonium chloride, trimethyl tallow quaternary ammonium chloride and dimethyl bis (hydrogenated-tallow) ammonium chloride. Furthermore the synthesis routes of polyurethane/clay nanocomposite foams are investigated by premixed 3 wt% of organoclay with either polyol or isocyanate before adding the other monomer. The degrees of clay dispersion in polyurethane/clay nanocomposite foams are characterized by X-ray diffraction (XRD) and scanning electron microscopy (SEM). In addition the chemical reactivity between nanoclay and polyurethane are characterized by fourier transform infrared spectroscopy (FTIR). The physical property and mechanical properties of polyurethane/clay nanocomposite foams are carried out by density test, indentation force deflection test, hardness test, constant deflection compression set test and resilience (ball rebound) test. The thermal property of polyurethane/clay nanocomposite foams is investigated by thermogravimetric analyzer (TGA).

Part II: Effect of clay composition and organoclay loading on properties of polyurethane/clay nanocomposite foams.

After the appropriate surfactant and suitable synthesis route of polyurethane/clay nanocomposite foams from part I is selected. The ability of cation exchange between two types of clay, i.e., Sodium bentonite with CEC of 60 meq/100 g of clay (MMT) and Sodium bentonite with cation exchange capacity (CEC) of 90 meq/100 g of clay (MMJ), and the organoclay loading of polyurethane/clay nanocomposite foams which is varied at various ratios, i.e., 1, 3, 5, 7 and 10% by weight are also considered. The composition of each pristine clay is analyzed by X-ray fluorescence (XRF). Moreover, the mechanical and thermal properties of polyurethane nanocomposite foams are investigated via the method as it is already mentioned from Part I. Finally the relationship between degree of clay dispersion and mechanical and thermal properties of these materials be considered.



ศูนย์วิทยทรัพยากร
จุฬาลงกรณ์มหาวิทยาลัย

CHAPTER II

THEORY

2.1 Polyurethane Foams (PURFs)

Polyurethane products have been used in many applications. Over three quarters of the global consumption of polyurethane products is in the form of foams. [10] Polyurethane foams are categorized as flexible or soft, rigid, and semi-rigid form. Flexible polyurethane foams are widely used in engineering applications, especially in automotive seat cushions. [11] In terms of their cell structure, PURFs are classified into closed-cell, open-cell, and mixed type of foams, and are characterized by means of the percentage of closed cells. Closed-cell PURFs have better thermoinsulating properties and superior resistance to atmospheric factors. Open-cell PURFs are better soundproofing materials and are more permeable to gases and water vapour. [5] Foams may be flexible or rigid, depending upon whether their glass transition temperature is below or above room temperature, which in turn depends upon their chemical composition, the degree of crystallinity, and the degree of cross-linking.

2.2 Types of Polyurethane Foams

Three foam types are, in quantity terms, particularly significant: low density flexible foams, low density rigid foams and high density flexible foams

2.2.1 Low-density flexible foams

Low-density flexible foams, whose density is in the range of 10 to 80 kg/m³, are made from lightly cross-linked polymer with an open-cell macro-structure. There are no barriers between adjacent cells, which results in a continuous path in the foam, allowing air to flow through it. These materials are used primarily as flexible and

resilient padding materials to provide a high level comfort for the user. An example of the cellular structure is shown in Figure 2.1.

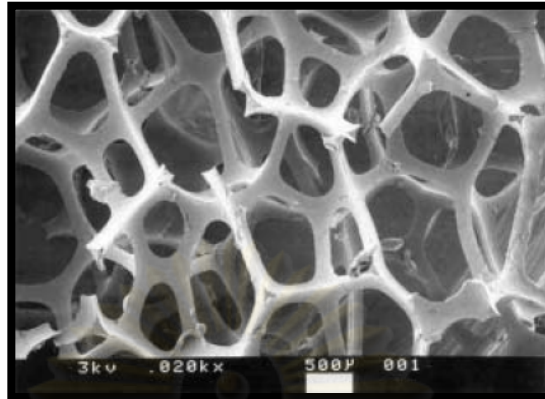


Figure 2.1: Scanning electron micrograph showing the open cells of flexible foam [12]

2.2.2 Low-density rigid foams

Low-density rigid foams are highly cross-linked polymers with an essentially closed cell structure and a density range of 28 to 50 kg/m³. Individual cells in the foam are isolated from each other by thin polymer wall, which effectively stop the flow of gas through the foam. These materials offer good structural strength in relation to their weight, combined with excellent thermal insulation properties. The cells usually contain a mixture of gases depending on their nature and relative proportion thus the foams will have different thermal conductivity. In order to maintain long-term performance it is necessary for the low thermal conductivity gases to remain in the cells, consequently more than 90% of the cells need to be closed. An example of the cellular structure is shown in Figure 2.2. Recently fully open celled rigid foams specifically developed for vacuum panel applications have been developed.

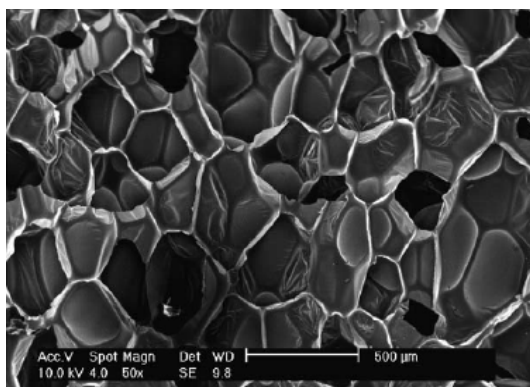


Figure 2.2: Scanning electron micrograph showing the closed cells of rigid foam [8]

2.2.3 High-density flexible foams

High-density flexible foams are defined as those having density above 100 kg/m^3 . This range includes moulded self-skinning foams and microcellular elastomers. Self-skinning or integral skin foam systems are used to make moulded parts having a cellular core and a relative dense, decorative skin. There are two types, i.e., those with an open cell core and an overall density in the range up to about 450 kg/m^3 and those with a largely closed cell or microcellular core and an overall density above 500 kg/m^3 . The microcellular elastomers have a much more uniform density in the range of 400 to 800 kg/m^3 and mostly closed cells, which are so small that they are difficult to see with naked eye. [13,14]

2.3 Raw Materials Used in Polyurethanes

Polyurethane foams are manufactured on the basis of polyether- or polyester urethanes and the main reactions involved in the production of all types of PURFs are based on the reactivity of isocyanates. [5,15] A typical reaction mixture for the production of PURFs consists of isocyanate, polyol, catalyst, blowing agent, and additives.

2.3.1 Isocyanates

The most common isocyanates are toluene diisocyanate (TDI) and 4,4' diphenylmethane diisocyanate (MDI). Other isocyanates that are used are generally blends with TDI and MDI. [13]

2.3.1.1 Toluene diisocyanate (TDI) (liquid, boiling point 120°C)

TDI is the most commonly available mixture of 80:20 and 65:35 of the 2,4 and 2,6 isomers as can be seen in Figure 2.3.

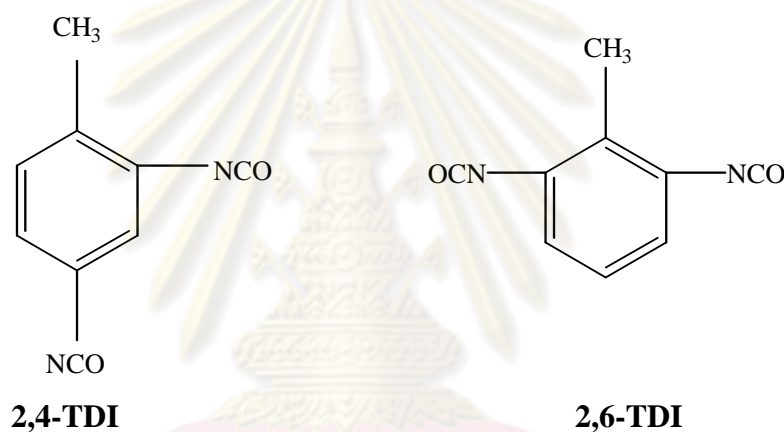


Figure 2.3: Toluene diisocyanate isomers used for PURFs manufacture [10,15]

TDI has a relatively high vapour pressure. It gives rise to the risk of airborne exposure to workers. As a consequence, it is quite difficult material to handle on site, in transport and in the laboratory; therefore, usage has been limited in favour of MDI which shows lower volatility. [10,15]

2.3.1.2 4,4' Diphenylmethane diisocyanate, or methylene diphenylene diisocyanate (MDI) (solid, melting point 38°C, boiling point 195°C)

Pure MDI is a crystalline solid at room temperature so it must be heated slightly in order to convert into a more manageable form, i.e., a fairly high viscosity liquid. [15]

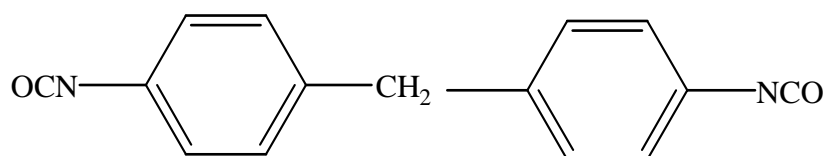


Figure 2.4: Molecular structure of MDI [15]

However, the main reason why TDI has been used for so long is that the cost of TDI production is considerably lower than MDI and, more importantly, the final properties of the foam are relatively better for TDI systems than for MDI based systems. [15]

2.3.2 Polyols

The polyol used for the manufacture of PURFs is usually either polyether or polyester type polyols. They are 'prepolymer' whose structure determines the final PURFs properties with a large dependence being on their molecular weight and functionality. Generally, flexible foam polyols have molecular weights of 1,000-6,500 g mol⁻¹, functionality 2.0-3.0 and hydroxyl value 28-160 mg KOH g⁻¹, whereas rigid foam polyols have molecular weights of 150-1,000 g mol⁻¹, functionality 2.5-8.0 and hydroxyl value 250-1,000 mg KOH g⁻¹. The rigidity of the foam can be increased by reducing the chain segment length between junction points-this effectively produces more tightly crosslinked networks. [10,15] In the foam industry, three types of polyol are prevalent; i.e., polyether polyol, polyester polyol and copolymer polyol. Each of them has its own advantages as summarized in Table 2.1. [10]

2.3.2.1 Polyether polyols

Approximately 90% of polyols used in PURFs production are hydroxyl-terminated polyethers due to their low cost and ease of handling (low viscosity). Polyether-based foams show better resilience and resistance to hydrolysis than polyester-based foams. They are produced by the ring opening of alkylene oxides using a polyfunctional initiator. Ethylene or propylene oxides are the most commonly used

polyols. The polyols used for making flexible foams have molecular weight ranging from 3,000 to 6,000 g mol⁻¹ whereas the molecular weight of rigid foam is approximately 500 g mol⁻¹ in order to reduce the distance between crosslinks. The reactions are base-catalysed. [15]

2.3.2.2 Polyester polyols

Compared with polyether polyols, polyester polyols tend to be more reactive, produce foams with better mechanical properties, are less susceptible to yellowing in sunlight and are less soluble in organic solvents. However, they are more expensive, more viscous; therefore, they are more difficult to handle. Consequently, they are only used in applications that require their superior properties. [15] Polyester polyols are made by condensation reactions between diols (and triols) and dicarboxylic acids such as: adipic acid, sebacic acid and m-phthalic acid as their formulas are shown in Figure 2.5.



Figure 2.5: Example of aliphatic and aromatic dicarboxylic acids used in the production of polyester polyols [15]

Table 2.1: Summary of foam polyol properties [10]

Properties	Polyether polyol	Polyester polyol	Copolymer polyol
Viscosity	low	high	medium
Hydrolytic stability	excellent	fair	excellent
Oil / Solvent stability	fair	excellent	good
Strength	fair	excellent	very good
Resilience	good	fair	excellent

2.3.3 Catalysts

Catalysts exert an influence upon the rate of competing reactions and have a major effect on the ultimate properties of the final foam. The formation of urea and urethane linkages establishes the physical properties of the polymer and these are dependent on the type and concentration of catalysts used. A typical catalyst system would consist of a mixture of a tertiary amine and organo-metallic compounds. Each catalyst type is specific for a particular chemical reaction. Catalyst mixtures are generally necessary to control the balance of the polymerization and the gas generation reactions, where both of them are exothermic reactions. Getting the correct balance of polymerization and foaming is of major importance in the production of closed cell foam. If too much gas is evolved before a sufficient amount of polymerization has taken place, the gas will burst through the weak cell walls. It then produce and open cell structure. On the other hand, if polymerization is completed before sufficient gas has been generated, high density foam will be obtained. Thus, blends of catalysts are required to balance the relative chemical reaction rates. [15]

2.3.4 Blowing agents

The most commonly used blowing agent is water. It produces carbon dioxide (CO₂) gas by the reaction with diisocyanate. Typical water concentrations are 3-5 parts of water per 100 parts of polyester polyol 1.8-5 parts of polyether polyol. The reaction of water with an isocyanate is exothermic and results in the formation of active urea sites which form crosslinks via hydrogen bonding. To reduce the high crosslink density

of the foam, auxiliary blowing agents are used to produce low density foams with a softer feel than water-blown foams, and to produce closed cell flexible foams. The auxiliary blowing agents used for this purpose are the chlorofluorocarbon and methylene dichloride. These materials volatilise due to the exothermic heat of reaction of isocyanates and increase the gas volume without increasing the degree of crosslinking. Due to the problems related to the earth's atmosphere, other types of auxiliary blowing agents such as hydro fluorocarbon which they do not contain chlorine were considered. [10,15]

2.3.5 Surfactants

Surfactants are essential additives used in PURFs formulations. They assist in mixing incompatible components of the formulation, controlling cell size, open cell content, and uniformity through reduce surface tension. The most important surfactants are based on water-soluble polyether siloxanes. It has been found that increasing the level of surfactant in the PURFs formulation causes a reduction in the rate of foam rise. This can be explained by the fact that increasing the surfactant level will effectively reduce functional group concentration. Consequently, the rate of foam rise, temperature rise, and overall reaction rate are reduced. There is a critical level of surfactant which the foam produced will suffer from coarse cell structure and collapse. Just above this critical level, good open cell foams are produced. At higher levels of surfactant, silicone foams with closed cell are produced. At much higher levels of surfactant, the foams produced show a high level of shrinkage, poor compression set and poor load-bearing capacity. [15]

2.3.6 Additives

2.3.6.1 Flame retardants

These are normally based on halogen or phosphorous containing compounds. The addition of small amounts of fire retardant has little or no effect on foam physical properties, but adverse effects are noticeable when higher amounts are used. [10,15]

2.3.6.2 Fillers

Particulate fillers tend to reduce flammability, increase compression resistance, compressive strength, and weight of seat cushion. Reinforcing fibrous fillers increase stiffness, heat resistance, and tensile strength. Typical fillers include carbon black, clay, calcium carbonate, glass fibres, and microspheres. Carbon fibres are used in high performance composites. [10,15]

2.3.6.3 Colouring materials

Pigments must be inert to isocyanates, stable at reaction temperatures, and free of contaminants that can affect foaming. [15]

2.3.6.4 Chain extenders/crosslinking agents

These are low molecular weight polyols or amines. They are generally used for producing foams of high flexibility by chain extension. Load-bearing capacity of foam is improved by augmenting the degree of crosslinking of the polymer by using polyfunctional reagents. [15]

Physical properties of the final PURFs are influenced by hydrogen bonding between the NH-groups in the urethane/urea linkage and either ether oxygen atoms in polyether or carbonyl oxygen atoms in polyester. Hydrogen atoms which are bonded to ether oxygen atoms are much weaker than those bonded to carbonyl oxygen atoms in polyester. This is the reason why polyether PURFs feel softer than those based on polyester polyols. Flexibility causes by the degree of crosslinking and is then determined largely by the functionality of the hydroxyl ended species (polyol). The use of highly branched polyols produces rigid foams with high crosslink density.

2.4 Basic Flexible Foam Chemistry

Flexible polyurethane foams consist essentially of two chemical inter-linked polymers:

(1) A urethane polymer formed by the reaction of a high molecular weight polyol that behaves as a soft segment and an isocyanate that may be di- or poly-functional. The resulting elastomeric polyurethane network gives the foam its stability, elasticity and mechanical strength.

(2) A urea polymer from the reaction of the isocyanate and water. The carbon dioxide generated acts as the blowing agent that forms the cellular network. The urea groups, physically linked through strong hydrogen bonds, phase separate forming hard segments that contribute to load-bearing properties.

To obtain low-density foam a high level of water, in molecular terms, is required. Thus, the urea reaction dominates the urethane reaction and is the main contributor to the overall foam exotherm.

Flexible foams can be made either by a one-shot process, where the urethane and urea reactions occur simultaneously, or in two-step process. In the latter the polyol is first reacted with an excess of isocyanate and the resulting isocyanate prepolymer reacted in a second step with water and the other additives. This effectively segregates the urethane and urea steps of the reaction, thus avoiding direct competition between the polyol hydroxyl groups and water. Because of its inherently higher cost the two-step process is reserved for more demanding applications.

2.4.1 Isocyanate reactions with hydroxyl

The most important reaction in the manufacture of polyurethanes is between isocyanate and hydroxyl groups as shown in Figure 2.6. The reaction product is a carbamate, which is called a urethane in the case of high molecular weight polymers. The reaction is exothermic and reversible going back to the isocyanate and alcohol.

Aliphatic primary alcohols are the most reactive and react much faster than secondary and tertiary alcohols due to steric reasons, but urethane made from tertiary alcohols do not regenerate free isocyanate instead dissociating to yield the

corresponding amine, alkene and carbon dioxide. The urethane back reaction starts at 250 °C for aliphatic isocyanates, but is closer to 200°C for aromatic isocyanates.

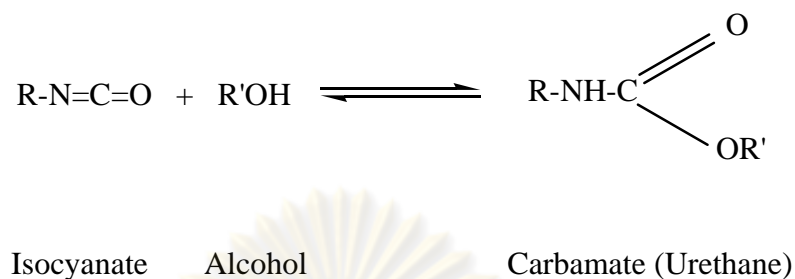


Figure 2.6: Urethane reaction [13]

2.4.2 Isocyanate reactions with water

The reaction of isocyanates with water to produce an amine and carbon dioxide is highly exothermic. The initial reaction product is a carbamic acid, which break down into carbon dioxide and a primary amine as shown in Figure 2.7. The amine will then react immediately with another isocyanate to form a symmetric urea. Due to the formation of carbon dioxide the water reaction is often used as a blowing agent as the level of blow can be tailored, simply by adjusting the amount of water in the formulation.

ศูนย์วิทยทรัพยากร
จุฬาลงกรณ์มหาวิทยาลัย

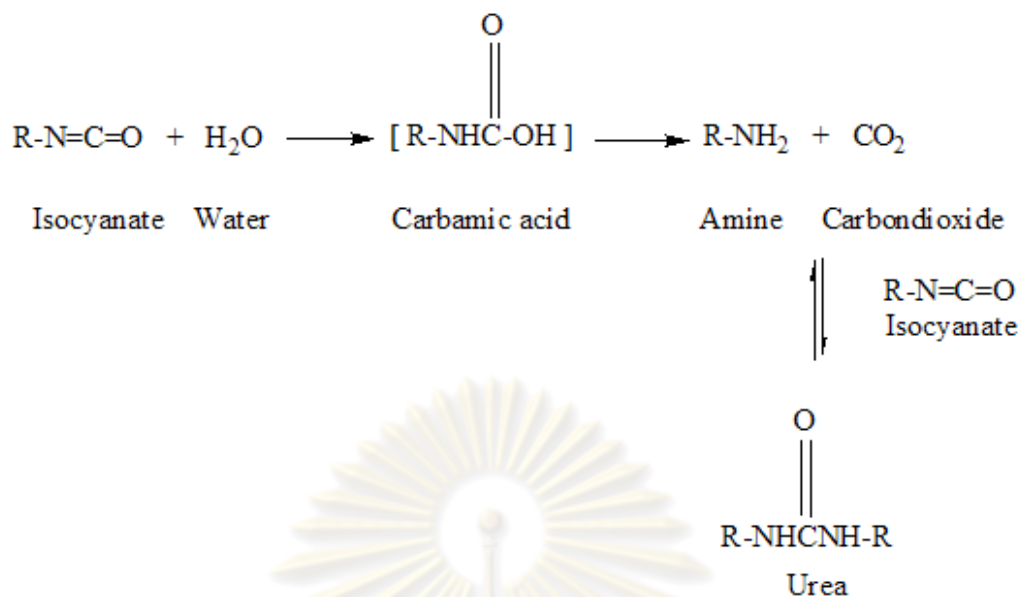


Figure 2.7: Water reaction [13]

Despite the high reaction exotherm the water reaction is generally slow in the absence of catalyst and one of the main reasons is that water is not very soluble in isocyanates such as MDI and TDI.

2.4.3 Isocyanate reactions with amines

Isocyanates react with primary and secondary amines to produce di- and tri-substituted urea respectively whilst tertiary amines form labile 1:1 adducts, but generally do not react with isocyanates as seen in Figure 2.8.

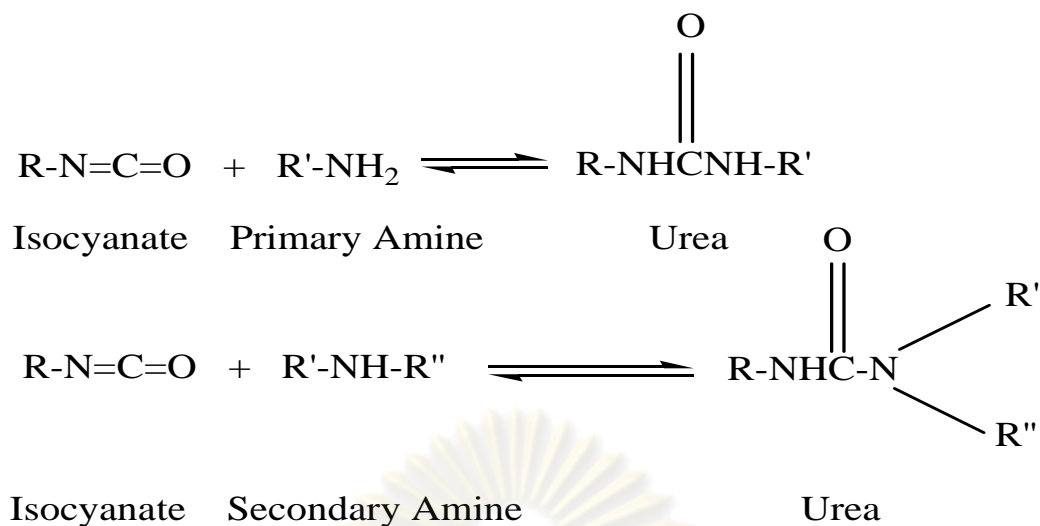


Figure 2.8: Urea formation [13]

These conversions are exothermic and diamines are used as chain extending and curing agents in polyurethane manufacture. The resulting polyurea segments increase the potential for crosslinking.

2.4.4 Isocyanate reactions with urethanes

An allophanate group is the result of the exothermic reaction of isocyanate with the active hydrogen on a urethane group, Figure 2.9.

ศูนย์วิทยาศาสตร์
จุฬาลงกรณ์มหาวิทยาลัย

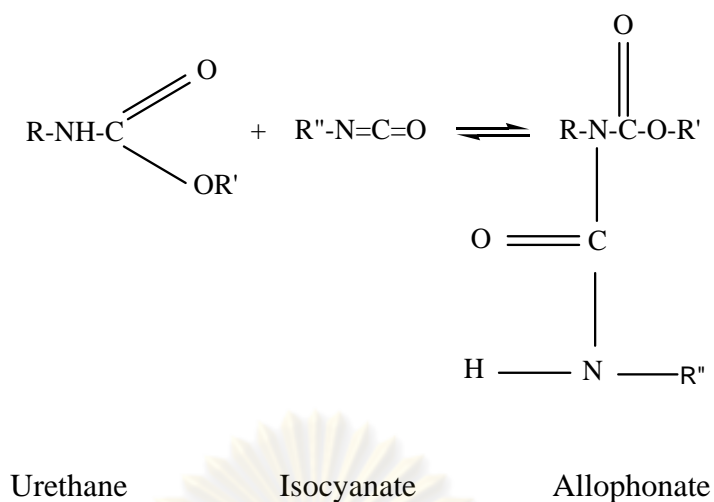


Figure 2.9: Allophonate formation [13]

The various stages of foam development are shown in Table 2.2.

Table 2.2: Timeline of foam development [13]

Time	Foam development	Physical event	Chemical event	Morphology
0 seconds		Raw material mixing, air nucleation		
5 seconds	Cream, initial rise	Froth formation	Urea reaction, CO ₂ saturation	
20 seconds	Rising foam	Viscosity increase, bubble expansion and coalescence, window thinning, gas diffusion	Urethane reaction, molecular weight increase	Beginning of hard domain formation
60-90 seconds	End of rise	Cell opening blow-off	Hydrogen bond formation	Phase separation (urea aggregate formation)
3 hours > 1 day	Cure	Hardness development		

2.5 Flexible Foam Processing

There are two principal kinds of flexible foam processing: production of moulded foam and production of slabstock.

2.5.1 Moulded flexible foam

In production of moulded, pouring is discontinuous. To mould foam, a weight of formulation mix is either poured into a heated mould that is then closed, or injected into a closed mould. In either case, the mould is equipped with ports to allow air to escape as the foam rises to fill the mould.

Moulded foams are typically made for use in automotive seating and headrests and in furniture seating. The foam is produced in essentially the shape in which it is to be used. Moulds are made of cast aluminum, although reinforced plastic and ceramic moulds have been used. Typically, the mould is preheated to 50°C, and the mould surface is treated with a mould release agent, usually a wax in a volatile hydrocarbon or an emulsion. A metered quantity of formulation mix is poured into the mould and the mould is clamped shut. In a few minutes, foam appears at the mould ports, the extrusion time. After a mould residence time of from two to ten minutes, the mould is opened, the moulded piece is removed by hand or mechanically, and the mould is conditioned for reuse (cleaned of flash and periodically treated with mould release). A number of moulds may be mounted on a carousel for parts production, with the moulded parts put on a conveyer after demould and passed through an oven to accelerate surface cure.

The moulded foam is usually treated in some way to ensure that foam cells are open, to prevent shrinkage and distortion on cooling. This treatment may be crushing or vacuum shock to burst open the still-closed cell windows of the foam. Moulded foam does not achieve its final properties for some time, as the curing reactions may take several hours to complete and climatic conditions (principally absolute humidity) play a role. Foams are regularly given at least 24 hours to cure before testing and humidity may be controlled during this time, for example 20°C and 50% relative humidity. [16]

2.5.2 Slabstock flexible foam

In slabstock production, formulated mix is poured continuously, usually into a paper support, which is moved from the pouring site as the foam rises, to form buns that may be 1.2-2.4 m wide, 1.5 m. high, and 15 m long or more. The continuous pouring of one bun may take 5 to 10 minutes before pouring is stopped and preparations are made to pour another bun.

In making slabstock foam, a traverse-mounted mixhead moves across the width of a paper form in which the foam formulation is continuously poured. The paper form containing the reacting foam is moved forward on a flat conveyor at a constant speed in the range of 5-18 cm/sec. The paper is either a wide strip of kraft paper folded to a U shape, or a separate bottom strip and two side strips, and may be either silicone- or polyolefin-coated. The paper conveyor is often inclined downward from the pour zone and is followed by a series of roller conveyors to produce a bun of risen foam that can be 60 m long.

In the first stage, while the rising bun in the paper form is moving on the flat conveyor, sidewalls are used to support the paper form and rising foam. Toward the end of foam rise, the bun blows, as gas bubbles break the top surface of the foam, and carbon dioxide, auxiliary blowing agent, some isocyanate, and amine catalyst volatilize. These gases must be contained in ventilation system, usually a tunnel through which the foam is conveyed. Before the buns harden, the paper removed. This removal is usually done 5 to 10 minutes after pour. The bun, which is now itself-supporting, can be trimmed. Flexible slab foams, however, do not reach their physical properties for at least 12 hours and usually 24 hours. The good thermal insulation properties of the foams and the highly exothermic reactions during foaming lead to temperatures at the center of the bun in the range of 140°C to 170°C. Some formulations may turn yellowish (scorch) in the center, and formulations with very high in water have self-ignited in the absence of proper attention to bun size and formulation reactivity.

Flexible foam buns are usually held in a storage area during cooling and curing. Thereafter, the buns are cut, usually in slices, for further fabrication.

The slab foaming process, outline above, leads to a bun that may be 1.5 m. high with a crowned top. Due to friction with the paper sides as the foams rises, the center of the bun rises higher than the sides. If the bun is very wide, around 2.4 m, the top may

be double-crowned, settling slightly in the middle. In any case, the crown is unstable as foam in slicing and fabrication. [16]

2.6 Clay and Organoclay

2.6.1 Clay

Clay minerals are group of hydrous layered magnesium or aluminosilicates (phyllosilicates) containing several main elements as iron, alkaline, and alkaline earth metals. The crystalline lattices are classified as three-dimensional, two-dimensional (layered) or mono-dimensional (fibrous structures). Clay used in this research is two-dimensional layered, which each magnesium or aluminosilicate is essentially composed of two types of sheets, octahedral and tetrahedral sheet. A continuous linkage of SiO_4 tetrahedra through sharing of three oxygen atoms with three adjacent tetrahedra produces a sheet with a planar network as seen in Figure 2.10. In such a sheet the tetrahedral silica groups are arranged in the form of a hexagonal network, which is repeated indefinitely to form a phyllosilicate with the composition $[\text{Si}_4\text{O}_{10}]^{4-}$ as shown in Figure 2.11. A side view of the tetrahedral sheet shows that it is composed of three parallel atomic planes, which are composed of oxygen, silicon, and oxygen, respectively. [1719]

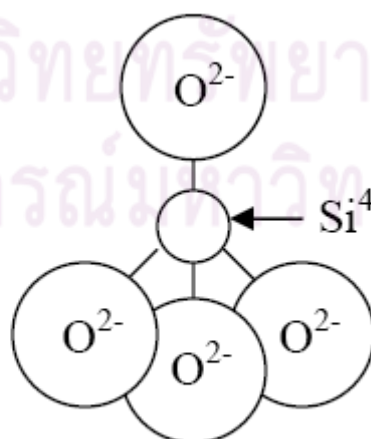


Figure 2.10: Silicon-Oxygen Tetrahedron, (SiO_4) [9]

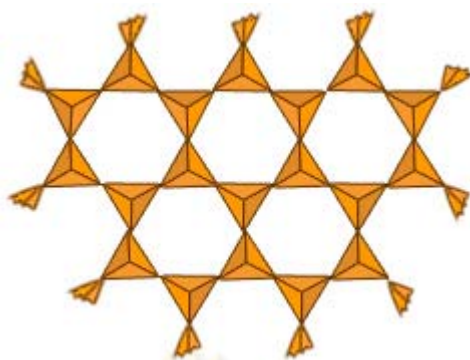


Figure 2.11: The tetrahedral sheet, $[\text{Si}_4\text{O}_{10}]^{4-}$ (Top view) [20]

An octahedral sheet is obtained through condensation of single $\text{Mg}(\text{OH})_6^{4-}$ or $\text{Al}(\text{OH})_6^{3-}$ octahedron as seen in Figure 2.12. Each O atom is shared by three octahedra, but two octahedra can share only two neighboring O atoms. In this sheet the octahedral groups are arranged to form a hexagonal network, which is repeated indefinitely to form an $[\text{Mg}_6\text{O}_{12}]^{12-}$ or $[\text{Al}_4\text{O}_{12}]^{12-}$ layer. [17]

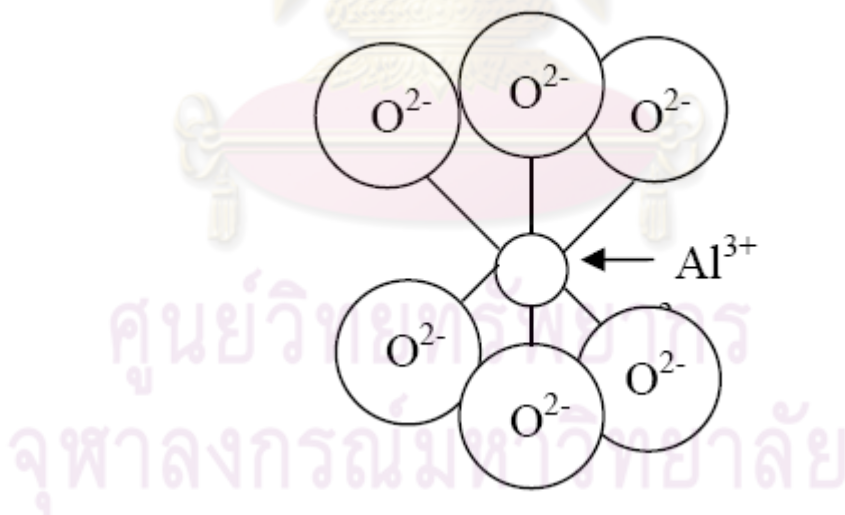


Figure 2.12: Aluminum Octahedron, $\text{Al}(\text{OH})_6^{3-}$ [9]

The hydrated aluminosilicates can be neutral or ionic exchangers and the groups treated in this work involve basically the phyllosilicates of the smectite group (sometimes known as the montmorillonite group), which consist of tetrahedral-

octahedral-tetrahedral (TOT) layer group. The common groups of the phyllosilicate minerals occurring in soils and sediments are listed in Table 2.3. [17]

Table 2.3: Classification scheme and ideal chemical composition of clay minerals in soils and sediments [17]

Group	Subgroup	Ideal chemical composition
Smectite	Beidellite	$[(Al_{4.00})(Si_{7.50-6.80}Al_{0.50-1.20})O_{20}(OH)_4]Na_{0.50-1.20}$
	Montmorillonite	$[(Al_{3.50-2.80}Mg_{0.50-1.20})(Si_8)O_{20}(OH)_4]Na_{0.50-1.20}$
	Nontronite	$[(Fe_{4.00})(Si_{7.50-6.80}Al_{0.50-1.20})O_{20}(OH)_4]Na_{0.50-1.20}$
	Hectorite	$[(Mg_{5.50-4.80}Li_{0.50-1.20})(Si_8)O_{20}(OH)_4]Na_{0.50-1.20}$
	Saponite	$[(Mg_{6.00})(Si_{7.50-6.80}Al_{0.50-1.20})O_{20}(OH)_4]Na_{0.50-1.20}$

Montmorillonite is one in the smectite group which has a low thermal expansion coefficient and high gas barrier properties. The composition of the montmorillonite is variable and depends on its own genesis, which is attributed to the characteristic of different cationic exchange capacity. A small fraction of the tetrahedral Si atom is isomorphically substituted by Al and/or a fraction of the octahedral atoms (Al or Mg) is substituted by atoms of lower oxidation number. The resulting charge deficiency is balanced by hydrated cations, mainly K, Na, Ca, and Mg, of which more than 80% is located between the parallel clay layers as shown in Figure 2.13. These ions are hydrated due to the fact that, in nature, smectite are formed in aqueous environments. Because they are hydrated, these cations are only loosely held by the negatively

charged clay layers. Smectite saturated with other cations dissociate in aqueous suspensions into exchangeable cations and tactoids, which are composed of several parallel TOT layers, held together by electrostatic forces by some of the exchangeable cations that remain in the interlayer space. Water and polar organic molecules are attracted by the exchangeable cations and may intercalate between the layers, causing the structure to expand in the direction perpendicular to the layers. The interlayer space between the TOT layers, obtained as a result of the expansion of the clay, has special chemical properties. The swelling of this space depends on several factors, such as the exchangeable cation, the humidity of the environment, the vapor pressure, and the temperature. [17,19]

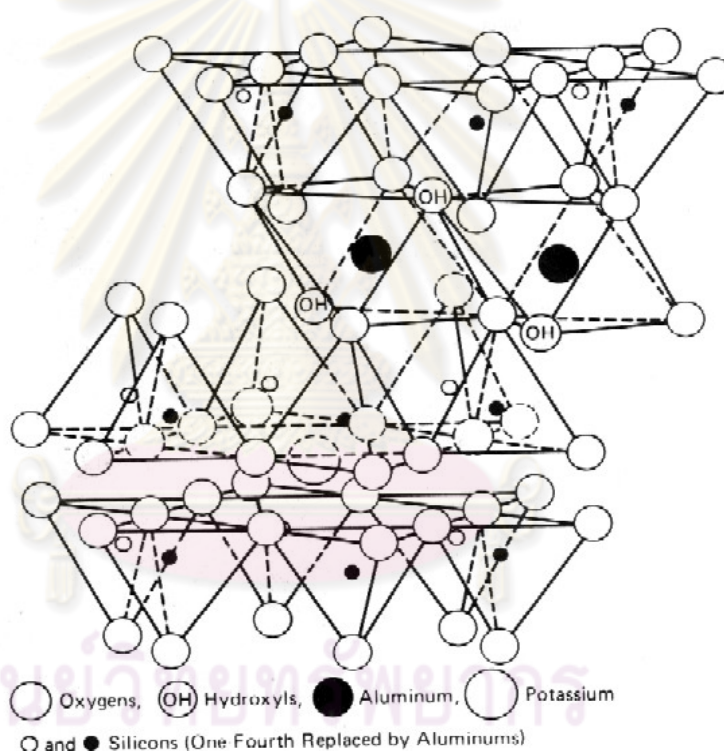


Figure 2.13: Structural scheme of the montmorillonite [21]

2.6.2 Organoclay

In the present clay minerals are used as fillers in different products. The interactions between organic matter and clay minerals are among the most widespread reactions in nature. The interactions include cation exchange and adsorption of polar

and nonpolar molecules. Smectite and especially montmorillonite have been the most studied minerals of all clay. These minerals are able to swell and adsorb polar organic compounds into their interlayer space. The presence of small inorganic cations in the interlayer makes this space hydrophilic. However, inorganic exchangeable cation can also be replaced by a quaternary ammonium cation in the interlayer. This treatment is used to enhance the hydrophobic properties of the clay. This modified clay is commonly referred to as “organoclay”. There are two types of organoclay: those saturated with large quaternary ammonium cations with one or two long alkyl chains and those saturated with small quaternary ammonium aliphatic and aromatic cations. Some investigators use the term “organophillic clay” for the first type and the “adsorptive clay” for the organoclay saturated with small quaternary ammonium cations. For example, the exchange reaction between an inorganic metallic cation, M^{m+} , initially saturating a smectite mineral, M^{m+} -Smec, and an aqueous solution of an aliphatic ammonium salt such as ethylammonium chloride, $C_2H_5NH_3Cl$, can be formulated by the following equation [17] :



2.7 Polymer/Clay Nanocomposites

Polymers have been successfully reinforced by glass fibers and other inorganic materials. In these reinforced composites, the polymer and additives are not homogeneously dispersed on a nanometer level. If nanometer range dispersion could be achieved, the mechanical and barrier properties might be further improved. Clay mineral is a potential nanoscale additive because it comprises silicate layers in which the fundamental unit is 1 nm thick planar structure. Also, it undergoes intercalation with various organic molecules. The intercalation causes an increase in the distance between silicate layers, which is dependent on the molecular size of the organic molecule. The dispersion of clay minerals in polymer matrix can be classified in three different types of nanocomposite; i.e., conventional composites, intercalated nanocomposite and exfoliated nanocomposite as shown in Figure 2.14. [22]

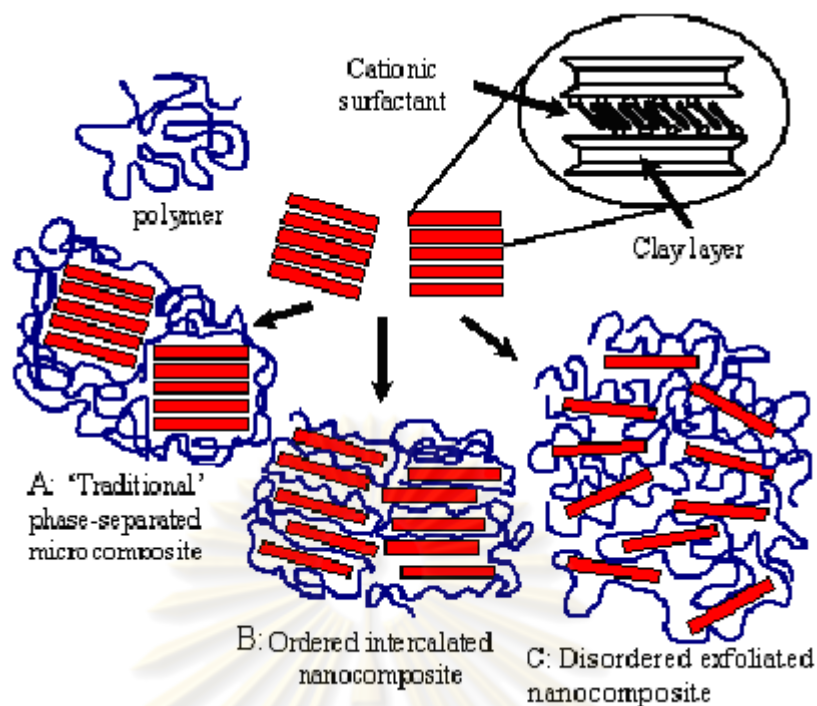


Figure 2.14: Illustration of the three different types of polymer/clay nanocomposites: (a) conventional composite, (b) intercalated nanocomposite, (c) exfoliated nanocomposite [23]

In a conventional composite the registry of the clay nanolayers is retained when mixed with the polymer. There is no intercalation of the polymer into the clay structure. Consequently, the clay fraction in conventional clay composites plays little or no functional role and acts mainly as a filling agent for economic considerations. Intercalated nanocomposites are formed when polymer chains are inserted into the clay galleries with fixed interlayer spacing. Exfoliated nanocomposites are formed when the silicate nanolayers are individually dispersed in the polymer matrix. The average distance between the segregated layers is dependent on the clay loading. Exfoliated nanocomposites show greater phase homogeneity than intercalated nanocomposites. More importantly, each nanolayer in an exfoliated nanocomposite contributes fully to interfacial interactions with the matrix. This structural distinction is the primary reason why the exfoliated clay state is especially effective in improving the reinforcement and other performance properties of clay composite materials. [22]

In general, polymer/clay nanocomposites can be prepared via in situ intercalative polymerization of monomers, polymer intercalation by the solution

method and melt intercalation. In situ polymerization involves the insertion of a suitable monomer into the clay galleries followed by polymerization. In the solution route, the organoclay and the polymer are dispersed in a polar organic solvent. Selection a proper solvent is the primary criterion to achieve the desired level of exfoliation of organoclay in the polymers. Solution intercalation method is not an effective way to prepare commercial nanocomposites because of high costs of solvent, which are also environmental unfriendly. Furthermore, a compatible polymer/clay solvent system is not always available. Melt intercalation is broadly applicable to many commodity and engineering polymers. Melt compounding is a flexible and commercial process capable of producing a variety of products on large volume scales. Moreover, the high shear environment of the melt extruder can assist the delamination or exfoliation of clay platelets. The disadvantage of melt intercalation is related to a low thermal stability of the onium modifiers. [19,24]

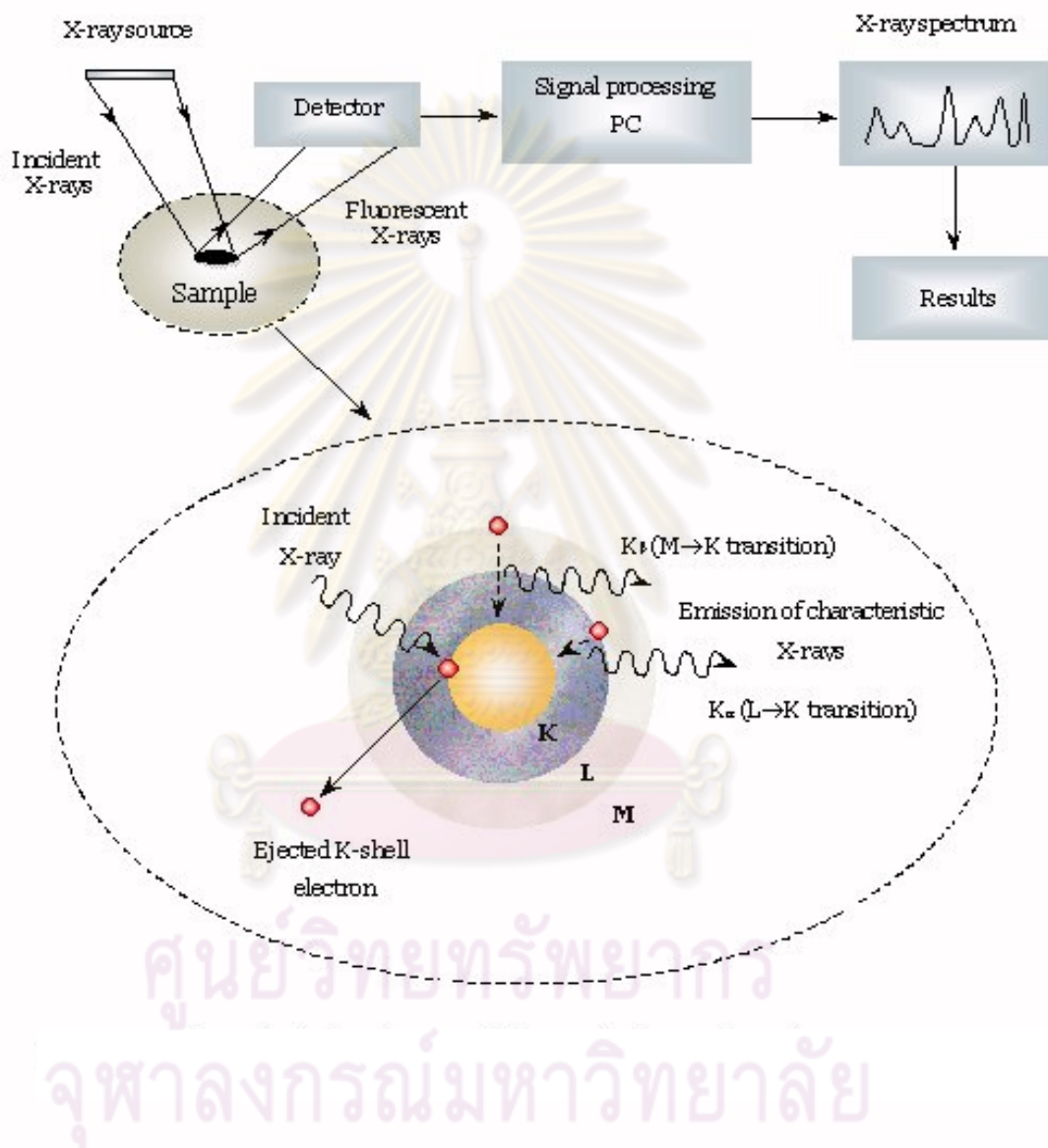
2.8 Polymer Characterizations

2.8.1 The composition of pristine clay

2.8.1.1 X-ray fluorescence (XRF)

XRF is a non-destructive analytical technique used to identify and determine the concentrations of elements present in solid, powdered and liquid samples. XRF is capable of measuring elements from Beryllium (Be) to Uranium (U) and beyond at trace levels and up to 100%. Additionally, X-rays are used to excite a sample and generate secondary X-rays. The X-rays broadcast into the sample by X-ray fluorescence spectrometers eject inner-shell electrons. Outer-shell electrons take the place of the ejected electrons and emit photons in the process. The wavelength of the photons depends on the energy difference between the outer-shell and inner-shell electron orbital. The amount of X-ray fluorescence is very sample dependent and quantitative analysis requires calibration with standards that are similar to the sample matrix. The solid samples used with X-ray fluorescence spectrometers are usually powdered and pressed into a wafer or fuse in a borate glass. The sample is then placed in the sample chamber of the XRF spectrometer, and irradiated with a primary X-ray

beam. The X-ray fluorescence is measured either in simultaneous or sequential modes, and is recorded with either an X-ray detector after wavelength dispersion or with an energy-dispersive detector. A typical XRF spectroscopy arrangement is shown in Figure 2.15 which includes a source of primary radiation (usually a radioisotope or an X-ray tube) and equipment for detecting the secondary X-rays.



2.8.2 Degree of clay dispersion

2.8.2.1 X-ray diffraction (XRD)

XRD is a technique used to determine the interlayer spacing of clay and organoclay, based on their characteristic diffraction behavior under X-ray irradiation of a known wavelength.

Diffraction can occur when electromagnetic radiation interacts with a periodic structure whose repeat distance is about the same as the wavelength of the radiation. Visible light, for example, can be diffracted by a grating that contains scribed lines spaced only a few thousand angstroms apart, about the wavelength of visible light. X-rays have wavelengths on the order of angstroms, in the range of typical interatomic distances in crystalline solids. Therefore, X-ray can be diffracted from the repeating patterns of atom that are characteristic of crystalline materials.

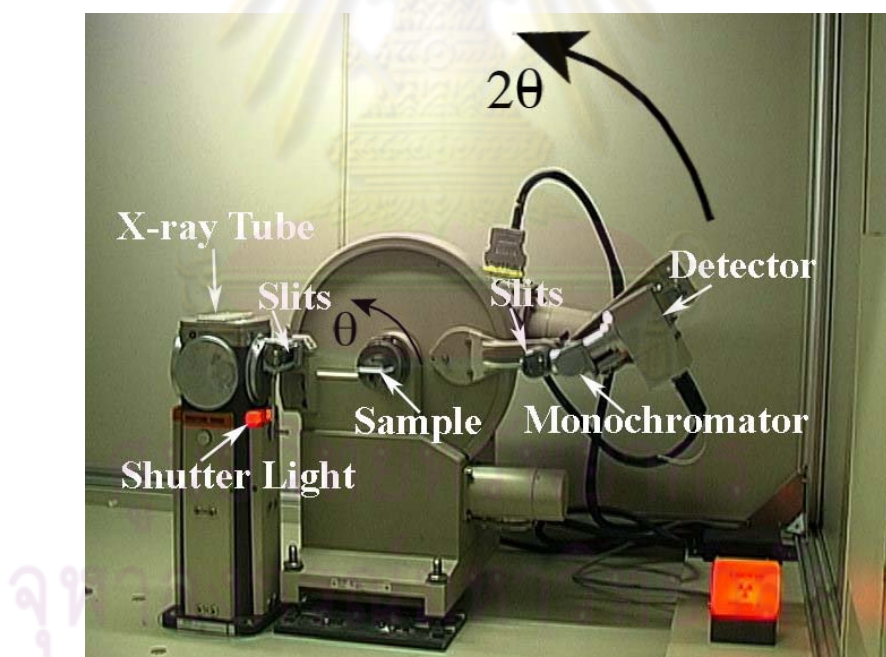


Figure 2.16: The composition of X-ray diffractometer [26]

The results from XRD analysis have been classified into three major types depending on the pattern of graph as shown in Figure 2.17.

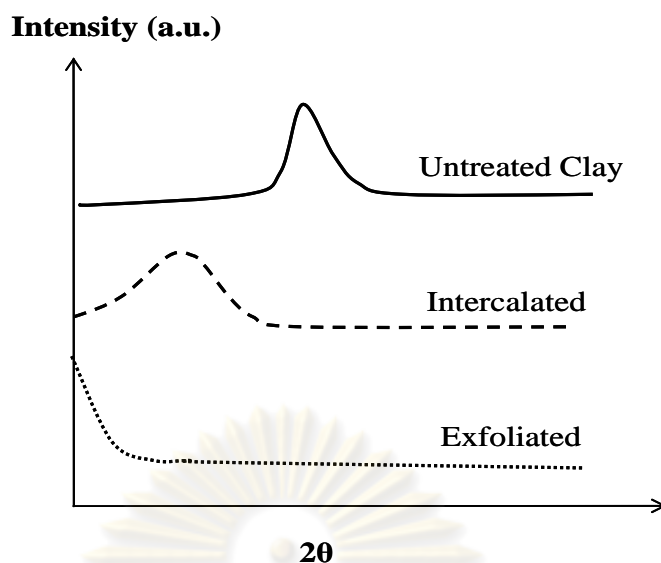


Figure 2.17: Diagram of X-ray diffraction analysis

As shown in Figure 2.17, the top line shows the diffraction curve of untreated clay. The organoclay, which is treated by ion exchange method with organic cation (surfactant) such as a quaternary ammonium ion, are mixed with polymer matrix in order to form nanocomposites. If the layered silicates of clay in polymer matrix are expanded but its layer still be in order, the diffraction curve is shown as a middle line in Figure 2.17. This curve shows a peak, which is shifted to a lower angle. If the silicate layers of clay in polymer matrix are delaminated as an individual layer and distributed randomly in the polymer matrix, the diffraction curve is shown as a bottom line in Figure 2.17. There is no peak appeared in this curve.

The interlayer spacing of clay and organoclay (or degree of clay dispersion) is calculated by the Bragg's equation. Bragg's law is derived by physicists W.H. Bragg and his son. It was determined the spacing between the planes in the atomic lattice by the following equation:

$$n\lambda = 2d \sin \theta$$

- Where:
- n = Peaks correspond to the {001} basal reflection ($n=1$)
 - λ = The wavelength of the X-ray radiation used in the diffraction experiment (angstroms), which equals to 1.542 \AA when $\text{CuK}\alpha$ was used.

- d = The spacing between the planes in the atomic lattice (Å)
 θ = The angle between the incident ray and the scattering planes
(degrees)

2.8.3 Morphology characterization

2.8.3.1 Scanning electron microscope (SEM)

SEM is a type of electron microscope that creates various images by focusing a high energy beam of electrons onto the surface of a sample and detecting signals from the interaction of the incident electrons with the sample surface. The surface of the sample is sputter coated in a vacuum with an electrically conductive layer of gold. The coated dry sample is now placed in a vacuum so that the electron beam can move without interference. Electricity is passed through the wire and then focused by magnets onto the sample. When the electrons from the gun strike the surface coating of gold, electrons are reflected back off the specimen to a detector, this is transmitted to a television screen where the image is viewed and photographed. The SEM is used to examine biological materials (such as micro-organisms and cells), a variety of large molecules, metals and crystalline structures, and the characteristics of various surfaces.

2.8.4 The chemical reactivity between nanoclay and polyurethane

2.8.4.1 Fourier transform infrared spectroscopy (FTIR)

Attenuated total reflectance (ATR) techniques are well established in FTIR spectroscopy for the direct measurement of solid and liquid sample without sample preparation. ATR accessory operates by measuring the changes that occur in a totally internally reflected infrared beam when the beam comes into contact with a sample, as shown in Figure 2.18.

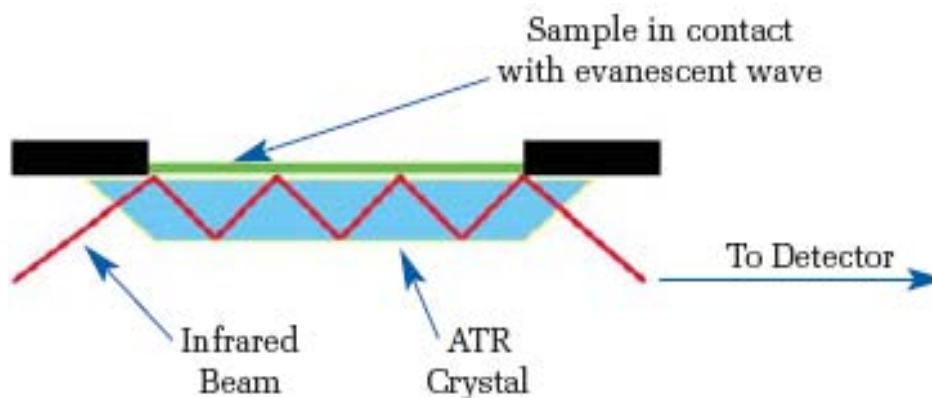


Figure 2.18: A multiple reflection ATR system [27]

An infrared beam is directed onto an optically dense crystal with a high refractive index at a certain angle. This internal reflectance creates an evanescent wave that extends beyond the surface of the crystal into the sample held in contact with the crystal. It can be easier to think of this evanescent wave as a bubble of infrared that sits on the surface of the crystal. This evanescent wave protrudes only a few microns ($0.5\ \mu\text{m} - 5\ \mu\text{m}$) beyond the crystal surface and into the sample. Consequently, there must be good contact between the sample and the crystal surface. In region of the infrared spectrum where the sample absorbs energy, the evanescent wave will be attenuated or altered. The attenuated energy from each evanescent wave is passed back to the IR beam, which then exits the opposite end of the crystal and is passed to the detector in the IR spectrometer. The system then generates an infrared spectrum. The infrared absorption band assignments of polyurethane foams are given in Table 2.4.

ศูนย์วิทยทรัพยากร
จุฬาลงกรณ์มหาวิทยาลัย

Table 2.4: Infrared absorption band assignments of polyurethane foams [28]

Frequency (cm ⁻¹)	Band assignment
3305-3361	-NH
2277	Isocyanate
1730	Free urethane
1715-1710	Soluble urea
1697-1695	Free urea
1661	Intermediate urea
1645-1640	H-bonded urea
1625-1655	Carbonyl
1710-1700	H-bonded urethane
1697	Soluble D-urea
1638	Associated D-urea
1595	Phenyl
1415	Isocyanurate
1220	Urethane (-C-O-)

2.8.5 Physical characterization

2.8.5.1 Apparent density

Apparent density test is obviously important to the performance and economics of foam because it measures how much of foam is air and how much is polymer. A carefully cut parallelepiped of foam is weighed and its dimension are measured. The weight to volume ratio is expressed in kg/m³. [10]

2.8.6 Mechanical characterizations

2.8.6.1 Hardness

Foam hardness has a major influence on the comfort factor of the furniture, bedding or automotive product in which, it is used. Therefore, it is important to know how much force is required to give a particular deflection or how much weight it can support. Hardness test was performed according to JIS K6301 with Auto Urethane H/N Tester. It **measures the depth** of an indentation in the material created by a given force on a standardized presser foot. This depth is dependent on the hardness of the material, its viscoelastic properties, the shape of the presser foot, and the duration of the test. JIS K6301 Auto Urethane H/N Tester allows for a measurement of the initial hardness, or the indentation hardness after a given period of time. The basic test requires applying the force in a consistent manner, without shock measuring the hardness (depth of the indentation). If a timed hardness is desired, force is applied for the required time and then read.

2.8.6.2 Indentation force deflection (IFD)

Indentation force deflection test (IFD) consists of measuring the force necessary to produce designated indentation in the foam product, for example, 25 and 65% deflections. A large sample, measuring $40 \times 40 \times 10 \text{ cm}^3$, is compressed with a standard indenter smaller than the foam surface. IFD values are reported for 25 and 65% indentation or other indentation. There are also other values derived from IFD test, such as support factor and guide factor.

2.8.6.2.1 Support factor (Sag factor)

Support factor is the ratio of the 65% indentation force to the 25% indentation force deflection determined after 1 min of rest. Most specifications are based on the 25% IFD value of 10 cm. foam. The support factor thus indicates what 65% IFD value would be acceptable for a particular application. The 65% IFD measures the support region of the stress-strain curve. Seating foams with low support factors will usually bottom out and give inferior performance.

$$\text{Support factor (SF)} = (65\% \text{ IFD} / 25\% \text{ IFD})$$

2.8.6.2.2 Guide factor

Guide factor is the ratio of the 25% indentation force deflection to the density after a 1 min rest. Most specifications do not have a density requirement; therefore the product with the highest guide factor has the cost advantage but not necessarily the performance advantage.

$$\text{Guide factor} = (25\% \text{ IFD} / \text{density})$$

2.8.6.3 Constant deflection compression set

Constant deflection compression set test method consists of deflecting the foam specimen to a specified deflection, exposing it to specified conditions of time and temperature and measuring the change of the specimen after a specified recovery period. The result is the percentage thickness loss, expressed by reference to the original thickness, as follow:

$$C_t = [(t_0 - t_f) / t_0] \times 100$$

Where:

C_t = compression set expressed as percentage of the original thickness

t_0 = original thickness of test specimen

t_f = final thickness of test specimen

Constant deflection compression set is used to assess the ability of the cellular plastics to recover after prolonged compression. The greater the compression set value, the less is the elastic recovery of the material.

2.8.6.4 Resilience (ball rebound)

Resilience is the ratio of the energy imparted to a material, e.g. from an object striking it, to the energy returned to the object. To evaluate the resilience of cellular plastics, a ball rebound test is commonly used. The apparatus consist of a clear plastic tube with a series of calibrated circles inscribed on it to measure the rebound height.

The test consists of dropping a steel ball onto a foam sample and monitoring the height of rebound. The resilience value is the ratio of the rebound height to the original drop height, as seen below

$$\text{Resilience (\%)} = (\text{Rebound height} / \text{Original drop height}) \times 100$$

In generally, the higher resiliency, the more durable the foam will be with compression force.

2.8.7 Thermal characterization

2.8.7.1 Thermogravimetric analysis (TGA)

TGA is a type of testing that is performed on samples to determine changes in weight in relation to change in temperature. The analyzer usually consists of a high-precision balance with a pan loaded with the sample. The sample is placed in a small electrically heated oven with a thermocouple to accurately measure the temperature. The atmosphere may be purged with an inert gas to prevent oxidation or other undesired reactions. A computer is used to control the instrument. The percent weight loss of a test sample is recorded while the sample is being heated at a uniform rate in an appropriate environment. The loss in weight over specific temperature ranges provides an indication of the composition of the sample, including volatiles and inert filler, as well as indications of thermal stability. TGA is commonly employed in research and testing to determine characteristics of materials such as polymers, to determine degradation temperatures, absorbed moisture content of materials, the level of inorganic and organic components in materials, decomposition points of explosives, and solvent residues. It is also often used to estimate the corrosion kinetics in high temperature oxidation.

CHAPTER III

LITERATURE REVIEWS

Numerous researches have described various factors that influenced on the mechanical and thermal properties of thermoplastic polyurethane/clay nanocomposites and polyurethane/clay nanocomposite foams such as degree of clay dispersion, chemical structure of surfactant and organoclay loading. In this chapter, the literature reviews on both types of polyurethane/clay nanocomposites are summarized as follows.

3.1 Effect of preparation method

Several routes are developed to achieve a high degree of dispersion of the clay nanoplatelet that are, (i) in situ polymerization of monomers which were initially intercalated between layered silicates, (ii) melt intercalation and (iii) combination with a polymer solution. [24] Depending on method of preparation and the nature of the components used in research such as layered silicates, organic cation and polymer matrix, three main types of composites which are conventional composite, intercalated nanocomposite and exfoliated nanocomposite may be obtained. When the silicate layers are completely and uniformly dispersed in a continuous polymer matrix, an exfoliated or delaminated structure is obtained. The delaminated structure has outstanding advantages because it makes the entire surface of clay layers available for the polymer and maximizes polymer/clay interactions. In addition the interfacial bonding between the polymer matrix and the reinforcing materials will be dramatically increased. [19,29]

3.2 Effect of chemical structure of surfactant

The interaction of quaternary alkyl ammonium cations with clay is affected by the size and structure of the alkyl group, the clay types, solution conditions and the nature of the exchange cation. The longer chain length of the alkyl group in the ammonium ion produces better hydrophobicity and generates better compatibility between the hydrophobic polymer and the hydrophilic negatively charged layered

silicates. [18,19] Therefore, proper selection of surfactant depends mainly on the type and polarity of polymer matrix used, i.e., a polar polymer such as nylon 6 (PA-6), exhibits a higher level of exfoliation with an organoclay based on a surfactant with one alkyl tail, while nanocomposites made from non-polar polymers, such as polypropylene, polyethylene, and various copolymers show completely opposite trends. [19] Chavarria et al. (2006) investigated the effect of chemical structure of surfactant on the morphology and mechanical properties of thermoplastic polyurethane nanocomposites prepared by melt processing. The chemical structures of the alkyl ammonium surfactants used to form the organoclay are shown in Figure 3.1.

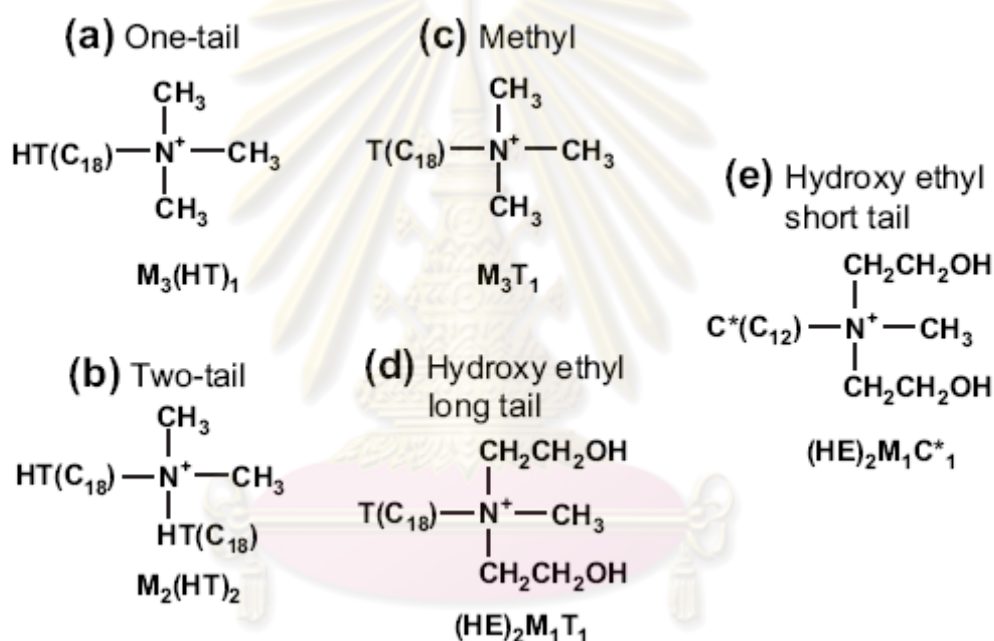


Figure 3.1: Molecular structure of the amine used to form organoclay [30]

They reported that the alkylammonium compound consisting of one alkyl tail is more effective than that having two alkyl tails in forming exfoliated nanocomposites, hydroxyl ethyl groups on the amine rather than methyl groups, and a longer alkyl tail as opposed to a shorter one leads to higher clay dispersion and stiffness enhancement for thermoplastic polyurethane nanocomposites. Overall, the organoclay containing hydroxyl ethyl functional groups produce the best dispersion of organoclay particles and the highest matrix reinforcement, while the one containing two alkyl tails produces the poorest. [30] Furthermore, Rehab et al. (2005) demonstrated that modified

montmorillonite with different chemical structure and percentage of clay leads to various degree of the dispersion in the polymer matrix, which is related to mechanical properties of nanocomposites. [7] These results are similar to the one described using another structures in polyurethane nanocomposites which indicate that the improved mechanical strength depends on characteristics of the modifier. [6,8]

3.3 Effect of organoclay loading

There are many researches that focus on effect of organoclay loading on mechanical properties of composites. Xiong et al. (2004) presented that the tensile strength increased dramatically with increasing organoclay content and reached maximum strength at 5 wt% organoclay content. The strength value began to decrease when organoclay content is over 5 wt%. The reason is mainly attributed to the agglomeration of organoclay particles above critical content of clay. However the elongation at break of the nanocomposites decreased with increase of organoclay. In addition, when organoclay content is below 5 wt%, the elongation at break slightly decreases. This response is related to the interaction between the pure polyurethane and nanoclay and the dispersion of organoclay in the polyurethane matrix. [6] Furthermore numerous studies have shown that the addition of very low percentage of organoclay (3-5 wt%) leads to significant enhancement in many properties such as stiffness and strength [1,31], flame retardancy [2] and thermal stability.

3.4 Effect of soft segment and hard segment in polyurethane structure

Since polyurethane structure is composed of short, alternating polydisperse blocks of soft and hard segments. Therefore polyurethanes exhibit a broad range of physical, thermal and mechanical properties due to the available options in selecting the chemicals such as different kind of diols [7,32], molecular weights of the various components [33,34], and the ratios in which they are reacted. [35,36] These different factors result in different capability to improve properties of polyurethane/clay nanocomposites. Pattanayak et al. (2005) investigated the effect of polyether and polyester soft segments on clay exfoliation and on mechanical and thermal properties of the composite materials. The result showed that composite of polyesterpolyol shows

much better improvement in tensile properties and tear strength than its polyetherpolyol counterpart. The study also showed that hydrogen bonding has no effect on mechanical properties and clay particles showed no influence on hard segment hydrogen bonding. [32]

3.5 Effect of the clay-monomer mixing sequence on clay dispersion

Xia Cao et al. (2005) studied the effect of the clay-monomer mixing sequence on clay dispersion and preparation method of polyurethane/clay nanocomposite foams, 5 wt% organoclay (MMT-OH) was premixed with either polyol or isocyanate before adding the other monomer. [8]

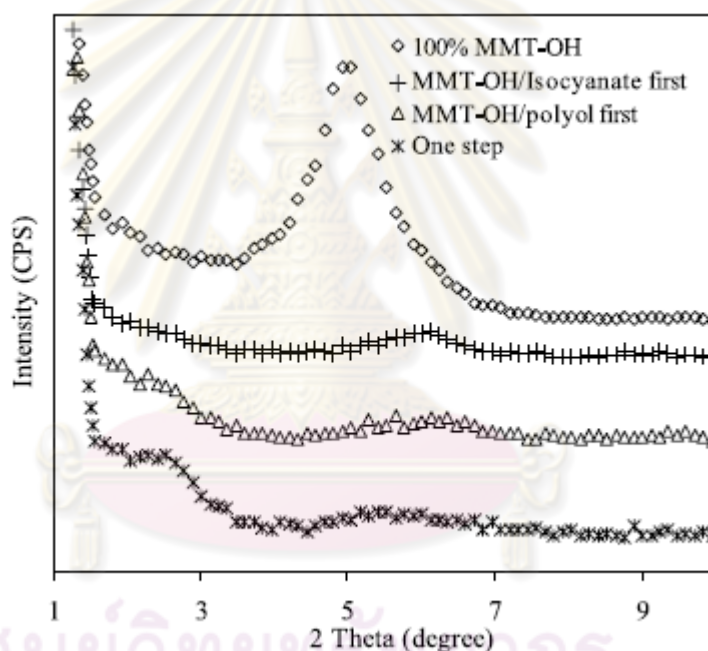


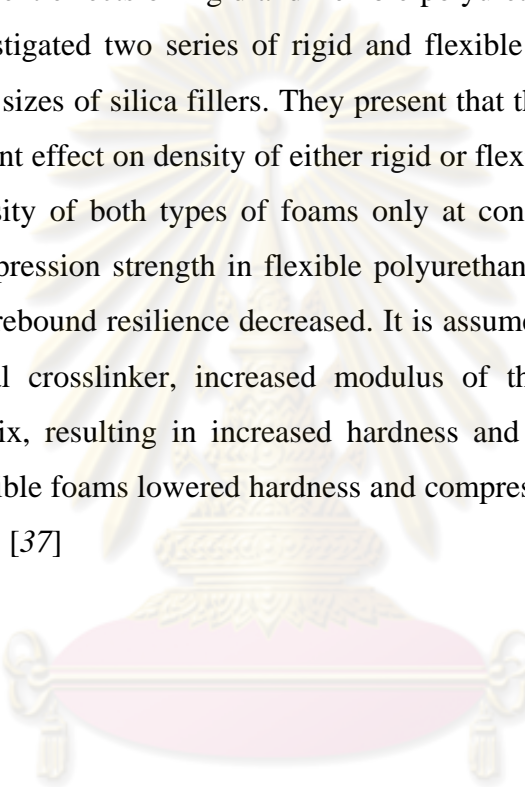
Figure 3.2: XRD of 5 wt% MMT-OH/PU nanocomposites prepared by different mixing procedures

As shown in Figure 3.2, it might be presumed that the nanocomposite prepared by two-step processes offered better clay dispersion than the one-step approach. A shoulder at $2\theta = 2.6^\circ$ on the XRD curve appeared when MMT-OH was premixed with polyol first. This shoulder completely disappeared when the clay was first mixed with isocyanate. This difference is a result of the reaction between the isocyanate monomers and the hydroxyl groups on alkyl chains of MMT-OH. Furthermore, the relative viscosity of the MMT-OH/isocyanate suspension is higher than that of the MMT-

OH/polyol suspension, and the presence of a catalyst further increases the viscosity. This provides further evidence of better clay dispersion in isocyanate because of the reaction between isocyanate and hydroxyl groups on the clay surface.

3.6 Effect of the filler sizes on polyurethane foam properties

Micro and nano silica fillers although of the same chemical origin, show considerably different effects on rigid and flexible polyurethane foam properties. Javni et al. (2002) investigated two series of rigid and flexible polyurethane foams which prepared with two sizes of silica fillers. They present that the micro silica filler did not show any significant effect on density of either rigid or flexible foams while nano silica increased the density of both types of foams only at concentration above 20%. The hardness and compression strength in flexible polyurethane foams with nano silica is increased and the rebound resilience decreased. It is assumed that the nano filler, as an additional physical crosslinker, increased modulus of the flexible segment in the polyurethane matrix, resulting in increased hardness and compression strength. The micro filler in flexible foams lowered hardness and compression strength, but increased rebound resilience. [37]



ศูนย์วิทยทรัพยากร
จุฬาลงกรณ์มหาวิทยาลัย

3.7 Effect of shape and chemical structure of nanoparticle on thermal and mechanical properties of polyurethane foam

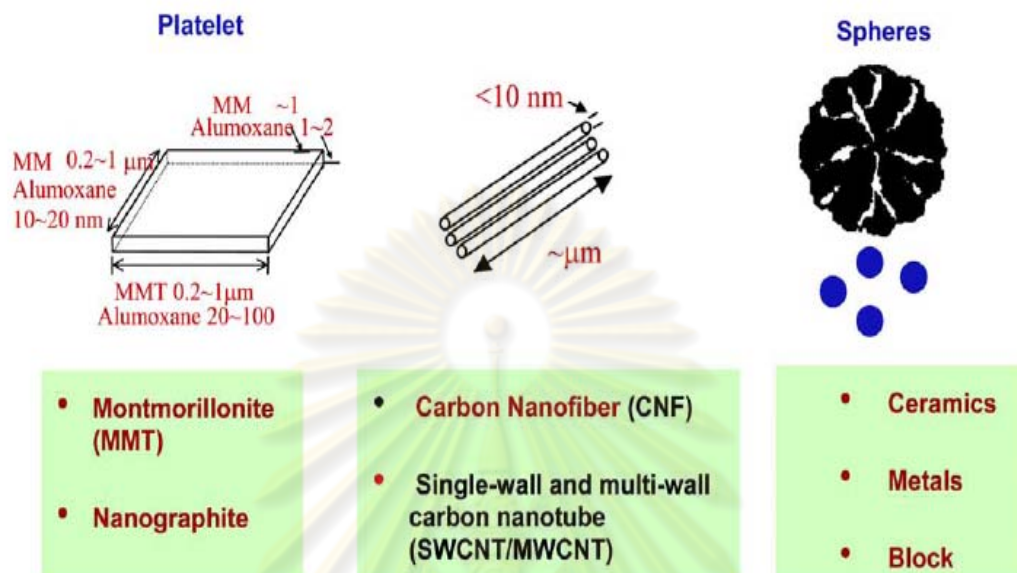


Figure 3.3: Different nanoparticle

Recently, the effects of different types of nanoparticle on thermal and mechanical performance of rigid polyurethane foam were investigated. Three different types of nanoparticle, namely spherical TiO_2 , platelet nanoclay, and rod-shape carbon nanofibers (CNFs) are considered. In all cases only 1 wt% nanoparticle is used. It is observed that CNFs infused polyurethane foam shows the highest and TiO_2 infused polyurethane foam shows the lowest enhancement in all the performed thermal and mechanical tests. This could be due higher interfacial stress transfer attributed by the higher aspect ratio of CNFs nanoparticle. [38]

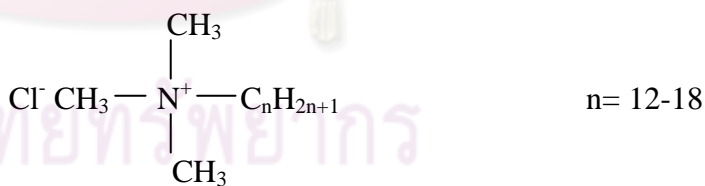
CHAPTER IV

EXPERIMENTS

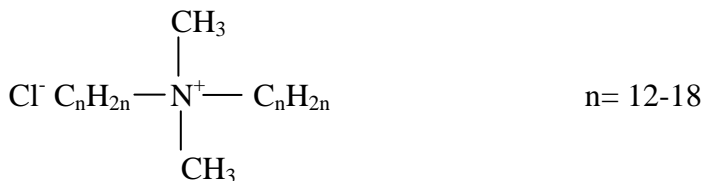
4.1 Materials

Isocyanate and polyol used in this work are kindly supported by BASF Polyurethanes (Thailand) Limited. Sodium bentonite (KUNIPIA-F), MMJ with cation exchange capacity (CEC) of 90 meq/100 g of clay was supplied by Kunimine Industrial Co., Ltd., Japan. Sodium bentonite (SAC), MMT with CEC of 60 meq/100 g of clay was provided by Thai Nippon Chemical Industry Co., Ltd., Thailand.

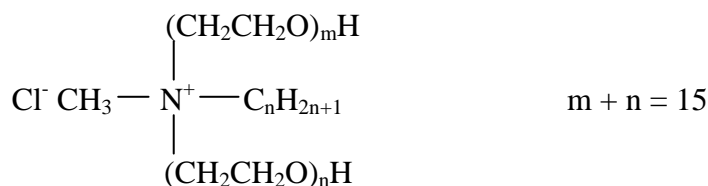
Surfactant that are used for ion-exchange reaction in this research are trimethyl tallow quaternary ammonium chloride (ARQUAD ®T-50) (MW = 347.5 g/mol and 50 %assay), dimethyl bis (hydrogenated-tallow) ammonium chloride (ARQUAD ®2HT-75) (MW = 585.5 g/mol and 75 %assay) and Octadecylmethyl [polyoxyethylene (15)] ammonium chloride (Ethoquad 18/25) (MW = 994 g/mol and 95 %assay). Their structures are shown in Figure 4.1. They are supplied by Akzo Nobel Co., Ltd., Thailand.



Trimethyl tallow quaternary ammonium chloride, (1T)



Dimethyl bis (hydrogenated-tallow) ammonium chloride, (2T)



Octadecylmethyl[polyoxyethylene (15)] ammonium chloride, (2TOH)

Figure 4.1: Molecular structure of amine salts

4.2 Preparation of Polyurethane/Clay Nanocomposite Foams

4.2.1 Determination of cation exchange capacity value of clay

Cation exchange capacity (CEC) is the capacity of the soil for ion exchange of cations such as calcium (Ca^{2+}), magnesium (Mg^{2+}), potassium (K^{1+}) and sodium (Na^{1+}) and the acidic cations, hydrogen (H^{1+}) and aluminum (Al^{3+}). The amount of these positively charged cations a soil can hold is described as the CEC and is expressed in milliequivalents per 100 grams (meq/100g) of soil. The larger this number, the more cations the soil can hold. The CEC value is determined by standard test method for methylene blue index of clay according to ASTM C 837-99. The procedures of this test method are shown as follows:

- 1) Weigh out 2.00 g of clay that has been dried in accordance with the procedure in test method C 324 and place in the 600 ml beaker.
- 2) Add 300 ml of distilled water to the beaker and stir with the mixer until the clay is uniformly dispersed.
- 3) Determine the pH of the slurry and add sufficient sulfuric acid to bring the pH within the range from 2.5 to 3.8. Continue stirring while the pH is being adjusted and continue stirring for 10 to 15 min after the last addition of acid.

- 4) Again test the slurry for pH, Adding additional acid if necessary to restore the pH to the 2.5 to 3.8 range.
- 5) With the slurry still under the mixer, fill the buret with the methylene blue solution add 5 ml of the solution to the slurry, and stir for 1 to 2 min.
- 6) Remove a drop of the slurry, using the dropper or the glass stirring rod, and place on the edge of the filter paper.
- 7) Observe the appearance of the drop on the filter paper. The end point is indicated by the formation of a light blue halo around the drop. Continue adding the methylene blue solution to the slurry in 1.0 ml increments with 1 to 2 min of stirring after each addition, then testing, until the end point is reached.
- 8) After the end point is reached, continue stirring for 2 min and retest.

NOTE: The methylene blue index was calculated using a multiple factor where the specimen size is 2.00 g and the methylene blue titrating solution is 0.01 N as follows:

$$MBI = \frac{0.01 \times V}{2} \times 100$$

Where:

MBI = methylene blue index for the clay in meq/100 g clay

V = milliliters of methylene blue solution required for the titration

4.2.2 Preparation of organoclay

The inorganic exchangeable cations can also be replaced with different organic cations by a simple ion exchange reaction. A variety of organic cations may be used in this regard to form organoclay which has organophilic property [13]. The procedures of modification of clay are shown as follows:

- 1) Add 400 g of sodium montmorillonite into a tank which contains 20 L of distilled water and stirred intensively for 3 hours until homogeneous phase was appeared. A tank is then heated up to 70°C.

- 1) Add trimethyl tallow quaternary ammonium chloride into another tank which contains 20 L of distilled water at 70°C and stirred intensively to dissolve it for about 10 minutes.
- 2) The solution of ammonium salt of trimethyl tallow quaternary ammonium chloride was poured into dispersed sodium montmorillonite and stirred vigorously at 70°C for 1 hour.
- 3) The solid part was filtered and washed with distilled water for several times.
- 4) The solid part was dried in an oven at 80°C for 3 to 4 days until it dries and then mortared and sieved respectively.
- 5) Step 1 to 5 was repeated with other surfactants.

NOTE: The weight of surfactant was calculated as follows:

$$g_{surf.} = \frac{CEC \times conc. \times Mw \times kg_{clay}}{\% assay}$$

Where:

- $g_{surf.}$ = Weight of surfactant ($g_{surf.}$)
- CEC = Cation exchange capacity of untreated clay (meq/ g_{clay})
- conc. = Concentration of surfactant (mmol_{surf.})
- Mw = Molecular weight of surfactant ($g_{surf.}/mol_{surf.}$)
- kg_{clay} = Weight of untreated clay (kg_{clay})
- % assay = Effectiveness of surfactant

The abbreviations of clay and organoclay samples were identified as shown in Table 4.1.

Table 4.1: The abbreviations of clay and organoclay samples

Clay formula	Abbrev.	Clay formula	Abbrev.
Thai clay	MMT	Japan clay	MMJ
MMT + 1T	MT1T	MMJ + 1T	MJ1T
MMT + 2T	MT2T	MMJ + 2T	MJ2T
MMT + 2TOH	MT2TOH	MMJ + 2TOH	MJ2TOH

4.2.3 Preparation of polyurethane/clay nanocomposite foams

Neat flexible polyurethane and polyurethane/clay nanocomposite foams were prepared via mould processing. The specifications of neat flexible polyurethane foams are shown in Table 4.2.

Table 4.2: Reaction test of neat flexible polyurethane foams system

Reaction of cushion	Polyol 648.38 g : Isocyanate 271.62 g
Density	50.00 kg/m ³
Water content	3.10 - 3.30 %
Viscosity	2,150 - 2,550 mPa
Temperature	21 °C

Part I: Effect of chemical structure of surfactant and the mixing sequence between nanoclay and monomer on properties of polyurethane/clay nanocomposite foams.

The density of all specimens was fixed at 50.00 kg/m³. The preparations of polyurethane/clay nanocomposite foams are shown as follows:

1) Premixed organoclay with polyol first

Organoclay 3% by weight of polyol is adding into polyol, the solution was mixed by an impeller at 2,000 rpm until the clay is uniformly dispersed. Using Mettler Toledo DL 38 Karl Fischer Titrator to determine the water content of slurry and add sufficient water to bring the water content within the range from 3.10 to 3.30 %.

Thereafter, the premixed polyol and isocyanate were placed on chill water to cool down the temperature until 21 ± 2 °C was reached. Then mixing them together for another 8 second. The mixer of all ingredients was mixed by an impeller at 1,500 rpm and it is poured into a preheated mould at 65°C. In a few minutes, foam appears at the mould ports. After a mould residence time of from 4 to 6 minutes, the mould is opened and then removed.

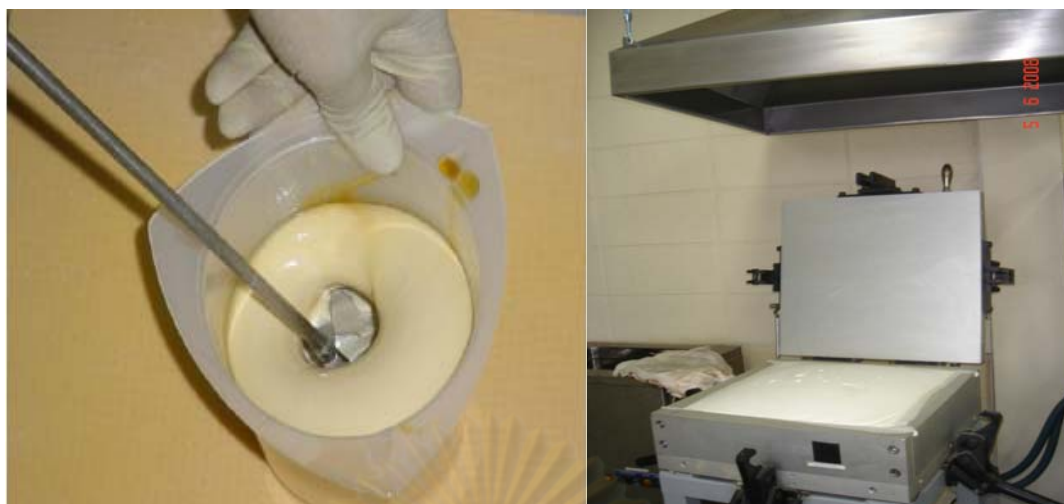
2) Premixed organoclay with isocyanate first

Organoclay 3% by weight of isocyanate is adding into isocyanate. Afterward, the solution was mixed by an impeller at 100 rpm until the clay is uniformly dispersed. Thereafter, the premixed isocyanate and polyol were placed on chill water to cool down the temperature until 21 ± 2 °C was reached. Then mixing them together for another 8 second. The mixer of all ingredients was mixed by an impeller at 1,500 rpm and it is poured into a preheated mould at 65°C. In a few minutes, foam appears at the mould ports. After a mould residence time of from 4 to 6 minutes, the mould is opened and then removed.

Furthermore, the preparation of nanocomposite with consists of the other types of surfactant, i.e., octadecyl methyl [polyethylene(15)] ammonium chloride, trimethyl tallow quaternary ammonium chloride and dimethyl bis (hydrogenated-tallow) ammonium chloride were repeated.

Part II: Effect of clay composition and organoclay loading on properties of polyurethane/clay nanocomposite foams.

After the appropriate surfactant and suitable route of polyurethane/clay nanocomposite foam synthesis from part I was selected. The organoclay which consists different ratios of organoclay (1, 3, 5, 7 and 10% by weight of organoclay loading) was repeated according to the method described above.



(a)

(b)

Figure 4.2: (a) Mixing of polyol and isocyanate (with or without nanoclay)
 (b) Flexible polyurethane mould foam processing

Table 4.3: The abbreviations of polyurethane/clay nanocomposite foams

Foam formula	Abbrev.
Neat PU	Neat PU
PU + 3% MTT (premixed with polyol)	PU_3%PMT
PU + 3% MT1T (premixed with polyol)	PU_3%PMT-1T
PU + 3% MT2T (premixed with polyol)	PU_3%PMT-2T
PU + 3% MT2TOH (premixed with polyol)	PU_3%PMT-2TOH
PU + 3% MTT (premixed with isocyanate)	PU_3%IMT
PU + 3% MT1T (premixed with isocyanate)	PU_3%IMT-1T
PU + 3% MT2T (premixed with isocyanate)	PU_3%IMT-2T
PU + 3% MT2TOH (premixed with isocyanate)	PU_3%IMT-2TOH
PU + 1% MT2TOH (premixed with isocyanate)	PU_1%IMT-2TOH
PU + 5% MT2TOH (premixed with isocyanate)	PU_5%IMT-2TOH
PU + 7% MT2TOH (premixed with isocyanate)	PU_7%IMT-2TOH
PU + 10% MT2TOH (premixed with isocyanate)	PU_10%IMT-2TOH
PU + 1% MJ2TOH (premixed with isocyanate)	PU_1%IMJ-2TOH
PU + 3% MJ2TOH (premixed with isocyanate)	PU_3%IMJ-2TOH
PU + 5% MJ2TOH (premixed with isocyanate)	PU_5%IMJ-2TOH
PU + 7% MJ2TOH (premixed with isocyanate)	PU_7%IMJ-2TOH
PU + 10% MJ2TOH (premixed with isocyanate)	PU_10%IMJ-2TOH

4.3 Specimen Characterizations

4.3.1 The composition of pristine clay

The composition of pristine clay powders were determined using X-ray fluorescence spectrometry (XRF). The results of this test method are shown in Table 5.1.



Figure 4.3: X-Ray fluorescence spectrometer

ศูนย์วิจัยทรัพยากร
จุฬาลงกรณ์มหาวิทยาลัย

4.3.2 Inorganic content in clay and organoclay

The inorganic content of pristine clay and organoclay was determined by weighing 2 g of sample in the ceramic crucibles and placing all crucibles into the furnace at 1000 °C for 4 hour to eliminate all organic material including the based polymer and surfactant. Thereafter, the remained ash in each crucible was weighed. The percentage of inorganic content was calculated from the weight loss. This test was repeated for 3 times for each sample.



Figure 4.4: Furnace

ศูนย์วิทยทรัพยากร
จุฬาลงกรณ์มหาวิทยาลัย

4.3.3 Degree of clay dispersion

The interlayer spacing of pristine clay, organoclay powders and polyurethane/clay nanocomposite foams were determined by X-ray diffraction on a D8 advance, BRUKER X-ray diffractometer using $\text{CuK}\alpha$ radiation (wavelength 1.542 Å) with voltage of 40kV and 30 mA. The interlayer spacing of each sample was determined by the Bragg's equation as shown in chapter 2.



Figure 4.5: X-ray diffractometer (D8 advance BRUKER German)

ศูนย์วิจัยทรัพยากร
จุฬาลงกรณ์มหาวิทยาลัย

4.3.4 Microscopic observation

The cellular morphologies and the degree of clay dispersion of the polyurethane/clay nanocomposite foams were investigated by a scanning electron microscope (SEM). Furthermore, SEM was applied to characterize the appearance of pristine clay. The SEM micrographs were taken after the foam samples were freeze-fractured in liquid nitrogen and the fracture surface was sputter-coated with thin film of gold with 300 Å in thickness. The accelerating voltage for the SEM was at 15 kV. In the current research, SEM (JEOL model JSM 5410LV) was used to characterize samples.



Figure 4.6: Scanning electron microscope (SEM)

ศูนย์วิจัยและพัฒนา
จุฬาลงกรณ์มหาวิทยาลัย

4.3.5 The chemical reactivity between nanoclay and polyurethane

Fourier transform infrared spectroscopy of polyurethane/clay nanocomposite foams were performed using a Spectrum GX FT-IR spectrometer from Perkin Elmer with an ATR accessory to determine the chemical bonding between the nanoclay and polyurethane. The micro domain structures of both neat and polyurethane/clay nanocomposite foams were also analyzed. The procedures of this test method are shown as follows:

- 1) Monitor the energy throughput with nothing in the beam. Check that the energy value is close to that obtained at the previous check. When the energy value falls to about three quarters of the original value the interferometer should be realigned. Use the realign function for instruments which realign automatically.
- 2) Record one scan of the background into the background memory area, then record one scan of the empty beam into one of the spectral memory areas. The result will be the total incident radiation line or 100% transmission of the spectrometer. Check that the noise level meets specification.
- 3) Record the background spectrum and check it for the presence of excessive water vapour. Check also the overall profile and the presence of any spurious bands or other unusual features.
- 4) Place the foam sample in a sample chamber, and then scan at a spectral range of 4,000 to 650 cm^{-1} with resolution of 4 cm^{-1} .



Figure 4.7: Fourier transform infrared spectrometer

4.3.6 Physical property

4.3.6.1 Apparent density

Foam density can be measured according to ASTM D 3574-05 (Test A). The density was calculated from the mass and volume of each specimen and is commonly measured in kilograms per cubic meter (kg/m^3)

$$\text{Density} = \frac{M}{V} \times 10^6$$

Where: M = mass of specimen, g

V = volume of specimen, mm^3



คุนยวทยทรพยากร
จุพาลงกรณ์มหาวิทยาลัย

4.3.7 Mechanical properties

4.3.7.1 Hardness

Hardness test was performed according to JIS K6301 using specimen with dimensions 50 mm length, 50 mm width and 25 mm in thickness. First, the initial thickness was measured. Afterward, the specimen was compressed downwards using a plate (100 mm in diameter) with a preload of 0.392 N. The specimen was compressed by 75% of its initial thickness at the speed of 50 mm/min. Then the load was removed immediately. Finally the specimen was compressed by 25% of its initial thickness at the speed of 50 mm/min. This condition was maintained and measured the load after 20 second later. The number of measurement was reported as the hardness (expressed in Newton). Only the averaged results from three tested specimens were reported.



Figure 4.8: Auto urethane H/N tester

4.3.7.2 Indentation force deflection (IFD)

The Indentation force deflection (IFD) test consists of measuring the force necessary to produce designated indentations in the foam product. The dimensions of each test specimen were 400 mm length, 400 mm width and 100 mm in thickness. The procedures were conducted according to ASTM D 3574 – 05 (Test B) by using a Universal Testing Machine (INSTRON Instrument, model 5567) and a flat circular indenter foot 203 mm in diameter with a preflex 4.5 N. The specimen was indented at 50 ± 5 mm/min 25% of specimen thickness and observes the force in kgf after 1 min. Without removing the specimen, the deflection was increased to 65% deflection, allowing the force to drift while maintaining the 65% deflection, and again observed the force in kgf after 1 min. Only the averaged results from three tested specimens were reported.



Figure 4.9: Indentation force deflection test

4.3.7.3 Constant deflection compression set

Constant deflection compression set was determined using compression set device, consisting of two flat plates so the plates are held parallel to each other by bolts or clamps and the space between the plates is adjustable to the required deflection thickness by means of spacers according to ASTM D 3574-05 (Test D). The dimensions of each test specimen were 50 mm length, 50 mm width and 25 mm in thickness. All specimens were placed in the two parallel plates and defect it to $50\pm 1\%$ of its thickness. Afterward, place the deflected specimens in the mechanically convected air oven at 70 ± 2 °C and 0% relative humidity for a period of 22 hours. Finally, remove the specimens immediately from the apparatus and measure the final thickness. Only the averaged results from three tested specimens were reported.



Figure 4.10: Constant deflection compression set test

4.3.7.4 Resilience (ball rebound)

Resilience or ball rebound was measured by dropping a steel ball on a foam specimen. The dimensions of each test specimen were 100 mm length, 100 mm width and 50 mm in thickness. This test method defined under ASTM D 3574 – 05 (Test H). The ball rebound tester consists of a 40 ± 4 mm inner diameter vertical clear plastic tube which a 16.03 ± 0.2 mm diameter ball is released by a magnet. Mount the steel ball on the release mechanism then drop it and measuring the maximum height of the rebound. If the ball strikes the tube on the drop or rebound, the value obtained is invalid. In order to minimize parallax error, the circles on the tube in the region where the percent rebound is read must appear as lines. Make an additional four drops on the same specimen at the same location but only the averaged results from five tested specimens were reported.



Figure 4.11: Resilience (ball rebound) test

4.3.8 Thermal property

4.3.8.1 Degradation temperature

The thermal behavior of pristine clay, organoclay and polyurethane/clay nanocomposite foams in terms of the decomposition temperature (T_d) and the char yield were determined by using a thermogravimetric analyzer (TGA, TA instruments, SDT Q600) as shown in Figure 4.8. About 10 mg of each formulation of the pristine clay and organoclay powder and 4 mg of polyurethane/clay nanocomposite foams were heated from 30 °C to 1000 °C at a heating rate of 10 °C/min under nitrogen atmosphere. The gas flow rate of the purged nitrogen was 100 ml/min. The sample was progressively heated, the changes in the weight of the sample were recorded. The weight changes were associated with the volatilization or decomposition of components within the sample. The weight loss of each sample was measured as a function of temperature. The T_d ranges and the char of all samples in this work were recorded.



Figure 4.12: Thermogravimetric analyzer.

CHAPTER V

RESULTS AND DISCUSSION

The influences of chemical structure of surfactant, the synthesis routes of polyurethane/clay nanocomposite foams, clay types as well as organoclay loading were investigated by studying their mechanical, thermal and physical properties as presented in this chapter.

5.1 The Composition of Pristine Clay

The composition of two sources of clay was analyzed by X-ray fluorescence spectrometer and the results are shown in Table 5.1 as follow:

Table 5.1: The composition of two sources of clay

Analyte	Compound	MMT	MMJ
		Concentration (%)	Concentration (%)
Na	Na ₂ O	1.619	3.243
Mg	MgO	1.823	2.867
Al	Al ₂ O ₃	12.329	20.089
Si	SiO ₂	80.078	70.187
P	P ₂ O ₅	0.024	0.013
S	SO ₃	-	0.433
Cl	Cl	0.035	0.024
K	K ₂ O	0.688	0.092
Ca	CaO	2.006	0.757
Ti	TiO ₂	0.204	0.148
Mn	MnO ₂	0.023	0.026
Fe	Fe ₂ O ₃	1.138	2.107
Zn	ZnO	0.005	-
Sr	SrO	0.016	0.008
Zr	ZrO ₂	0.012	0.006

It is performed to know the chemical compositions of the minerals that are presented in the clay. The data given in table 5.1 shows that silica and alumina oxide are presented in major quantities while other minerals are presented in trace amounts. As a result, MMT clay has concentration of silica oxide about 80 % while MMJ clay has concentration of silica oxide about 70 %.

5.2 Inorganic Content in Pristine Clay and Organoclay

The inorganic content of pristine clay and organoclay was determined by weighing remained ash of sample after burned at 1000 °C for 4 hour. The percentage of inorganic content and concentration values were calculated as shown in table 5.2. The result shows that MMT clay had higher percentage of inorganic content than that of MMJ clay. This result was in agreement with the XRF result of these clays as reported in table 5.1. MMJ clay had cation exchange capacity of 90 meq/100 g of clay and MMT clay had cation exchange capacity of 60 meq/100 g of clay. Compare between MT1T and MJ1T, it was found that surfactant can penetrate and reside in layered silicates of MMJ clay than those of MMT clay. However, different percentages of inorganic content are shown in different types of surfactant due to different molecular weight as well as structure of surfactant. Using single tail surfactant (1T) was found to show the highest percentage of inorganic content according to the lowest molecular weight of surfactant and small structure of surfactant. Furthermore, the 1T surfactant shows only 50% effectiveness of surfactant which was less than the others resulted into the less concentration value of surfactant which can penetrate to layered silicate. The more polar structure such as hydroxyl group surfactant (2TOH) shows the least percentage of inorganic content due to the highest molecular weight of surfactant and 95% effectiveness of surfactant which is the highest among the others. The calculation method of concentration value, which was fixed at 1.0 for this research, was found the error on some organoclay. A possible explanation is that the error during the investigation such as washing process and pre-mixing process might be occurred. The calculation of concentration value in table 5.2 was shown in appendix B.

Table 5.2: Percentage of inorganic content of clay and organoclay

Sample	Percentage of inorganic content (wt%)	Concentration value (mmol _{sur} /g _{clay})
MMT	91.86±0.23	-
MT1T	75.59±0.08	0.52
MT2T	67.45±4.60	0.77
MT2TOH	62.60±0.02	0.74
MMJ	90.19±0.30	-
MJ1T	65.67±0.04	0.60
MJ2T	55.84±0.02	0.88
MJ2TOH	50.06±0.08	0.85

5.3 Degree of Clay Dispersion

5.3.1 Effect of clay composition and chemical structure of surfactant on d-spacing of layered silicates

Figures 5.1 and 5.2 show the X-ray diffraction patterns of pristine clay and organoclay powder based on MMT clay and MMJ clay, respectively. Both types of clay were treated by different types of surfactant. The d-spacing and degree of clay dispersion were determined by calculated from 2θ position of first diffraction (001) peak which was determined by X-ray diffraction, using Bragg's equation. The pristine MMT clay shows a characteristic diffraction (001) peak at $2\theta = 7.21^\circ$ corresponding to a d-spacing of 1.22 nm. While the pristine MMJ clay shows a characteristic diffraction (001) peak at $2\theta = 7.28^\circ$ corresponding to a d-spacing of 1.21 nm. However, the diffraction (001) peak of the organoclay based on both types of clay which were treated by different types of surfactant was shifted toward lower angle compared to the pristine clay. It has been reported that the MT1T, MT2T and MT2TOH peaks were appeared at 3.89 , 2.66 and 2.50° corresponding to a d-spacing of 2.27, 3.31 and 3.52 nm respectively, followed the same trend as in organoclay based on MMJ clay. It has been reported that the MJ1T, MJ2T and MJ2TOH peaks were appeared at 4.24 , 2.83 and 2.58° corresponding to a d-spacing of 2.08, 3.12 and 3.42 nm respectively. These results indicated that the d-spacing of organoclay becomes larger than that of the

pristine clay because the surfactants had inserted in to the interlayer of layered silicates of clay which is consistent with previous studies [8]. The difference in d-spacing could be due to the different in actual surfactant concentration that penetrated between layered silicates. From table 5.2 it can be seen that, there is no significant change in surfactant concentration that was contained in MT2T and MT2TOH. Both of them had higher surfactant concentration than MT1T. This could make the interlayer spacing of MT2T and MT2TOH organoclay larger than that of MT1T organoclay. By the way, the organoclay which was treated by hydroxyl group surfactant (2TOH) shows the highest d-spacing of layered silicates due to the highest molecular weight of surfactant and has 95% effectiveness of surfactant which was highest than the others. These results were similar to organoclay based on MMJ. The results indicated that extend of d-spacing expansion is mainly dependent on the structure of surfactant and effectiveness of surfactant.

Figure 5.3 shows the X-ray diffraction patterns of organoclay powder based on the same type of surfactant (2TOH) comparing between two types of clay. MJ2TOH organoclay exhibited narrow peak with high intensity than MT2TOH. It can be seen that MT2TOH shows higher d-spacing than MJ2TOH because the pristine MMT clay had a characteristic diffraction (001) peak at lower angle compared to characteristic diffraction (001) peak of MMJ clay. MMT clay also has higher free silica content in clay composition than MMJ clay. Moreover, two different peaks of MJ2TOH and MT2TOH may be the results from different orientation of amine surfactant between layered silicates which are consistent with Limpanart's research. [39]

ศูนย์วิทยทรัพยากร
จุฬาลงกรณ์มหาวิทยาลัย

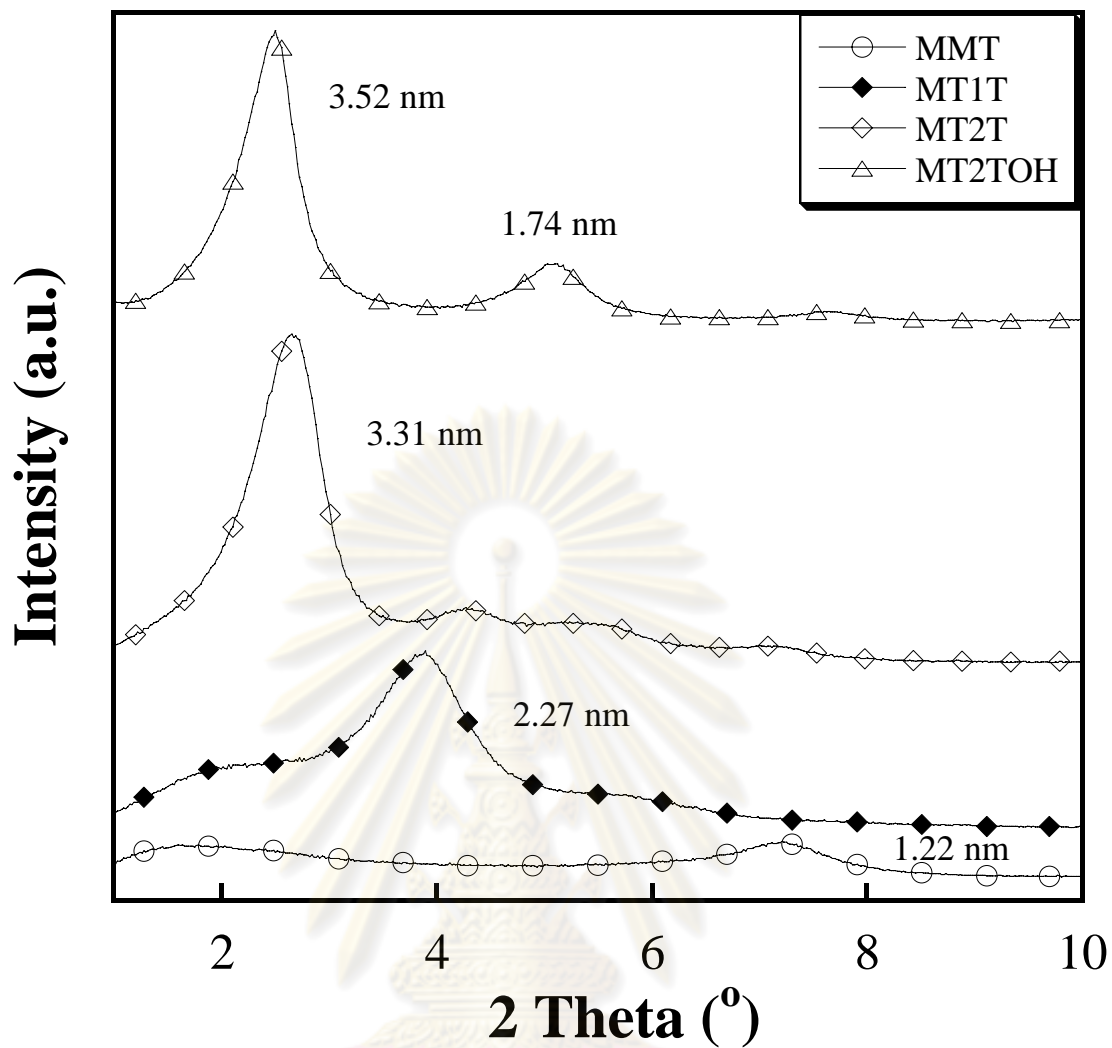


Figure 5.1: XRD patterns of pristine clay (MMT) and modified clay at $2\theta = 1-10^\circ$

ศูนย์วิทยทรัพยากร
จุฬาลงกรณ์มหาวิทยาลัย

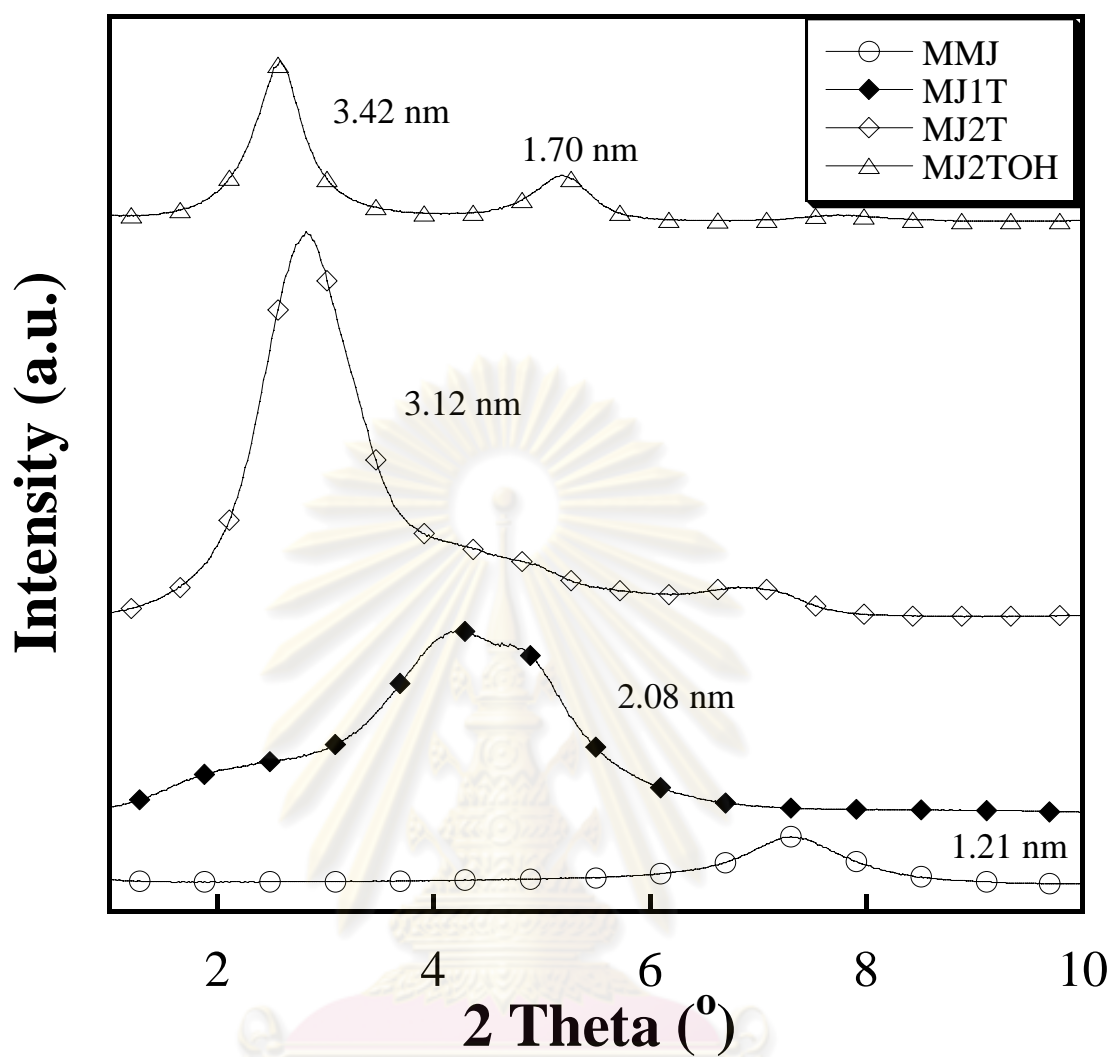


Figure 5.2: XRD patterns of pristine clay (MMJ) and modified clay at $2\theta = 1-10^\circ$

ศูนย์วิทยาศาสตร์
จุฬาลงกรณ์มหาวิทยาลัย

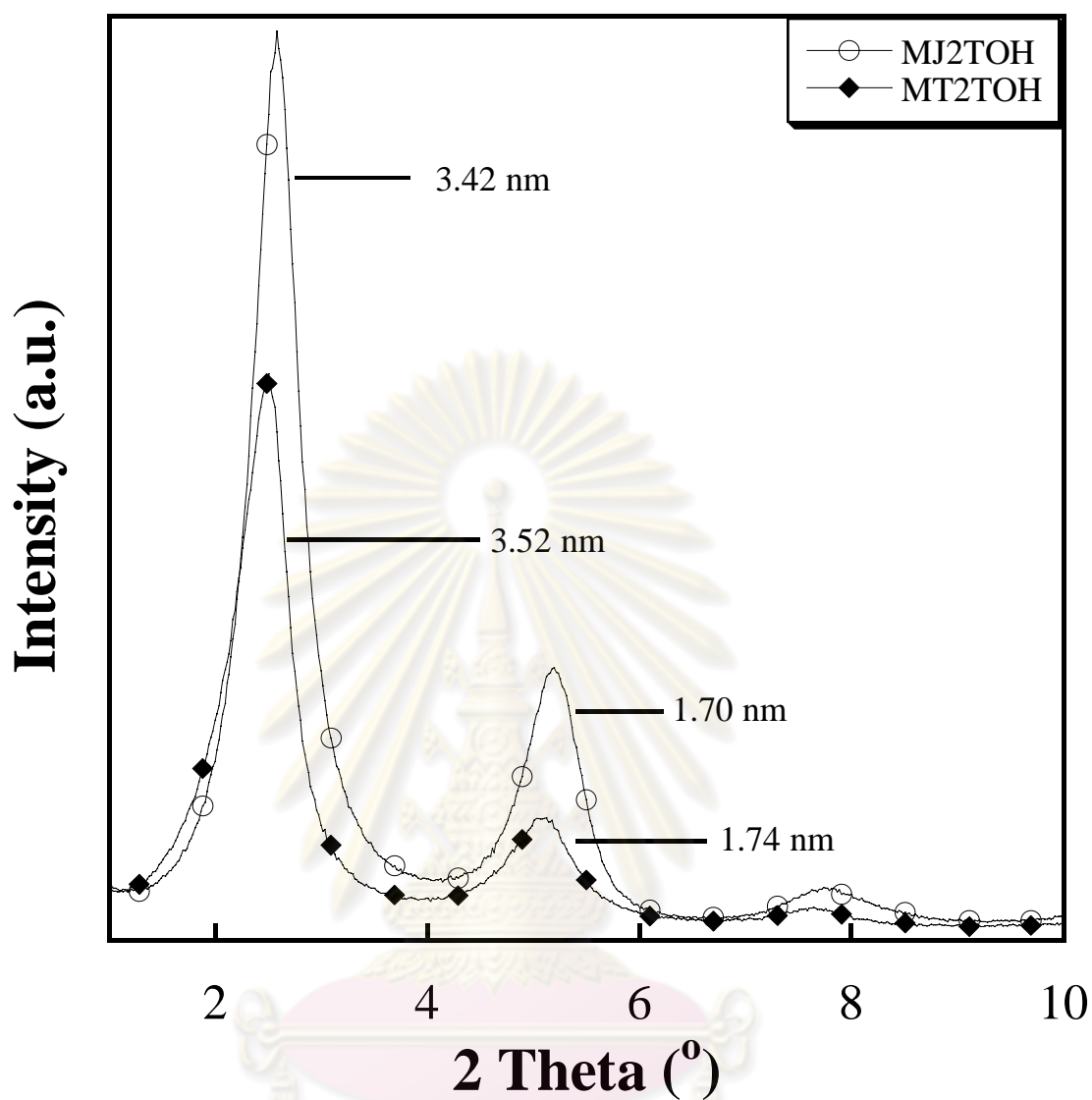


Figure 5.3: XRD patterns of modified clay, MJ2TOH and MT2TOH at $2\theta = 1-10^\circ$

ศูนย์วิจัยทรัพยากร
จุฬาลงกรณ์มหาวิทยาลัย

5.3.2 Effect of chemical structure of surfactant and mixing sequence between nanoclay and monomer on degree of clay dispersion

Flexible polyurethane/clay nanocomposite foams containing 3 wt% of organoclay was prepared via mould processing. The X-ray diffraction patterns of polyurethane/clay nanocomposite foams containing 3 wt% of organoclay, which were treated with different types of surfactant, at $2\theta = 1-10^\circ$ were shown in figure 5.4 and 5.5. To study the effect of mixing sequence on clay dispersion, figure 5.4 shows X-ray diffraction pattern in case of premixed 3 wt% of organoclay with polyol. The neat polyurethane foam exhibits an amorphous halo from $2\theta = 1-10^\circ$. However, the polyurethane/clay nanocomposite foams with different modifiers such as PU_3%PMT, PU_3%PMT-1T, PU_3%PMT-2T and PU_3%PMT-2TOH foams show characteristic diffraction peak at $2\theta = 2.45, 5.67, 1.42$ and 2.06° corresponding to a d-spacing of 3.60, 1.56, 6.23 and 4.27 nm, respectively. The results indicated that the polyurethane chain can intercalate into the layers of silicates as can be seen from the increasing of d-spacing of MMT for the nanocomposite foams premixed with polyol. The d-spacing of PU_3%PMT-2T becomes larger than that of the others, which resulted from the steric chain of the double tails surfactant. This suggests that the extent of gallery expansion is mainly dependent on the structure of the surfactant in the interlayer.

Figure 5.5 shows X-ray diffraction pattern in case of premixed 3 wt% of organoclay with isocyanate. The polyurethane/clay nanocomposite foams with different modifiers such as PU_3%IMT, PU_3%IMT-1T, PU_3%IMT-2T and PU_3%IMT-2TOH foams show characteristic diffraction peak at $5.97, 2.39, 2.15$ and 2.41° corresponding to a d-spacing of 1.48, 3.69, 4.11 and 3.66 nm, respectively. The results indicated that the polyurethane chain can intercalate into the layers of silicates as can be seen from the increasing of d-spacing of MMT for the nanocomposite foams premixed with isocyanate. The d-spacing of PU_3%IMT-2T becomes larger than that of the others, which results from the steric chain of the double tails surfactant. This suggests that the extent of gallery expansion is mainly dependent on the structure of the surfactant in the interlayer. Moreover, good dispersion of clay in the polyurethane matrix also exhibited through the modification of MMT with active surfactant

containing hydroxyl group. The presence of hydroxyl group enhances intra-gallery polymerization, which in turn leads to better clay dispersion.

Figure 5.6 shows XRD patterns of polyurethane/clay nanocomposite foams compared between using 3 wt% of modified clay premixed with isocyanate, PU_3%IMT-2TOH and 3 wt% of modified clay premixed with polyol, PU_3%PMT-2TOH at $2\theta = 1-10^\circ$. A shoulder at $2\theta = 5.6^\circ$ on the curve appeared when premixed 3 wt% of organoclay with polyol first. This shoulder completely disappeared when 3 wt% of organoclay was first premixed with isocyanate. This difference is a result of the reaction between the isocyanate monomers and the hydroxyl groups on alkyl chains of MT2TOH. This caused an increase of gallery spacing of clay to facilitate clay dispersion which is consistent with Cao's research. [8]

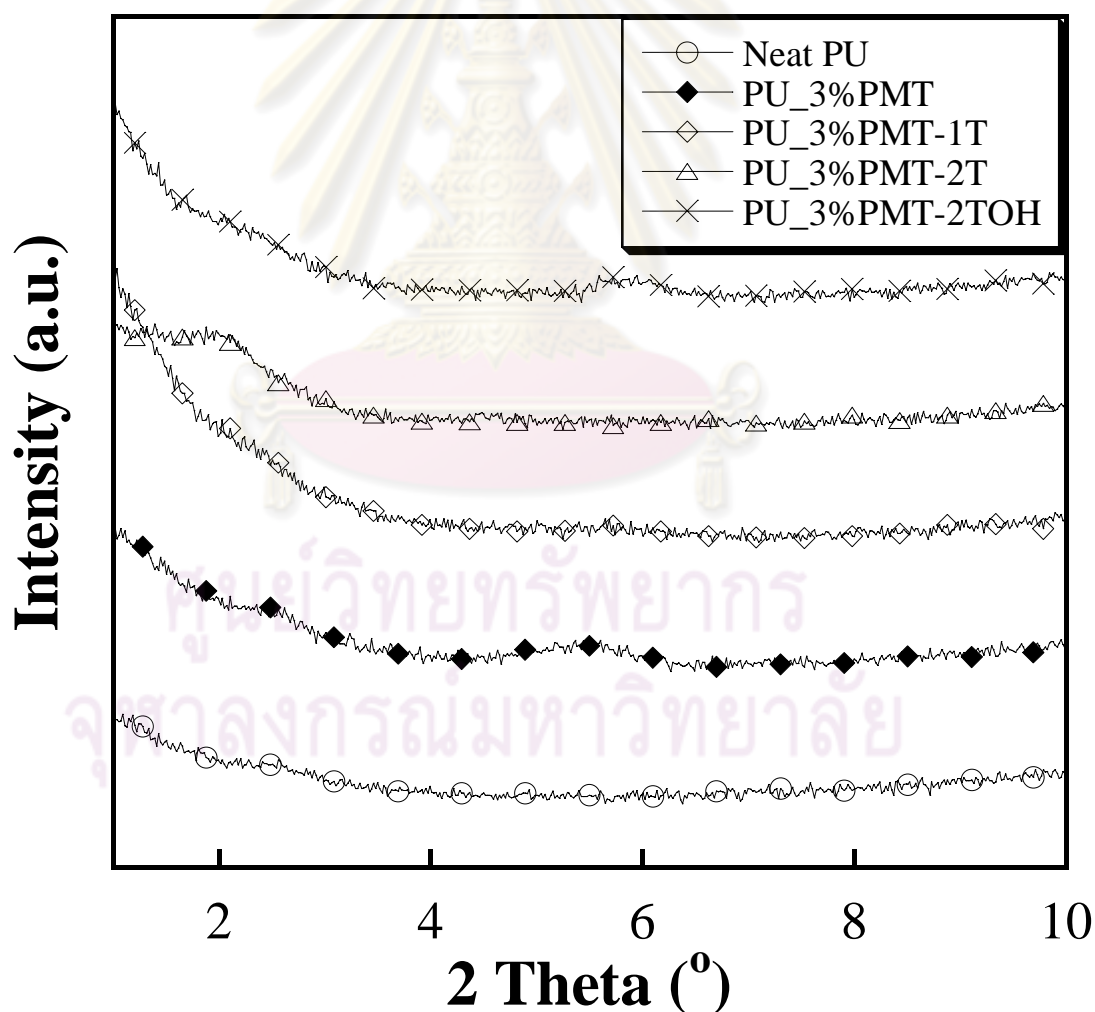


Figure 5.4: XRD patterns of polyurethane/clay nanocomposite foams by using 3 wt% of modified clay premixed with polyol at $2\theta = 1-10^\circ$

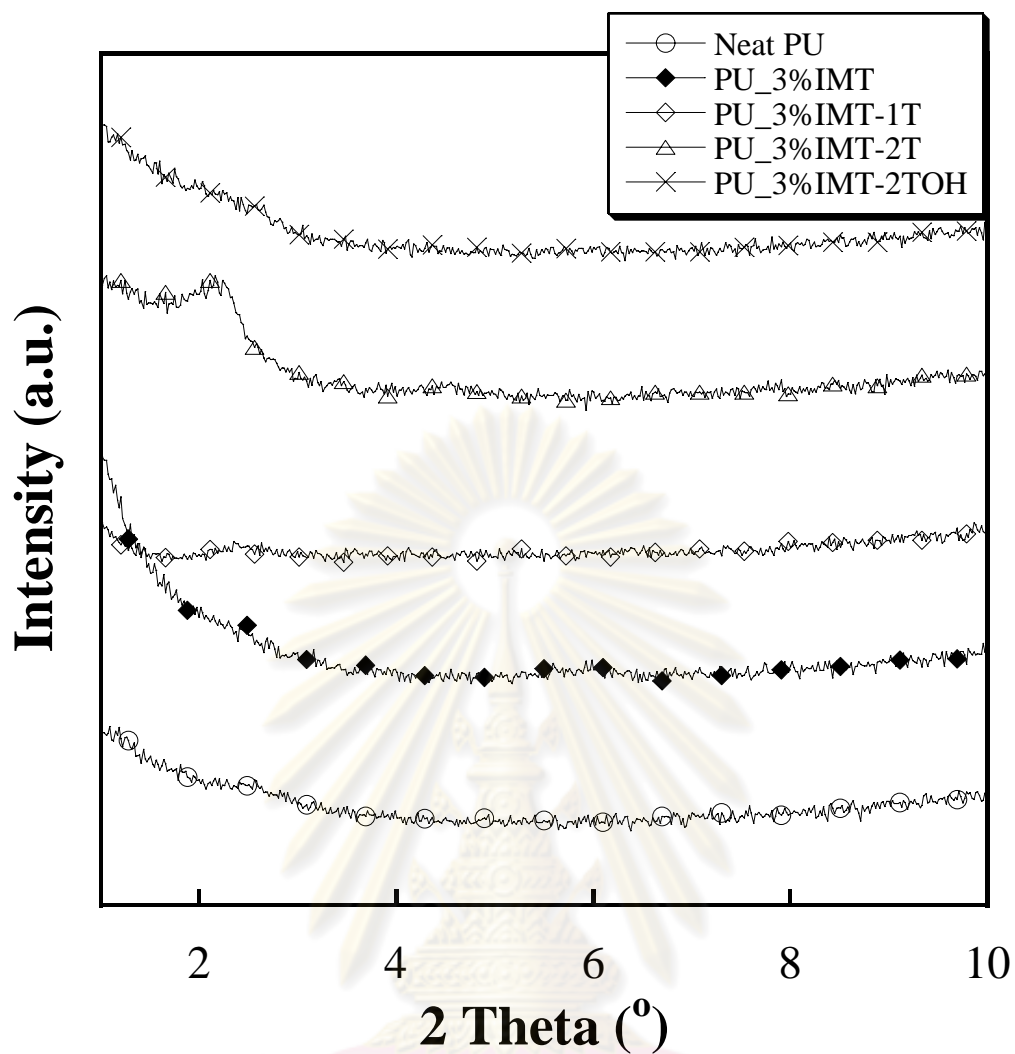


Figure 5.5: XRD patterns of polyurethane/clay nanocomposite foams by using 3 wt% of modified clay premixed with isocyanate at $2\theta = 1-10^\circ$

ศูนย์วิทยทรัพยากร
จุฬาลงกรณ์มหาวิทยาลัย

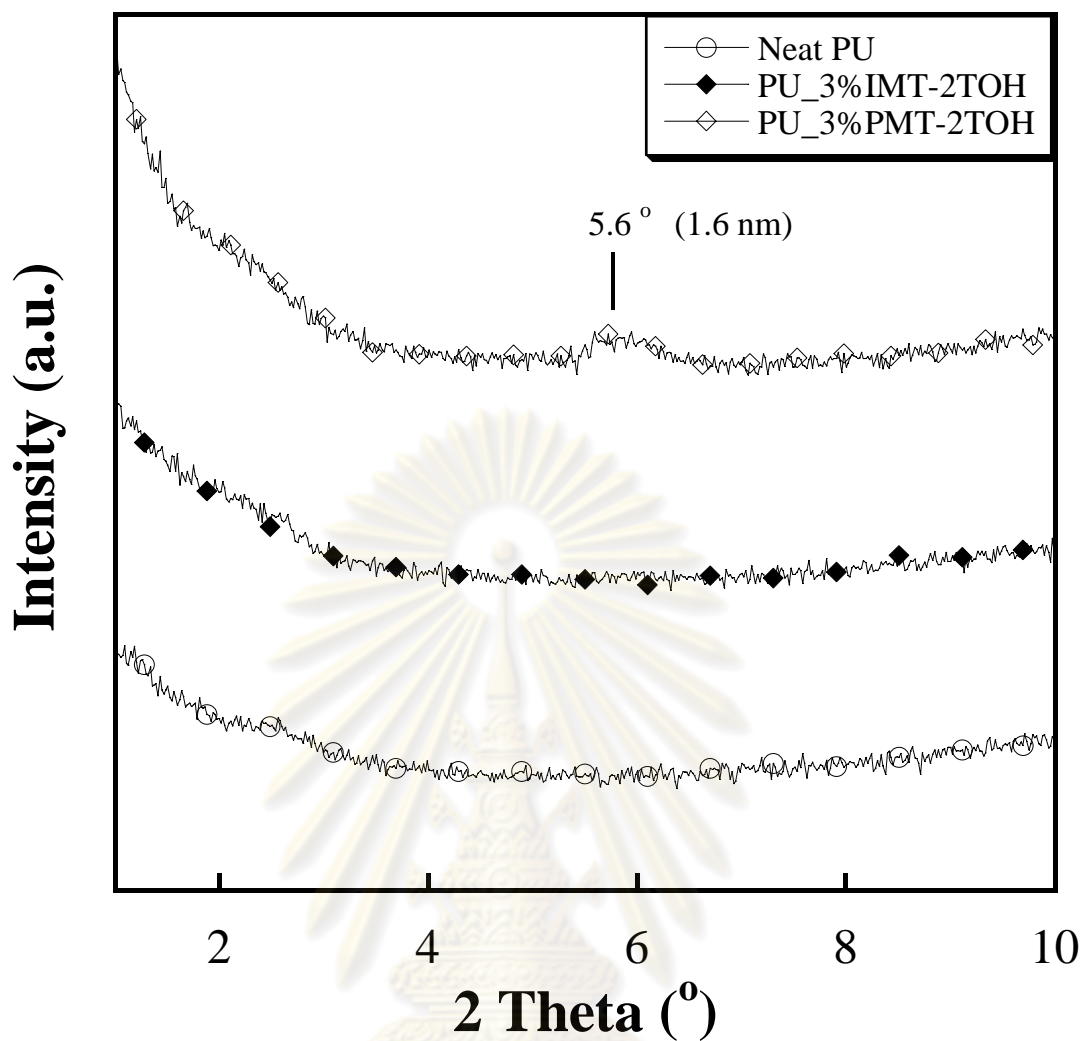


Figure 5.6: XRD patterns of polyurethane/clay nanocomposite foams compared between using 3 wt% of modified clay premixed with isocyanate, PU_3%IMT-2TOH and 3 wt% of modified clay premixed with polyol, PU_3%PMT-2TOH at $2\theta = 1-10^\circ$

จุฬาลงกรณ์มหาวิทยาลัย

5.3.3 Effect of clay composition and organoclay loading on degree of clay dispersion

The X-ray diffraction patterns of polyurethane/clay nanocomposite foams based on the same type of surfactant (2TOH) and using similar synthesis route comparing between two types of clay. It can be seen that PU_IMT-2TOH shows larger d-spacing than PU_IMJ2TOH because the pristine MMT clay had a characteristic diffraction (001) peak at lower angle compared to that of MMJ clay.

Figure 5.7 shows X-ray diffraction pattern of polyurethane/clay nanocomposite foams containing 0, 1, 3, 5, 7 and 10 wt% of MMT-2TOH modified clay premixed with isocyanate at $2\theta = 1-10^\circ$. The polyurethane/clay nanocomposite foams with different modifier such as PU_1%IMT-2TOH, PU_3%IMT-2TOH, PU_5%IMT-2TOH, PU_7%IMT-2TOH and PU_10%IMT-2TOH foams were observed at 1.87, 2.41, 1.91, 2.00 and 2.07° corresponding to an interlayer spacing of 4.72, 3.66, 4.61, 4.42 and 4.26 nm, respectively. The results did not show significant diffraction peak at 1, 3, 5, and 7 wt% of organoclay loading. These could identify that layered silicates in polyurethane foams had a good dispersion in range of 1-7 wt% of organoclay loading.

Figure 5.8 shows X-ray diffraction pattern of polyurethane/clay nanocomposite foams containing 0, 1, 3, 5, 7 and 10 wt% of MMJ-2TOH modified clay premixed with isocyanate at $2\theta = 1-10^\circ$. The polyurethane/clay nanocomposite foams such as PU_1%IMJ-2TOH, PU_3%IMJ-2TOH, PU_5%IMJ-2TOH, PU_7%IMJ-2TOH and PU_10%IMJ-2TOH foams were observed at 2.26, 2.20, 2.25, 2.25 and 2.24° corresponding to an interlayer spacing of 3.91, 4.00, 3.93, 3.93 and 3.95 nm, respectively. The results show that the diffraction intensity of MMJ-2TOH nanocomposite foams was gradually increased with increasing organoclay loading. The increase in diffraction intensity of XRD peak leads to high order of layered silicates that were dispersed into polyurethane matrix. This is evidence that good dispersion only worked at low clay content.

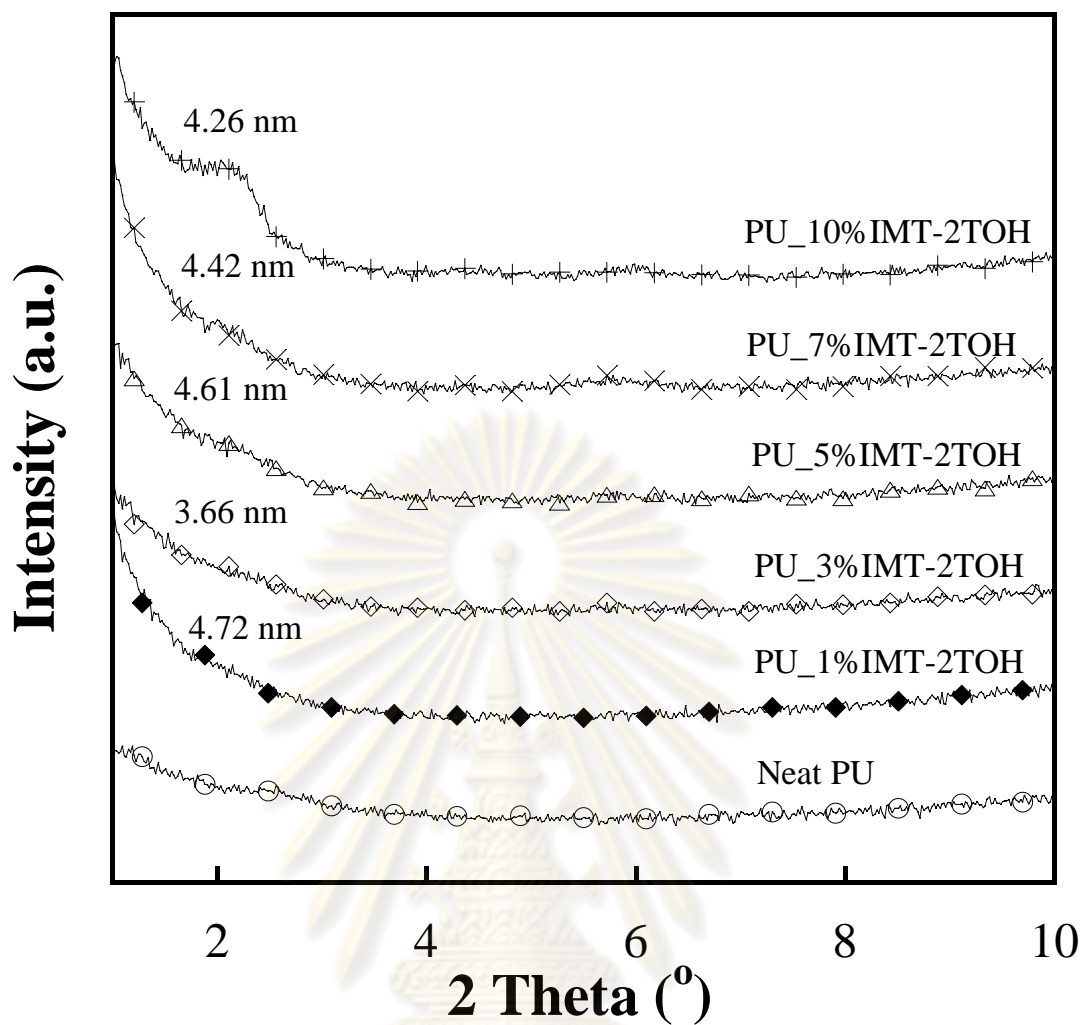


Figure 5.7: XRD patterns of polyurethane/clay nanocomposite foams containing 0, 1, 3, 5, 7 and 10 wt% of MMT-2TOH modified clay premixed with isocyanate at $2\theta = 1-10^\circ$

ศูนย์วิจัยทรัพยากร
จุฬาลงกรณ์มหาวิทยาลัย

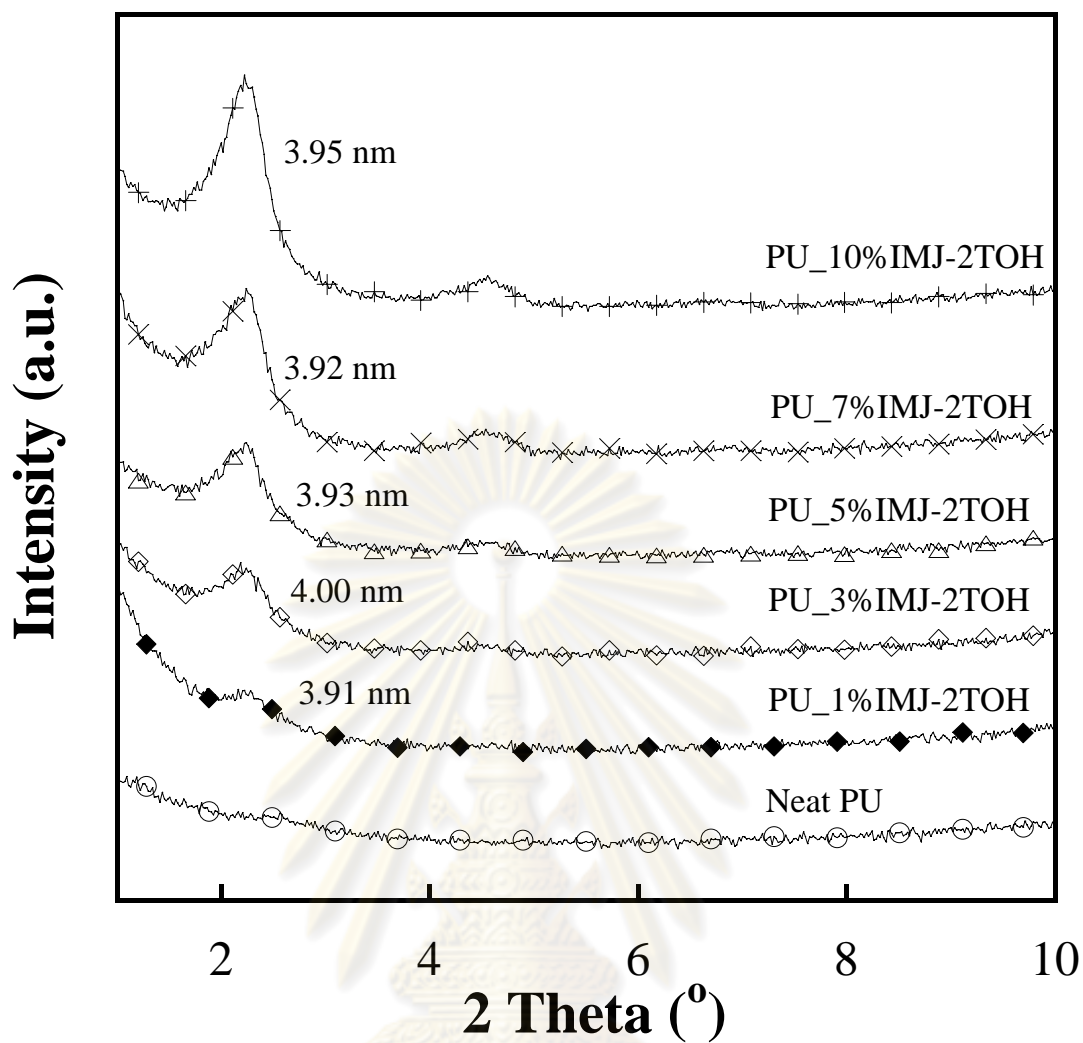


Figure 5.8: XRD patterns of polyurethane/clay nanocomposite foams containing 0, 1, 3, 5, 7 and 10 wt% of MMJ-2TOH modified clay premixed with isocyanate at $2\theta = 1-10^\circ$

ศูนย์วิทยทรัพยากร
จุฬาลงกรณ์มหาวิทยาลัย

5.4 Morphological Characterization

The cell structure of the flexible polyurethane foam was investigated by Scanning Electron Microscopy (SEM). The SEM micrographs of pristine clay are shown in figure 5.9. Due to the magnification of the SEM equipment; the detail of the individual clay platelet can not be seen. Furthermore, SEM micrographs of neat flexible polyurethane foam are shown in figure 5.10. The flexible polyurethane foam observed at 35X exhibits open-cell structure whose cell walls were broken and the structure consisted of mainly ribs. In addition, the effect of clay composition and organoclay loading on degree of clay dispersion of polyurethane/clay nanocomposite foams were characterized by SEM as shown in figure 5.11. It can be seen that polyurethane/clay nanocomposite foam based on MMJ clay had high degree of clay agglomeration that was caused by ultra fine size of MMJ clay. The agglomeration of nanoparticles is due to their high surface energy. As the size of nanoparticles is small, specific surface area is large and so as surface energy. Thus adhesive force between nanoparticles is strong and the particles easily agglomerate more than that of MMT clay. In high degree of clay agglomerated foams, poor properties were observed. Moreover, the agglomeration of nanoparticles was found to increase with increasing organoclay loading. These results are related with X-ray diffraction as mentioned above which can be suggested that good degree of clay dispersion only worked at low clay content.

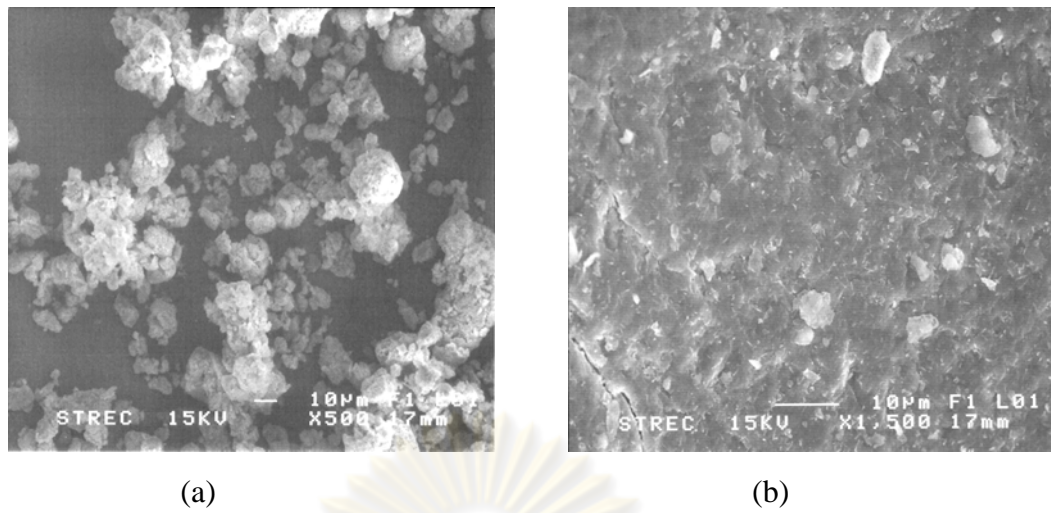


Figure 5.9: SEM micrographs of pristine clay (a) MMT, 500X (b) MMJ, 1500X

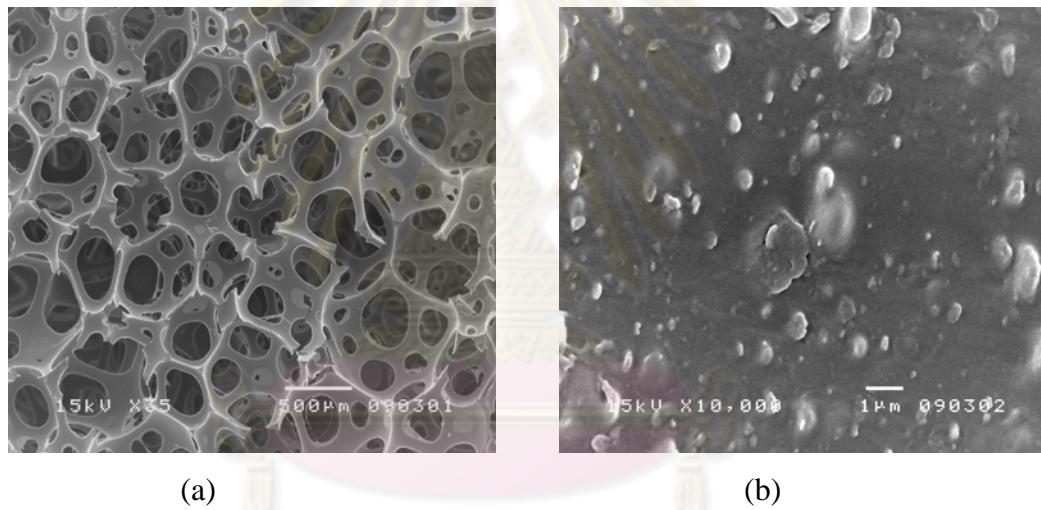


Figure 5.10: SEM micrographs of Neat PU foam (a) 35X (b) 10,000X

จุฬาลงกรณ์มหาวิทยาลัย

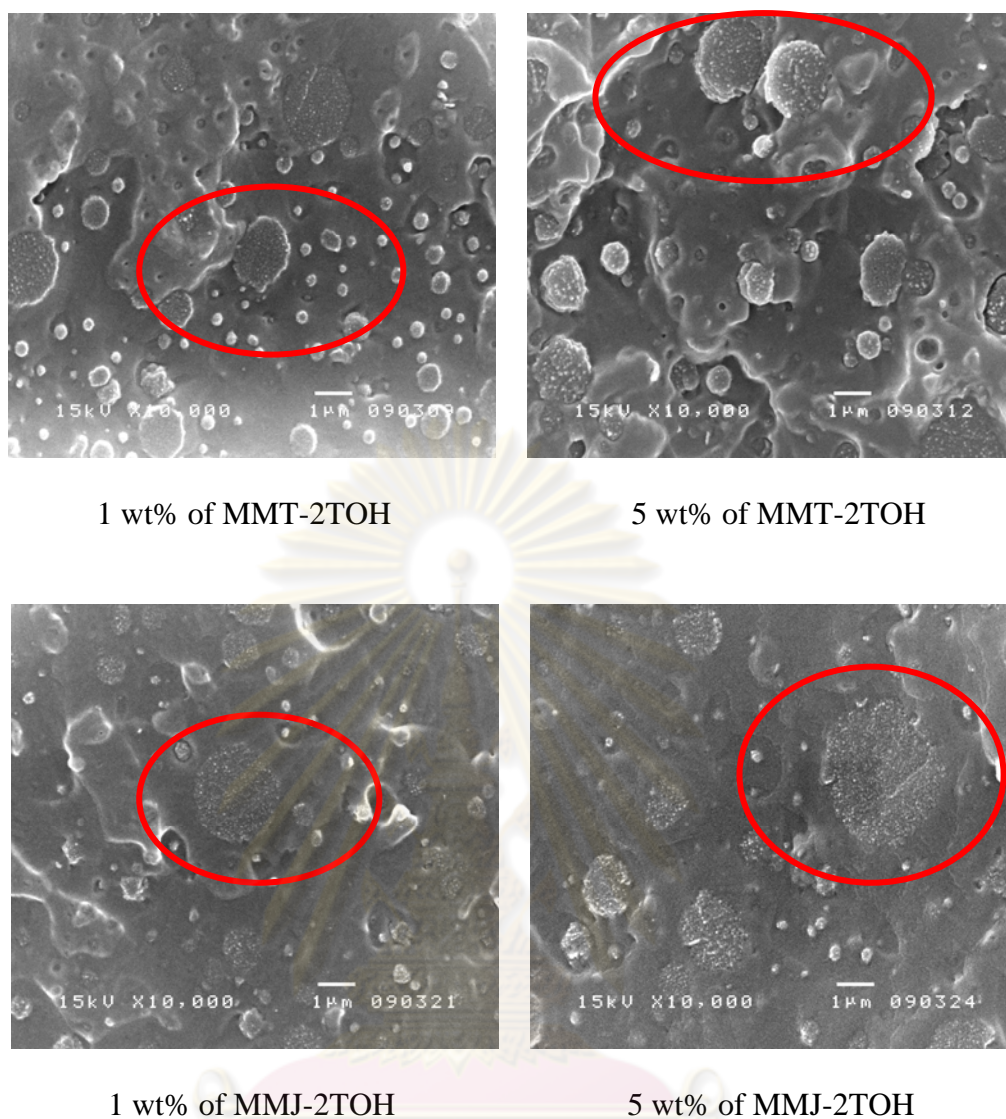


Figure 5.11: SEM micrographs of polyurethane/clay nanocomposite foams containing 1 and 5 wt% of MMT-2TOH and MMJ-2TOH modified clay premixed with isocyanate (10,000X)

5.5 The Chemical Reactivity between Nanoclay and Polyurethane

5.5.1 Effect of chemical structure of surfactant and mixing sequence between nanoclay and monomer

FTIR spectroscopy is a useful technique in identifying chemical species and functional groups of the polyurethane foam and determines the effect of chemical structure of surfactant and mixing sequence between nanoclay and monomer on hydrogen bond formation by the hard segments. The results of polyurethane/clay nanocomposite foams spectra are shown in Figure 5.13-5.16. Two main regions are of interest in this study, -NH absorption and -C=O stretching as depicted in figure 5.12. The possible functional groups acting as the proton acceptors in the hydrogen bonding with -NH (proton donor) are the urethane carbonyl (-C=O), the ether (-C-O-C) and the oxygen of the hydroxyl groups (-OH) on silicate layers. Figure 5.13-5.16, polyurethane/clay nanocomposite foams show the absence of -NCO peaks at 2270 cm^{-1} indicates completion of chain extension reaction. The -NH absorption peak at $\sim 3310\text{ cm}^{-1}$ was shown due to hydrogen-bonded -NH groups of urethane linkages. In this case, such hydrogen bonding can be formed with hard segment carbonyl and with soft segment ether linkages. The peak at $\sim 1707\text{-}1711\text{ cm}^{-1}$ is assigned to hydrogen bonded carbonyl (-C=O). This implies appreciable phase separation between hard and soft segment occurred and clay particles showed no influence on hard segment hydrogen bonding. [29] In addition, the peaks for hydrogen bond -NH group shifted from 3317 cm^{-1} in pristine polyurethane to slightly lower wave number in polyurethane/clay nanocomposite. This indicates that a majority of hydrogen bond -NH groups in these composites was associated with the ether linkages which are consistent with Pattanayak's research. [29]

Table 5.3 and table 5.4 show the ratio of areas under various characteristic peaks and the area under the -CH peak. It can be seen that the values of $A_{[\text{NH}]} / A_{[\text{CH}]}$ and $A_{[\text{CO}]} / A_{[\text{CH}]}$ have show no significant change in the present of clay particles, indicating that clay particles did not interfere with hydrogen bond formation by urethane -NH groups

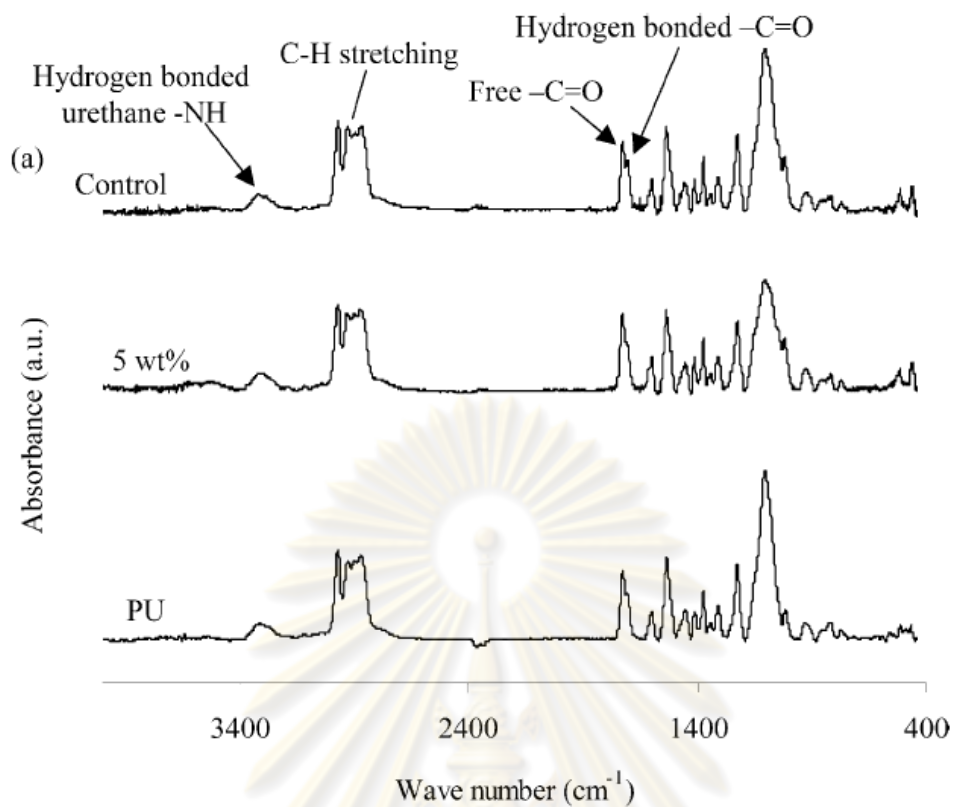


Figure 5.12: FTIR spectra of composites of polyether polyol [32]

ศูนย์วิทยทรัพยากร
จุฬาลงกรณ์มหาวิทยาลัย

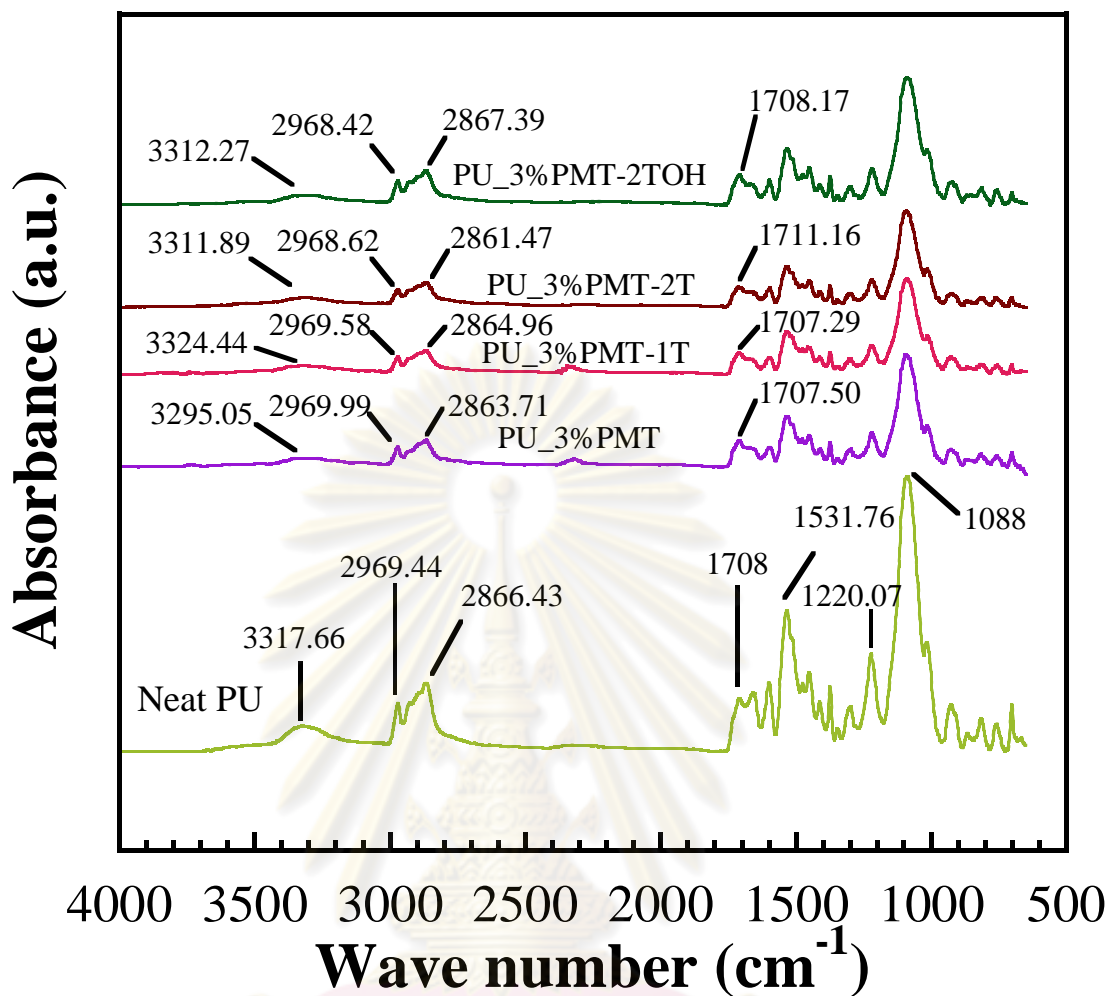


Figure 5.13: FT-IR spectra of polyurethane/clay nanocomposite foams by using 3 wt% of modified clay premixed with polyol

ศูนย์วิทยาศาสตร์
จุฬาลงกรณ์มหาวิทยาลัย

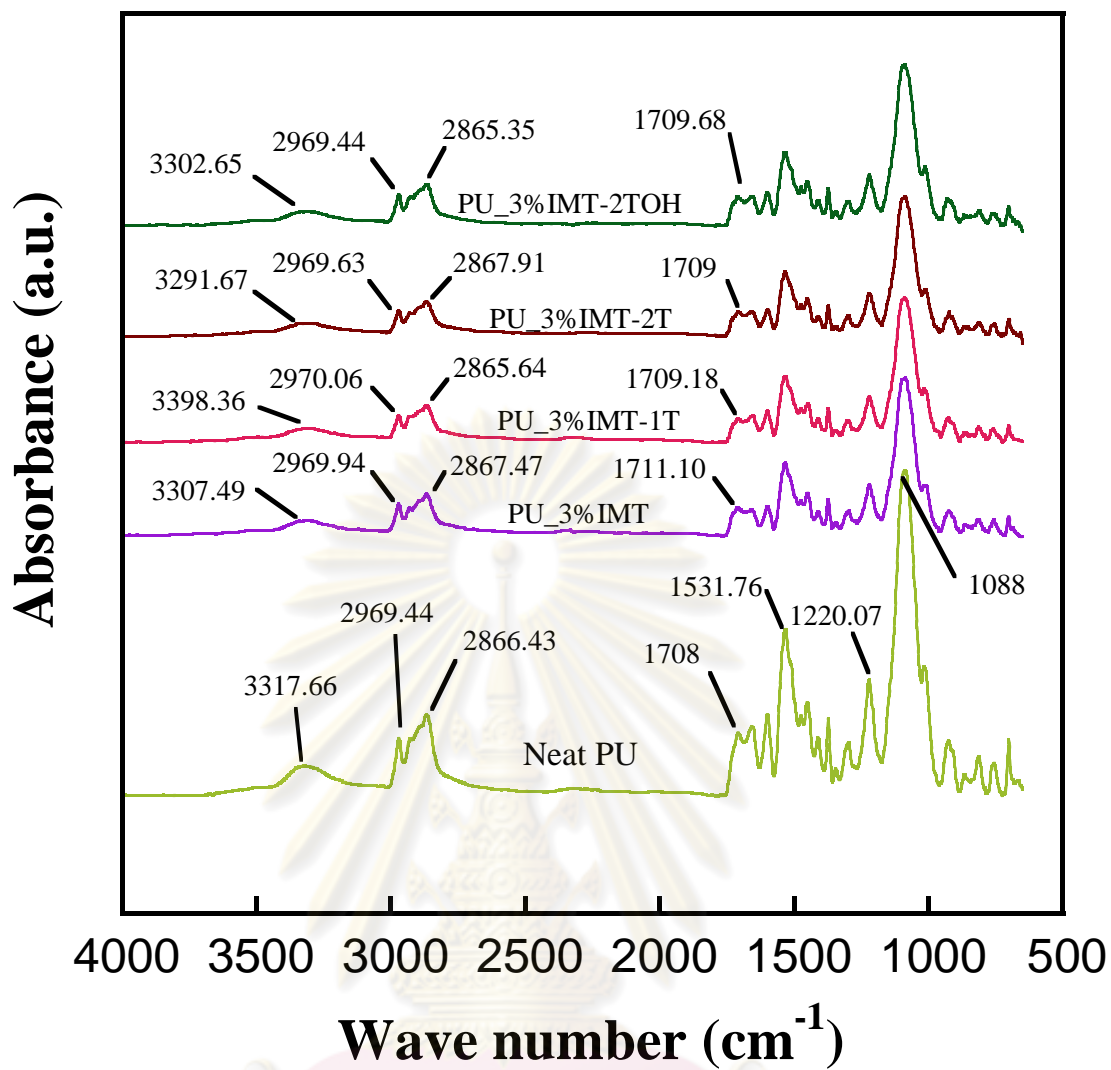


Figure 5.14: FT-IR spectra of polyurethane/clay nanocomposite foams by using 3 wt% of modified clay premixed with isocyanate

ศูนย์วิทยทรัพยากร
จุฬาลงกรณ์มหาวิทยาลัย

Table 5.3: Ratio of the area under the peak of hydrogen bond –NH ($A_{[NH]}$), C=O ($A_{[CO]}$) and –CH stretching ($A_{[CH]}$) of FTIR spectra (Part I)

Sample	Ratio	
	$A_{[NH]}/A_{[CH]}$	$A_{[CO]}/A_{[CH]}$
NEAT PU	1.06	0.19
PU_3%PMT	1.25	0.18
PU_3%PMT-1T	1.20	0.18
PU_3%PMT-2T	1.12	0.18
PU_3%PMT-2TOH	1.21	0.17
PU_3%IMT	0.65	0.10
PU_3%IMT-1T	0.73	0.10
PU_3%IMT-2T	1.15	0.15
PU_3%IMT-2TOH	1.02	0.18

5.5.2 Effect of clay composition and organoclay loading

The IR spectra of polyurethane/clay nanocomposite foams containing different amount of organoclay are shown in Figure 5.15 and 5.16, respectively. The positions of bands for distinctive functional groups in the IR spectra of the neat polyurethane and the polyurethane/clay nanocomposite foams are identical, confirming that the chemical structure of polyurethane were not altered by the presence of organoclay. Therefore, the effect of the intercalated layered silicates on the degree of phase separation in polyurethane can be determined solely from the extent of hydrogen bonding in the hard segments which is consistent with Tien's research. [35]

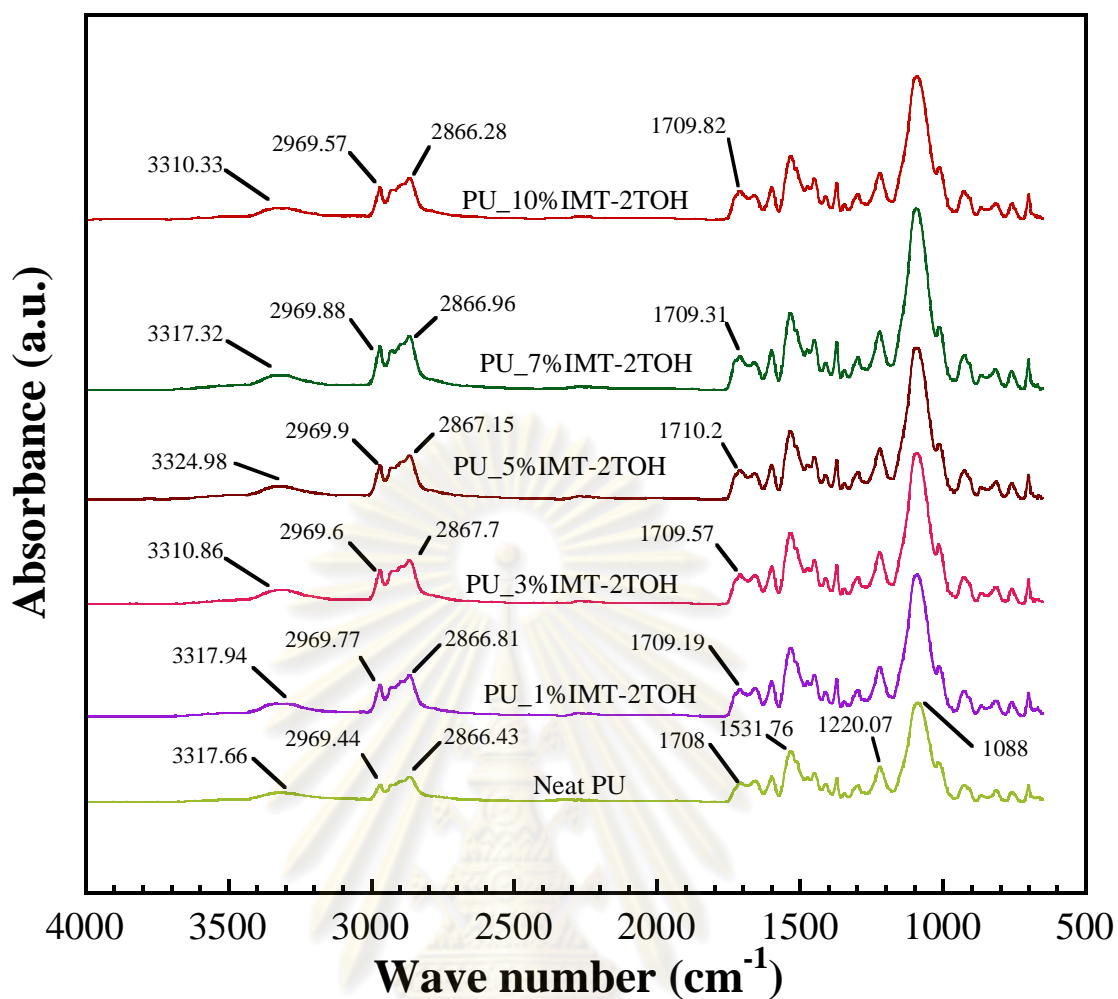


Figure 5.15: FT-IR spectra of polyurethane/clay nanocomposite foams containing 0, 1, 3, 5, 7 and 10 wt% of MMT-2TOH modified clay premixed with isocyanate

ศูนย์วิทยทรัพยากร
จุฬาลงกรณ์มหาวิทยาลัย

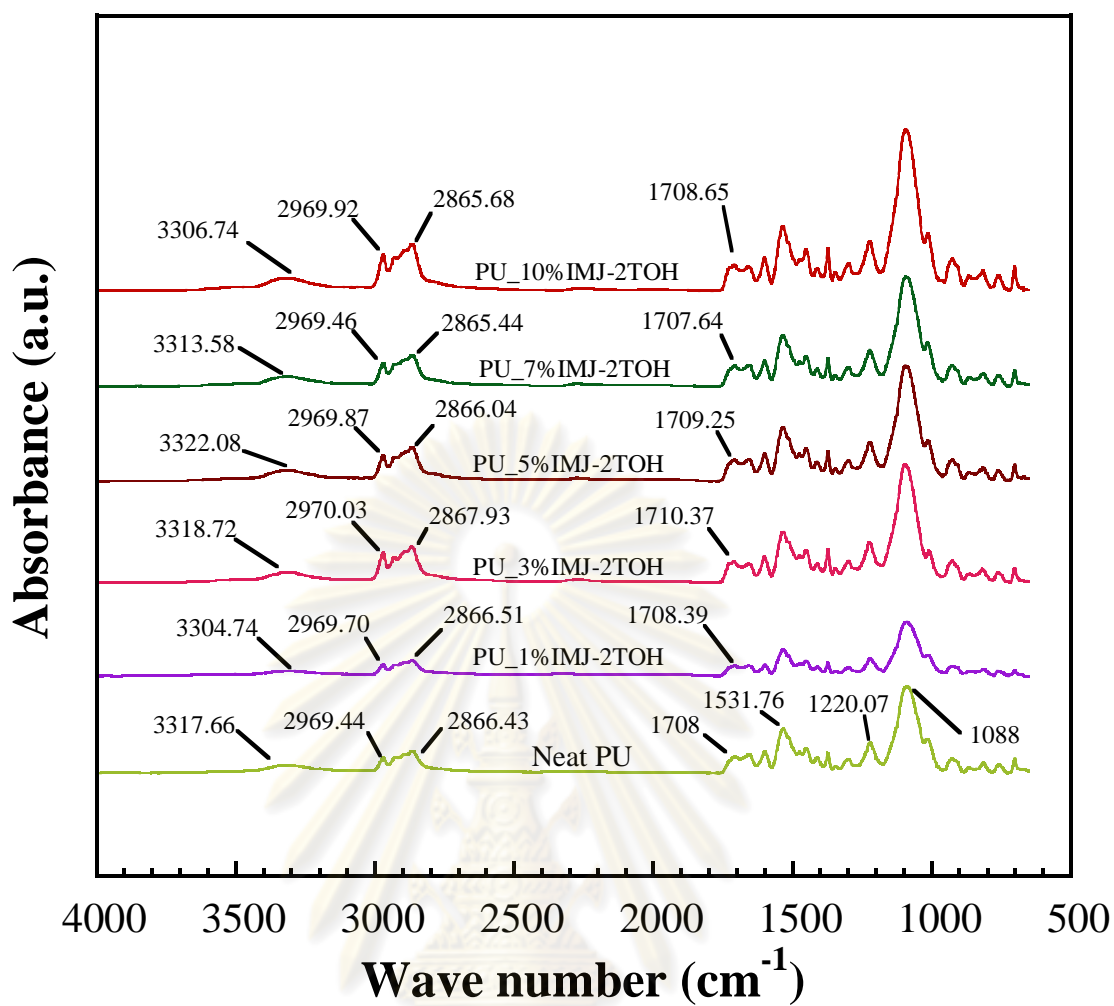


Figure 5.16: FT-IR spectra of polyurethane/clay nanocomposite foams containing 0, 1, 3, 5, 7 and 10 wt% of MMJ-2TOH modified clay premixed with isocyanate

ศูนย์วิทยทรัพยากร
จุฬาลงกรณ์มหาวิทยาลัย

Table 5.4: Ratio of the area under the peak of hydrogen bond –NH ($A_{[NH]}$), C=O ($A_{[CO]}$) and –CH stretching ($A_{[CH]}$) of FTIR spectra (Part II)

Sample	Ratio	
	$A_{[NH]}/A_{[CH]}$	$A_{[CO]}/A_{[CH]}$
NEAT PU	1.06	0.19
PU_1%IMT-2TOH	1.00	0.18
PU_3%IMT-2TOH	1.02	0.18
PU_5%IMT-2TOH	0.93	0.19
PU_7%IMT-2TOH	0.86	0.19
PU_10%IMT-2TOH	1.01	0.19
PU_1%IMJ-2TOH	1.11	0.17
PU_3%IMJ-2TOH	0.87	0.18
PU_5%IMJ-2TOH	1.04	0.18
PU_7%IMJ-2TOH	1.04	0.18
PU_10%IMJ-2TOH	1.04	0.18

ศูนย์วิทยทรัพยากร
จุฬาลงกรณ์มหาวิทยาลัย

5.6 Physical Property

5.6.1 Apparent density

The density of all specimens is fixed at $50.00 \pm 2 \text{ kg/m}^3$ by fixing the volume of mould. The results are shown in Table 5.4

Table 5.5: Weight and density of neat polyurethane and polyurethane/clay nanocomposite foams

Sample	Weight (g)	Density (kg/m^3)
Neat PU Foam	789.20	49.32
PU_3%PMT	800.15	50.00
PU_3%IMT	786.46	49.15
PU_3%PMT-1T	831.01	51.94
PU_3%IMT-1T	783.18	48.95
PU_3%PMT-2T	791.2	49.45
PU_3%IMT-2T	784.04	49.00
PU_3%PMT-2TOH	790.19	49.30
PU_3%IMT-2TOH	786.11	49.13

Sample	Weight (g)	Density (kg/m^3)
Neat PU Foam	789.20	49.32
PU_1%IMT-2TOH	782.26	48.89
PU_3%IMT-2TOH	766.90	47.93
PU_5%IMT-2TOH	745.60	46.60
PU_7%IMT-2TOH	775.18	48.45
PU_10%IMT-2TOH	777.97	48.62
PU_1%IMJ-2TOH	786.90	49.18
PU_3%IMJ-2TOH	761.25	47.58
PU_5%IMJ-2TOH	767.57	47.97
PU_7%IMJ-2TOH	773.60	48.35
PU_10%IMJ-2TOH	770.30	48.14

5.7 Mechanical Properties

5.7.1 Hardness

5.7.1.1 Effect of chemical structure of surfactant and mixing sequence between nanoclay and monomer

Hardness test was performed according to JIS K6301 with Auto Urethane H/N Tester. Figure 5.17 shows the hardness of polyurethane/clay nanocomposite foams using 3 wt% of modified clay premixed with isocyanate and 3 wt% of modified clay premixed with polyol with different types of surfactant. It can be seen that, the introduction of 3 wt% organoclay in to polyurethane foams is responsible for the enhancement of hardness. It is obvious that premixed modified clay with polyol before adding the other chemicals exhibit more hardness than premixed modified clay with isocyanate because isocyanate reduction are remarkably affected on hard segment in polyurethane/clay nanocomposite foams than adding small amount of modified clay. Additionally to study the effect of the type of surfactant it can be seen that for premixed modified clay with polyol the highest hardness was observed with nanocomposite with single tail surfactant (PU_3%PMT-1T) due to highest density. For premixed modified clay with isocyanate the highest hardness was observed with nanocomposite with double tails surfactant (PU_3%IMT-2T) which was consistent with the highest d-spacing of layered silicates as shown in figure 5.5. This result suggests that a good dispersion of layered silicate has been found to improve the mechanical properties.

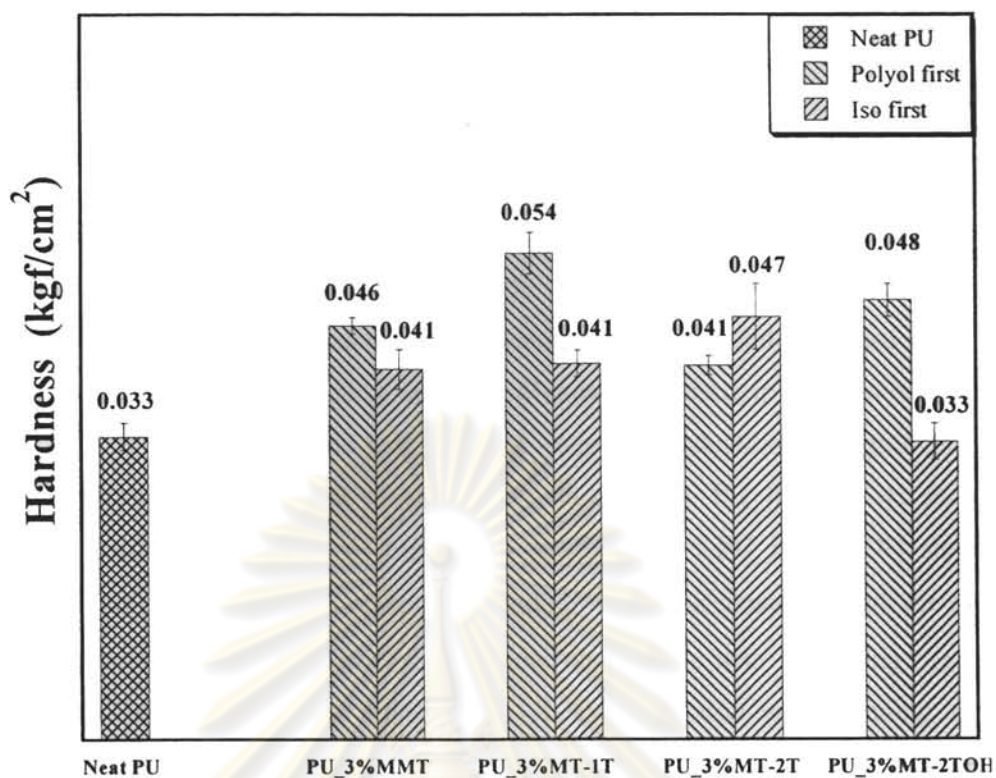


Figure 5.17: Hardness of polyurethane/clay nanocomposite foams by using 3 wt% of modified clay premixed with isocyanate and 3 wt% of modified clay premixed with polyol at different types of surfactant

ศูนย์วิทยทรัพยากร
จุฬาลงกรณ์มหาวิทยาลัย

5.7.1.2 Effect of organoclay loading and clay composition

Figure 5.18 shows the hardness of polyurethane/clay nanocomposite containing 0, 1, 3, 5, 7 and 10 wt% of modified clay, MMT-2TOH and MMJ-2TOH premixed with isocyanate. The results obviously demonstrated that the hardness decreased with an increase of organoclay content in 0-10 wt%. This can be due to the fact that, adding amount of organoclay premixed with isocyanate has been found to reduce the amount of isocyanate, thereby lowering cost of polyurethanes used in automotive industry. This may be taken as evidence that, effect of isocyanate reduction had significant effect than increased small amount of organoclay. In addition, PU_IMT-2TOH shows the highest hardness at 5 wt% of organoclay loading while PU_IMJ-2TOH shows the highest hardness at 1 wt% of organoclay loading. This was consistent with the fact that the agglomeration of nanoparticles was found to increase with increasing organoclay loading. These results also related with X-ray diffraction and scanning electron micrograph as mentioned above which can be suggested that good degree of clay dispersion only worked at low clay content.

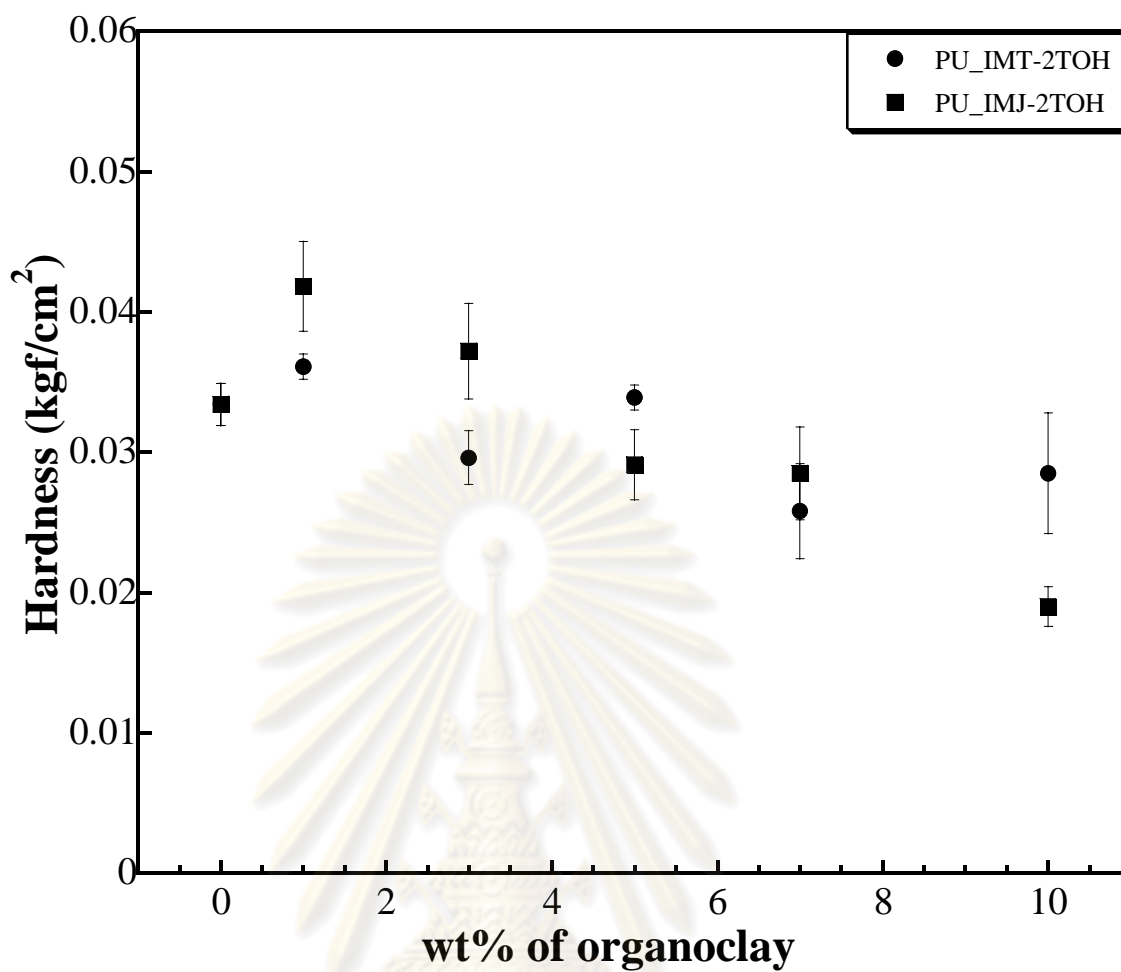


Figure 5.18: Hardness of polyurethane/clay nanocomposite foams containing 0, 1, 3, 5, 7 and 10 wt% of modified clay, MMT-2TOH and MMJ-2TOH premixed with isocyanate

ศูนย์วิทยทรัพยากร
จุฬาลงกรณ์มหาวิทยาลัย

5.7.2 Indentation force deflection (IFD)

5.7.2.1 Support factor (Sag factor)

Support factor is the ratio of the 65% indentation force to the 25% indentation force deflection determined after 1 min of rest. Most specifications are based on the 25% IFD value of 10 cm. foam. The support factor thus indicates what 65% IFD value would be acceptable for a particular application. The 65% IFD measures the support region of the stress-strain curve. Seating foams with low support factors will usually bottom out and give inferior performance.

$$\text{Support factor (SF)} = (65\% \text{ IFD} / 25\% \text{ IFD})$$

5.7.2.1.1 Effect of chemical structure of surfactant and mixing sequence between nanoclay and monomer

This parameter measures the seating quality of a piece of foam. Usually foams with higher density have higher support factor regardless of the type of foam. Seating foams with low support factors will usually bottom out and give inferior performance. The support factors of polyurethane/clay nanocomposite foams by using 3 wt% of modified clay premixed with isocyanate and 3 wt% of modified clay premixed with polyol at different types of surfactant are shown in Figure 5.19. The support factors of all 3 wt% of modified clay premixed with polyol foams were higher than that of neat polyurethane foam due to higher density. On the other hand, in case of premixed modified clay with isocyanate only PU_3%MT-1T shows higher support factor than neat polyurethane because isocyanate reduction remarkably affected on hard segment in polyurethane/clay nanocomposite foams than adding small amount of modified clay. Additionally to study the effect of the type of surfactant it was shown that for premixed modified clay with polyol the highest support factor were shown in untreated clay (PU_3%PMT) and double tails surfactant (PU_3%PMT-2T) due to high densities and for premixed modified clay with isocyanate the highest support factor was shown in single tail surfactant (PU_3%IMT-1T).

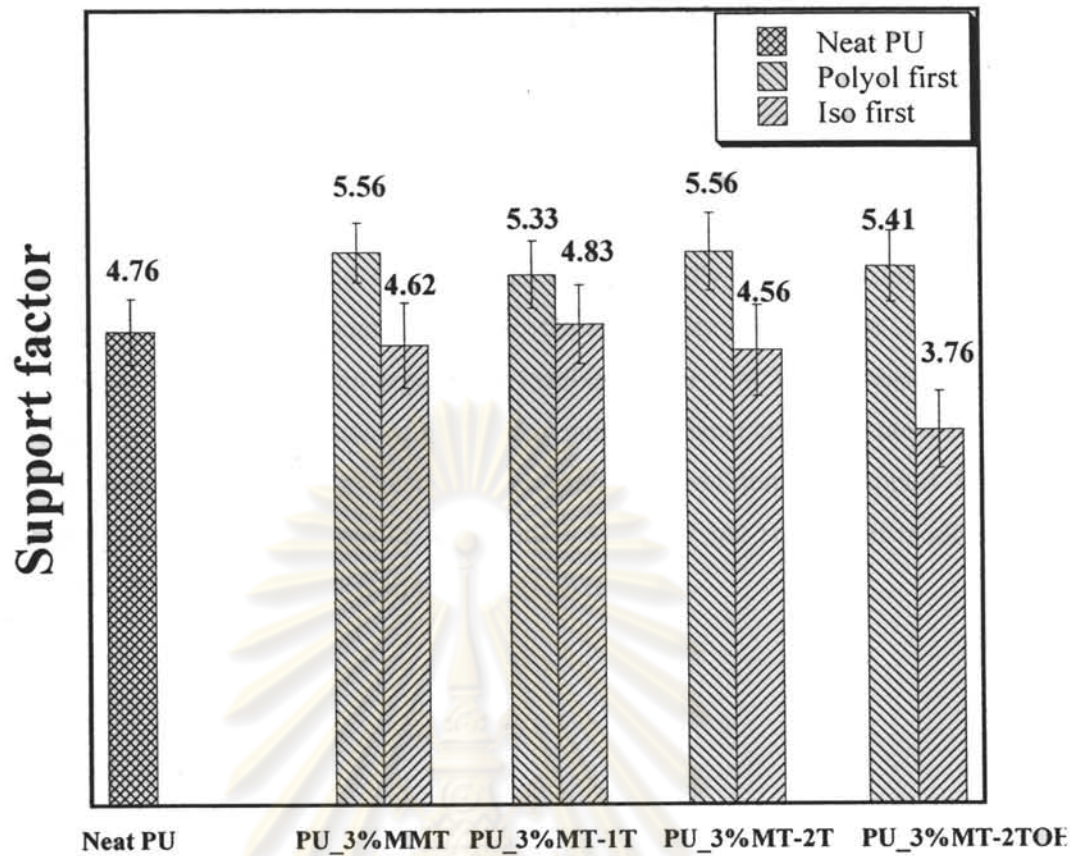


Figure 5.19: Support factor of polyurethane/clay nanocomposite foams by using 3 wt% of modified clay premixed with isocyanate and 3 wt% of modified clay premixed with polyol at different types of surfactant

ศูนย์วิทยทรัพยากร
จุฬาลงกรณ์มหาวิทยาลัย

5.7.2.1.2 Effect of clay composition and organoclay loading

Figure 5.20 shows the support factor of polyurethane/clay nanocomposite containing 0, 1, 3, 5, 7 and 10 wt% of modified clay, MMT-2TOH and MMJ-2TOH premixed with isocyanate. In case of PU_IMJ-2TOH, the results obviously demonstrated that the support factor increased dramatically with increasing organoclay loading and reached maximum value at 3 wt% organoclay loading. The support factor value began to decrease when organoclay loading is over 3 wt%. The reason is mainly attributed to the agglomeration of organoclay particles above critical content of clay as can be seen from scanning electron micrograph. In addition the support factor of polyurethane/clay nanocomposite containing 0, 1, 3, 5, 7 and 10 wt% of modified clay (PU_IMT-2TOH) was lower than that of PU_IMJ-2TOH.



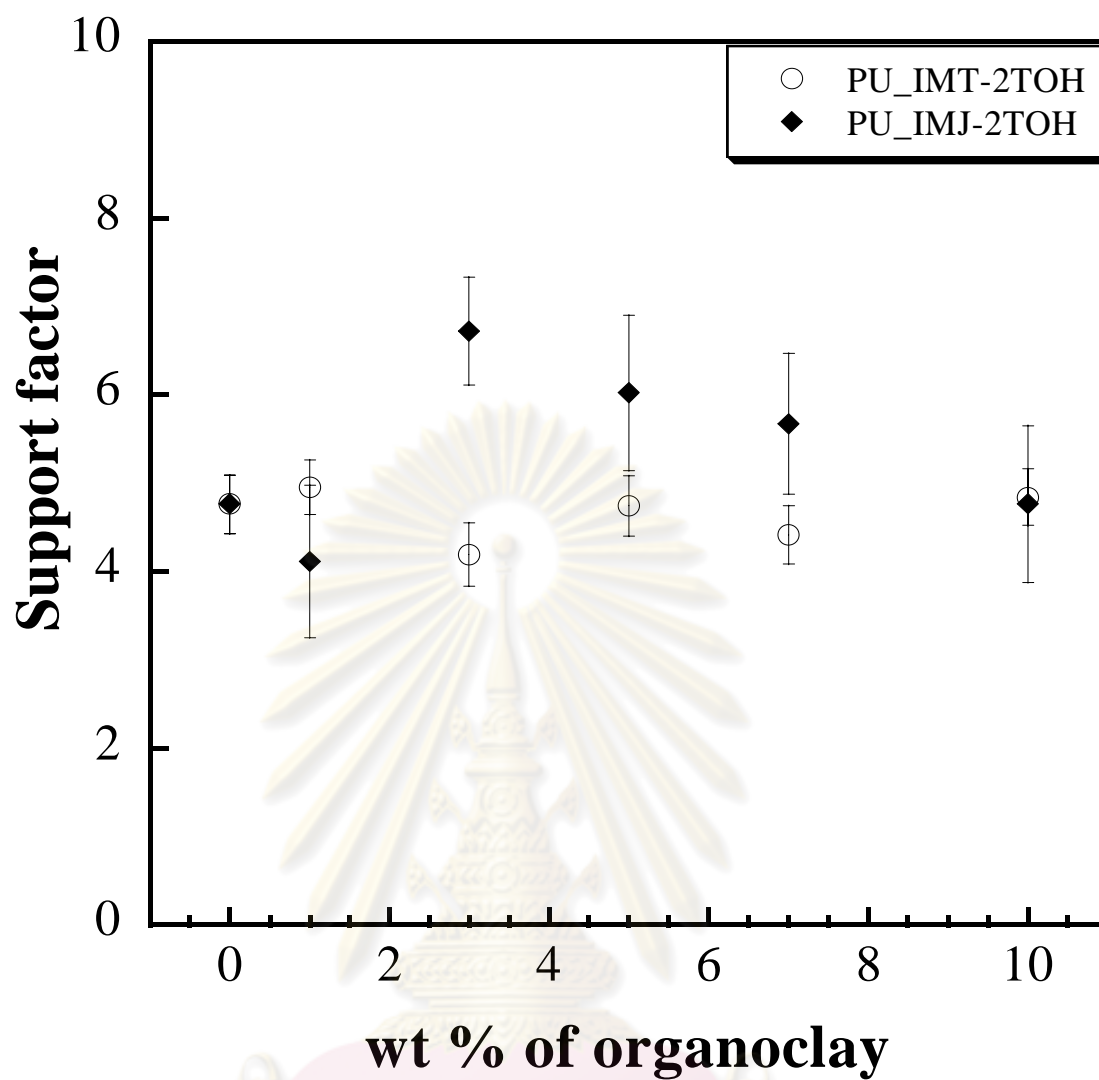


Figure 5.20: Support factor of polyurethane/clay nanocomposite foams containing 0, 1, 3, 5, 7 and 10 wt% of modified clay, MMT-2TOH and MMJ-2TOH premixed with isocyanate

5.7.2.2 Guide factor

Guide factor is the ratio of the 25% indentation force deflection to the density after a 1 min rest. Most specifications do not have a density requirement; therefore, the product with the highest guide factor has the cost advantage but not necessarily the performance advantage.

$$\text{Guide factor} = (25\% \text{ IFD} / \text{density})$$

5.7.2.2.1 Effect of chemical structure of surfactant and mixing sequence between nanoclay and monomer

Guide factor is useful in determining the relative firmness of foams with different density. The closer the densities, the better the comparison. When densities are different, the foam with the highest guide factor has the cost advantage, but may not necessarily have the performance advantage. Guide factor of polyurethane/clay nanocomposite foams by using 3 wt% of modified clay premixed with isocyanate and 3 wt% of modified clay premixed with polyol at different types of surfactant are shown in Figure 5.21. The guide factors of all 3 wt% of modified clay premixed with polyol foams were higher than that of neat polyurethane foam. Additionally to study the effect of the type of surfactant it was shown that for premixed modified clay with polyol the highest guide factor was shown in single tail surfactant (PU_3%PMT-1T) due to highest density and hydroxyl surfactant (PU_3%PMT-2TOH) due to highest d-spacing of layered silicates compared to MMT clay modified with other types of surfactant and for premixed with isocyanate the highest support factor was shown in hydroxyl surfactant (PU_3%IMT-2TOH) due to the highest d-spacing of layered silicate with lead to good dispersion.

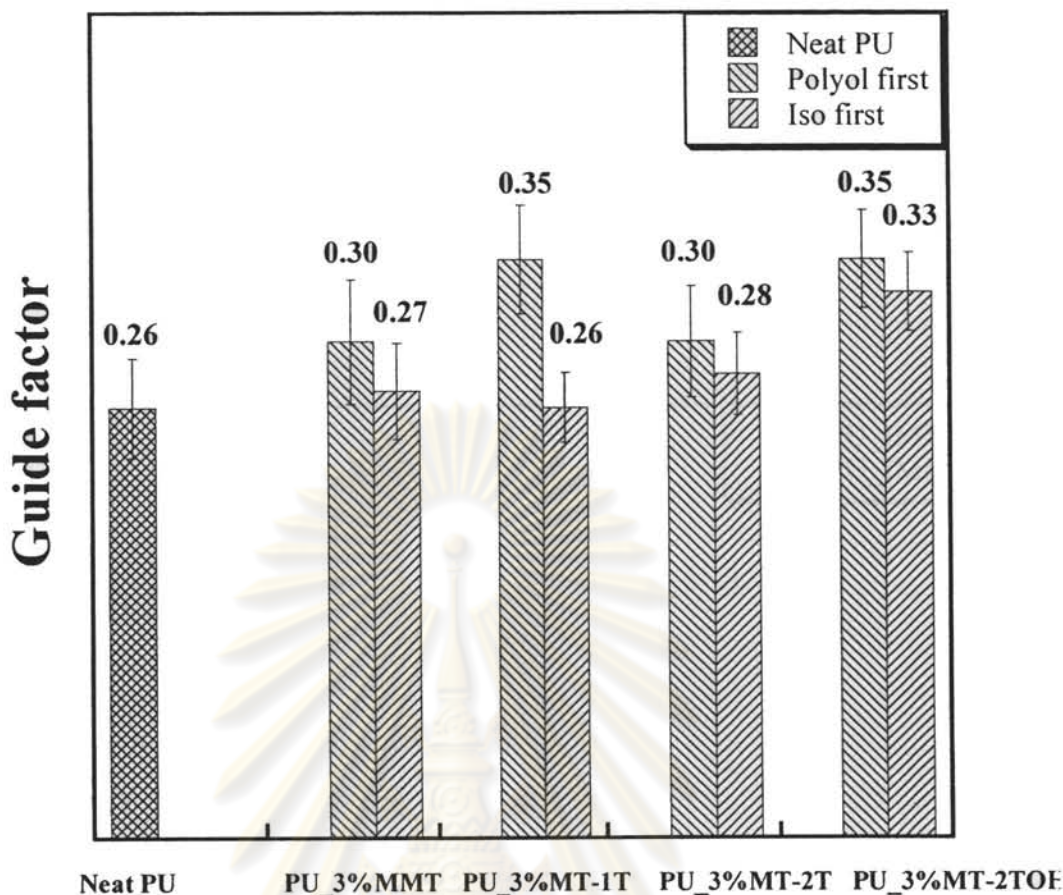


Figure 5.21: Guide factor of polyurethane/clay nanocomposite foams by using 3 wt% of modified clay premixed with isocyanate and 3 wt% of modified clay premixed with polyol at different types of surfactant

5.7.2.2.2 Effect of clay composition and organoclay loading

Figure 5.22 shows the guide factor of polyurethane/clay nanocomposite containing 0, 1, 3, 5, 7 and 10 wt% of modified clay, MMT-2TOH and MMJ-2TOH premixed with isocyanate. In case of PU_IMT-2TOH, the results obviously demonstrated that the guide factor increased dramatically with increasing organoclay loading and reached maximum value at 3 wt% organoclay loading. The guide factor value began to decrease when organoclay loading is over 3 wt%. The reason is mainly attributed to the agglomeration of organoclay particles above critical content of clay which was consistent with the results from scanning electron micrograph. It is interesting that the guide factor of polyurethane/clay nanocomposite containing 0, 1, 3,

5, 7 and 10 wt% of modified clay (PU_IMJ-2TOH) reached maximum value at 1 wt% organoclay content and then decreased when organoclay content is over 1 wt%. These results also related with X-ray diffraction and scanning electron micrograph as mentioned above which can be suggested that good degree of clay dispersion only worked at low clay content.

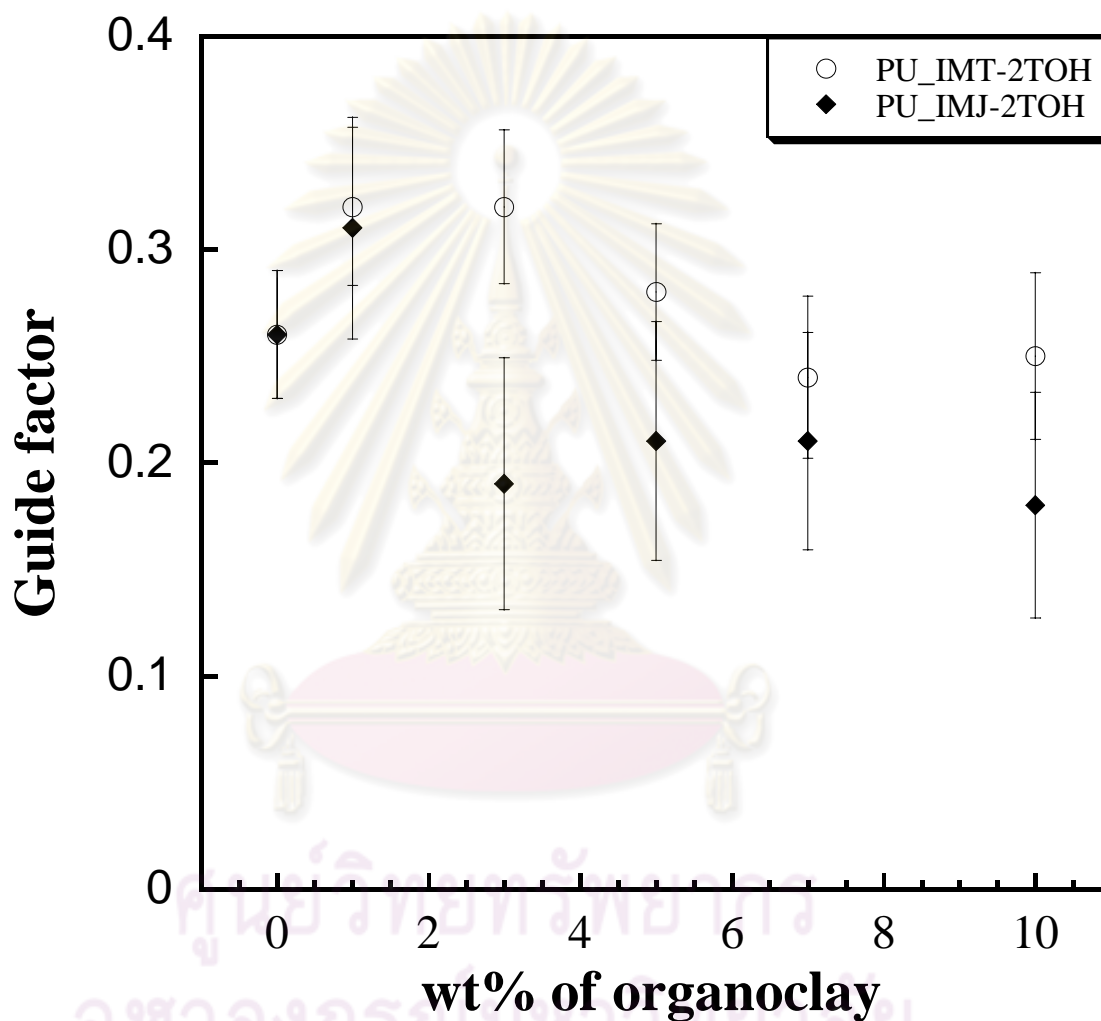


Figure 5.22: Guide factor of polyurethane/clay nanocomposite foams containing 0, 1, 3, 5, 7 and 10 wt% of modified clay, MMT-2TOH and MMJ-2TOH premixed with isocyanate

5.7.3 Constant deflection compression set

5.7.3.1 Effect of chemical structure of surfactant and mixing sequence between nanoclay and monomer

Constant deflection compression set is used to assess the ability of the cellular plastics to recover after prolonged compression. The greater the compression set value, the less the elastic recovery of the material is. Compression set value of polyurethane/clay nanocomposite foams by using 3 wt% of modified clay premixed with isocyanate and 3 wt% of modified clay premixed with polyol at different types of surfactant are shown in Figure 5.23. In case of premixed modified clay with polyol before, the results show that compression set value of polyurethane/clay nanocomposite foam was found to be higher when compared with neat polyurethane foam and the less value for this case are shown in untreated clay (PU_3%PMT) and clay which were treated by hydroxyl surfactant (PU_3%PMT-2TOH). On the other hand, in case of premixed with isocyanate, the compression set value of polyurethane/clay nanocomposite foam was found to be lower when compared with neat polyurethane foam due to isocyanate reduction which is strongly affected by hard segment in polyurethane/clay nanocomposite foams. The less value for this case are shown in untreated clay (PU_3%IMT) although PU_3%IMT was shown the less d-spacing compared to organoclay modified by other types of surfactant.

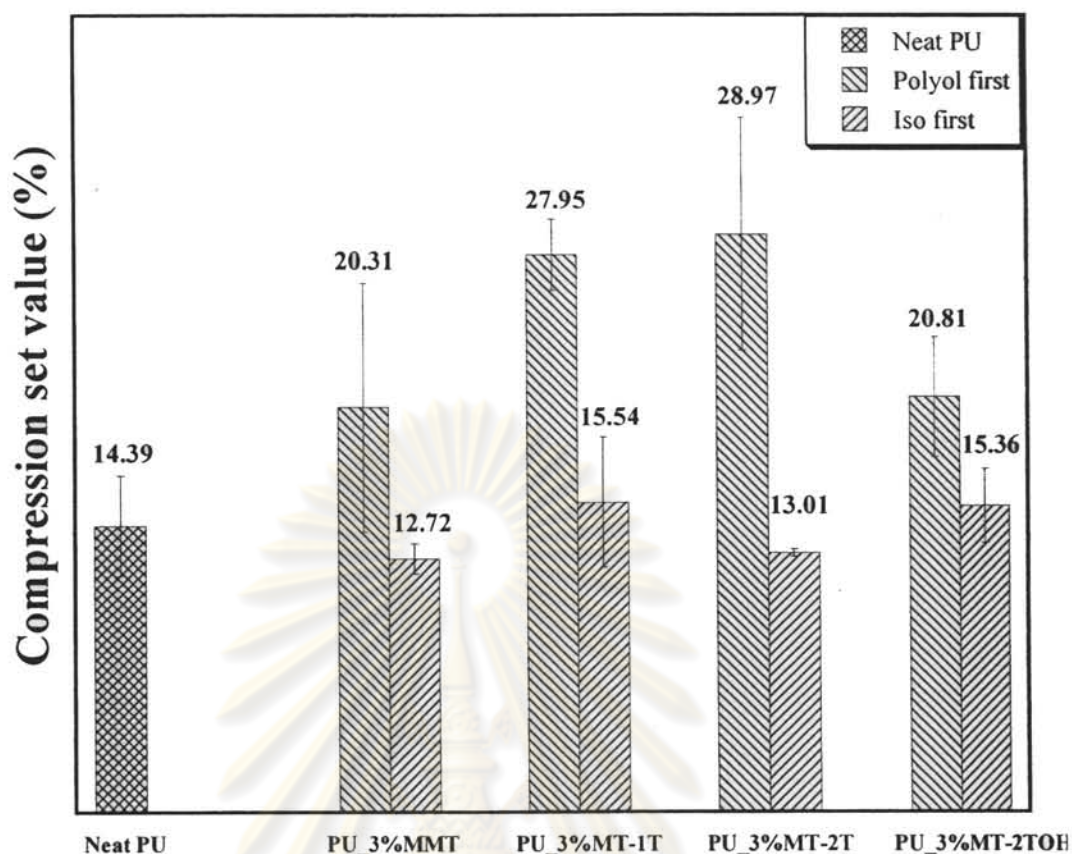


Figure 5.23: Compression set value of polyurethane/clay nanocomposite foams by using 3 wt% of modified clay premixed with isocyanate and 3 wt% of modified clay premixed with polyol at different types of surfactant

5.7.3.2 Effect of clay composition and organoclay loading

Figure 5.24 shows compression set value of polyurethane/clay nanocomposite foams containing 0, 1, 3, 5, 7 and 10 wt% of modified clay, MMT-2TOH and MMJ-2TOH premixed with isocyanate. The results obviously demonstrated that the compression set value decreased with an increase of organoclay loading in 0-10 wt%. This can be due to the fact that, adding organoclay premixed with isocyanate has been found to reduce the amount of isocyanate, thereby lowering cost of polyurethanes used in automotive industry. This may be taken as evidence that, isocyanate reduction had significant effect than increased small amount of organoclay due to the reduction of hard segment in polyurethane. In addition, it can be seen that the two types of clay was found to show

little effect. It is obvious that polyurethane/clay nanocomposite foams show greater elastic recovery of the material than neat polyurethane.

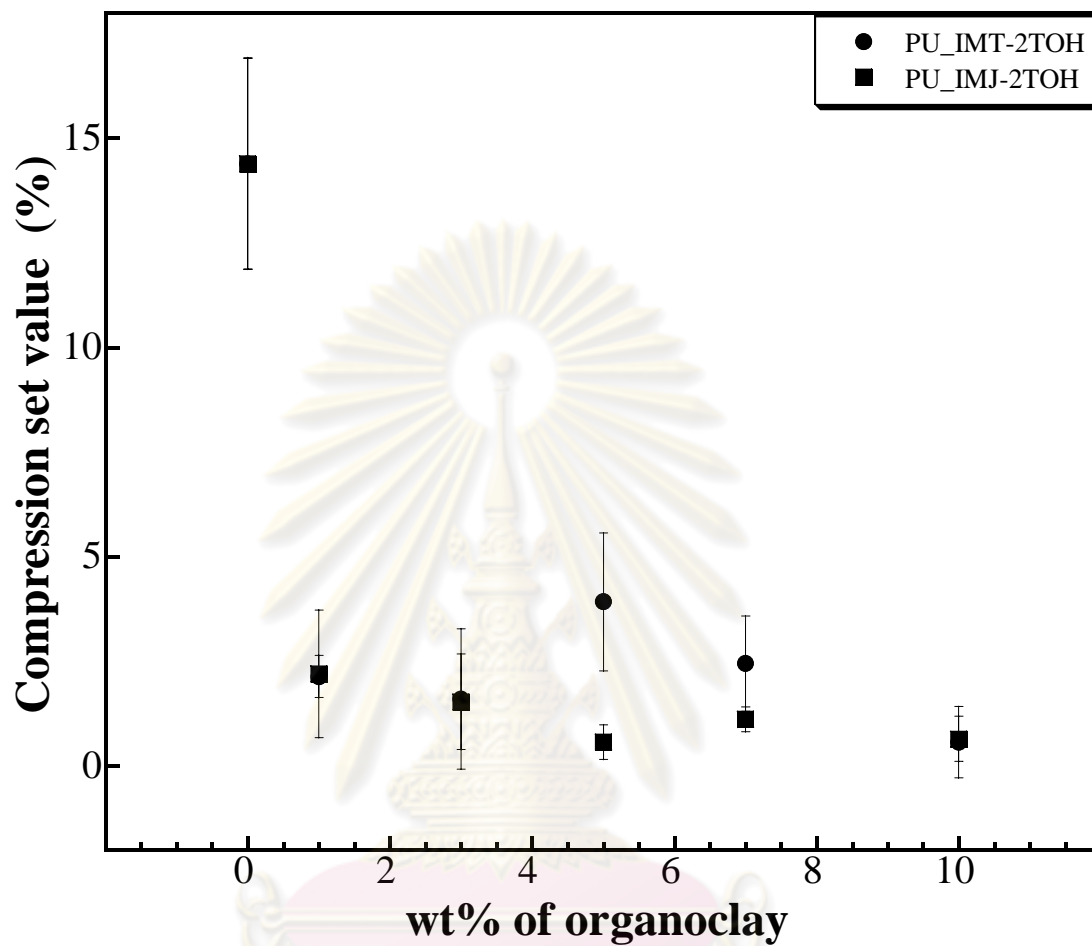


Figure 5.24: Compression set value of polyurethane/clay nanocomposite foams containing 0, 1, 3, 5, 7 and 10 wt% of modified clay, MMT-2TOH and MMJ-2TOH premixed with isocyanate

จุฬาลงกรณ์มหาวิทยาลัย

5.7.4 Resilience (ball rebound)

5.7.4.1 Effect of chemical structure of surfactant and mixing sequence between nanoclay and monomer

Resilience is an indicator of the surface elasticity or “springiness” of foam. Resilience can relate to comfort. Resilience is typically measured by dropping a steel ball onto the foam cushion and measuring how high the ball rebounds. Foam resilience ranges from about 40 percent ball rebound to as high as 70 percent rebound. Higher resilience in a foam often means that sofa seat cushions, for example, have a better “hand” or surface feel. Ball rebound value of polyurethane/clay nanocomposite foams by using 3 wt% of modified clay premixed with isocyanate and 3 wt% of modified clay premixed with polyol at different types of surfactant are shown in Figure 5.25. In case of premixed modified clay with polyol before, the results show that, resilience value of polyurethane/clay nanocomposite foam was found to be lower when compared with neat polyurethane foam and the highest value for this case is shown in untreated clay (PU_3%PMT). On the other hand in case of premixed modified clay with isocyanate, the resilience value of polyurethane/clay nanocomposite foam remained almost unchanged when compared with neat polyurethane foam due to reduction in isocyanate monomer. The highest value for this case is shown in single tail surfactant (PU_3%IMT-1T) and clay treated with hydroxyl surfactant (PU_3%IMT-2TOH) which were similar to resilience value of neat polyurethane foam.

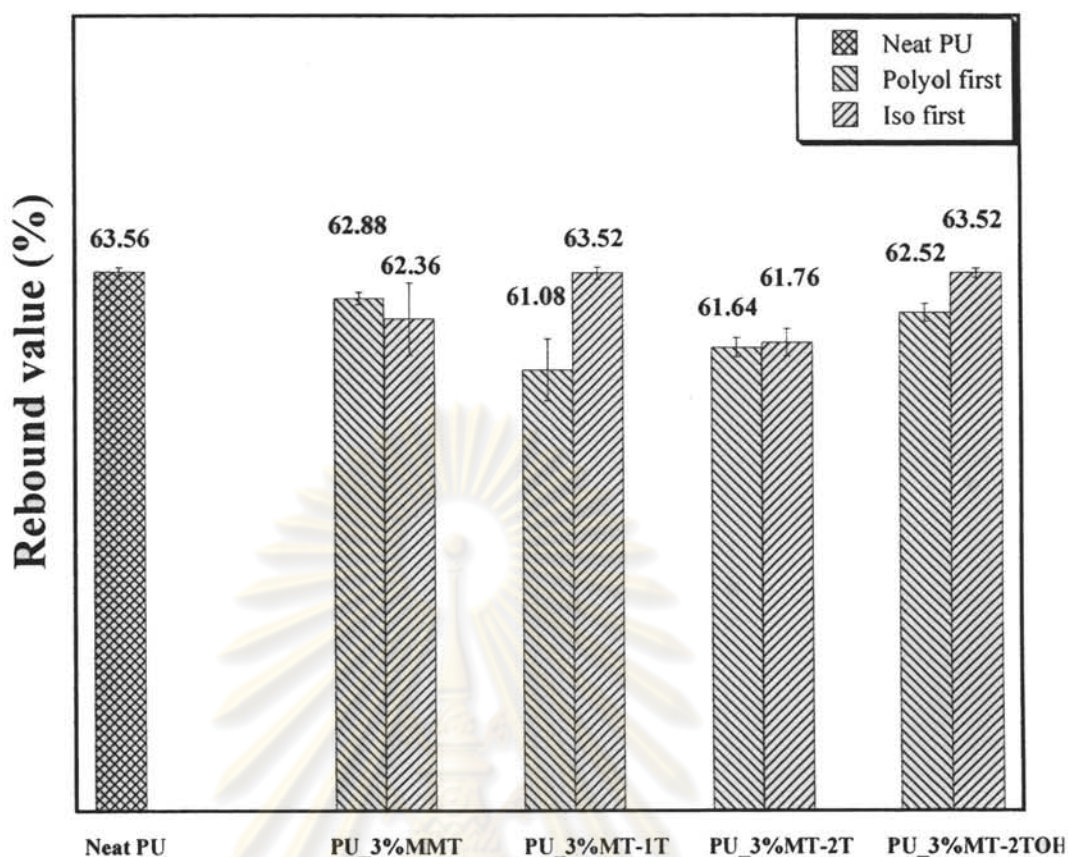


Figure 5.25: Resilience value of polyurethane/clay nanocomposite foams by using 3 wt% of modified clay premixed with isocyanate and 3 wt% of modified clay premixed with polyol at different types of surfactant

5.7.4.2 Effect of clay composition and organoclay loading

Figure 5.26 shows resilience value of polyurethane/clay nanocomposite foams containing 0, 1, 3, 5, 7 and 10 wt% of modified clay, MMT-2TOH and MMJ-2TOH premixed with isocyanate. The results obviously demonstrated that in case of PU_IMJ-2TOH, the results show that, the highest resilience value of polyurethane/clay nanocomposite foam was found at 1 wt% of organoclay loading. This result was associated with the highest resilience of PU_IMT-2TOH. This was consistent with the fact that the agglomeration of nanoparticles was found to increase with increasing organoclay loading. These results also related with X-ray diffraction and scanning electron micrograph as mentioned above which can be suggests that good degree of clay dispersion only worked at low clay content.

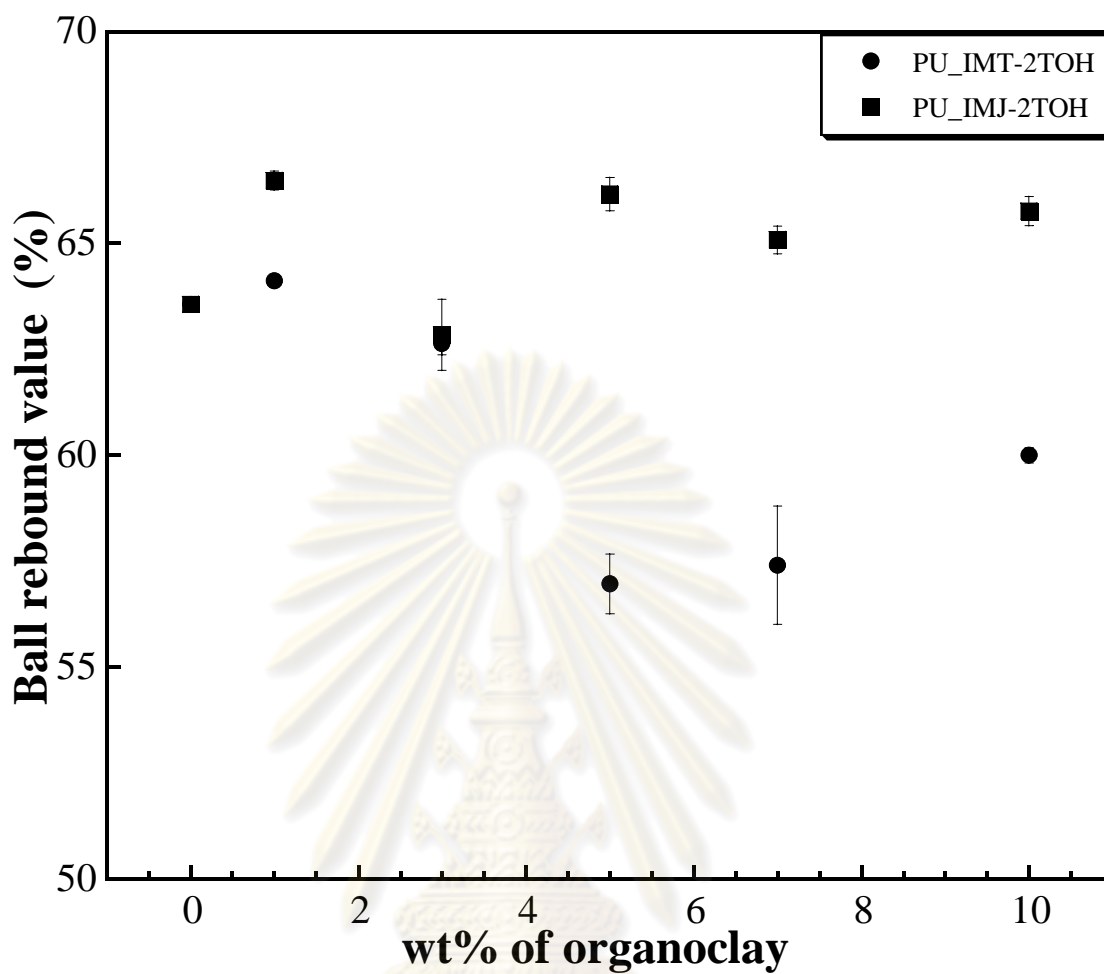


Figure 5.26: Resilience value of polyurethane/clay nanocomposite foams containing 0, 1, 3, 5, 7 and 10 wt% of modified clay, MMT-2TOH and MMJ-2TOH premixed with isocyanate

ศูนย์วิทยทรัพยากร
จุฬาลงกรณ์มหาวิทยาลัย

5.8 Thermal Property

5.8.1 Degradation temperature

5.8.1.1 Effect of clay composition and chemical structure of surfactant

Figure 5.27 shows thermogravimetric analysis curves of pristine clay (MMT) and modified clay which was carried out in a nitrogen atmosphere from room temperature to 800 °C at 10°C/min. The exchanged portion in the inter-galleries of silicates was determined by the weight residue difference of MT1T, MT2T and MT2TOH in the temperature range from 120 to 800 °C. As a results, MT1T, MT2T and MT2TOH show larger weight loss compared to MMT. Furthermore, the degradation temperature (T_d) is one of the key parameters need to be determined for thermal stability of polymer. The T_d , in this case, is defined as the temperature at 5% weight loss of samples. As evidently seen in the thermogram, the thermal decomposition in each organoclay was found to show single stage weight loss and T_d of MMT begins at about 675 °C whereas the T_d of MT1T, MT2T and MT2TOH are shown at 275, 275 and 300 °C, respectively. Thermal degradation of organoclay MT1T and MT2T begin at about 275 °C because the ammonium cation loss an amine and leaves and acid proton on the surface of the MMT.

Figure 5.28 shows thermogravimetric analysis curves of pristine clay (MMJ) and modified clay which were carried out in a nitrogen atmosphere from room temperature to 800 °C at 10°C/min. The exchanged portion in the inter-galleries of silicates was determined by the weight residue difference of MJ1T, MJ2T and MJ2TOH in the temperature range from 120 to 800 °C. The degradation temperature in each organoclay was found to show single stage weight loss and T_d of MMJ begins at about 500 °C whereas the T_d of MJ1T, MJ2T and MJ2TOH are shown at 250, 275 and 310 °C, respectively. The trend of thermogravimetric analysis of MMJ clay is similar to that of MMT clay.

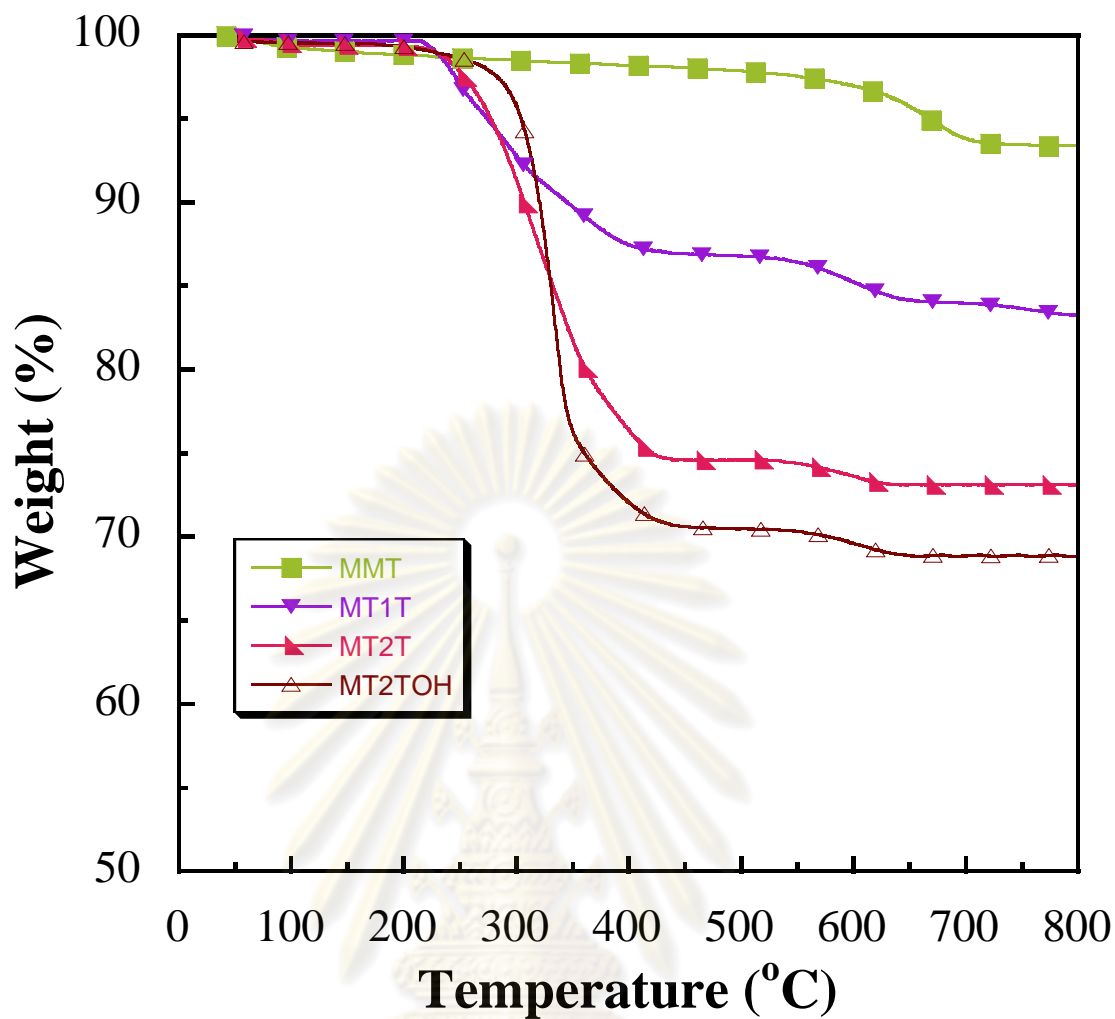


Figure 5.27: Thermal degradation of pristine clay (MMT) and modified clay

ศูนย์วิทยทรัพยากร
จุฬาลงกรณ์มหาวิทยาลัย

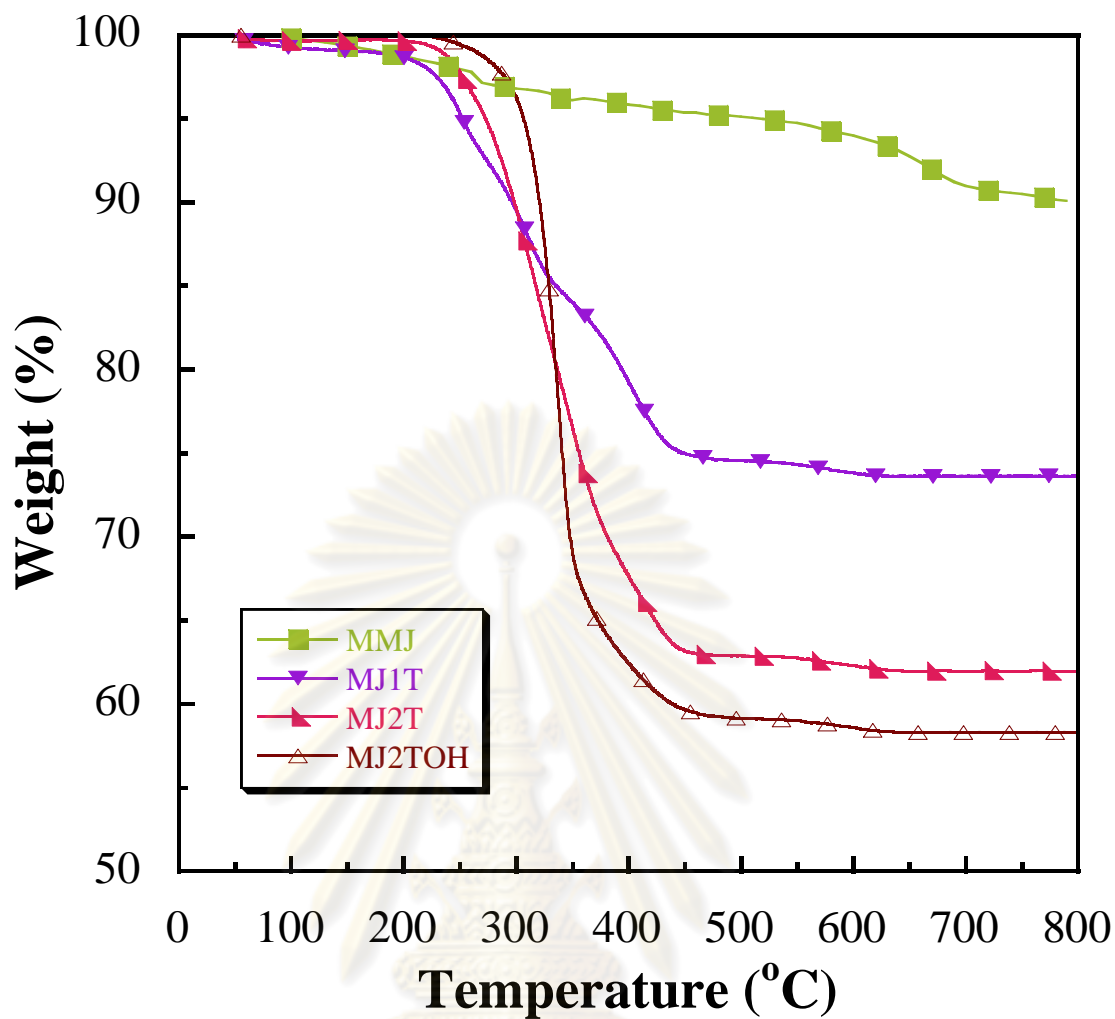


Figure 5.28: Thermal degradation of pristine clay (MMJ) and modified clay

ศูนย์วิทยทรัพยากร
จุฬาลงกรณ์มหาวิทยาลัย

5.8.1.2 Effect of mixing sequence between nanoclay and monomer

Figure 5.29 shows thermogravimetric analysis curves of neat polyurethane and polyurethane/clay nanocomposite foams compared between using 3 wt% of modified clay premixed with isocyanate, PU_3%IMT-2TOH and 3 wt% of modified clay premixed with polyol, PU_3%PMT-2TOH which were carried out in nitrogen atmosphere from room temperature to 800 °C at 10°C/min. As seen in the thermogram at 5% weight loss, the thermal decomposition in PU_3%IMT-2TOH was found to be slightly higher than that of the neat polyurethane foam, indicating the organoclay can enhance the heat resistance of polyurethane. The T_d of neat polyurethane was determined to be 243 °C whereas the T_d of PU_3%IMT-2TOH was shown at 255 °C which was attributed to the depolycondensation reaction. This result might be due to the reaction of isocyanate in polyurethane and hydroxyl of organoclay to increase a physical link through strong hydrogen bonds. In addition, it is observed from figure 5.29 that the decomposition behaviors of all foams are in the form of three steps of degradation stages. In the first and second stage, the urethane bonds decompose to form alcohols and isocyanates. Complete volatilization of resulting chain fragments is prevented by dimerisation of isocyanates to carbodiimides, which react with the alcohol groups to give relatively stable substituted ureas (second stage) that decompose in the third stage. Trimerization of isocyanates may also occur under certain conditions to yield thermally stable isocyanurate rings. The final step is the high temperature degradation of these stabilized structures to yield volatile products and a small quantity of carbonaceous char. [34]

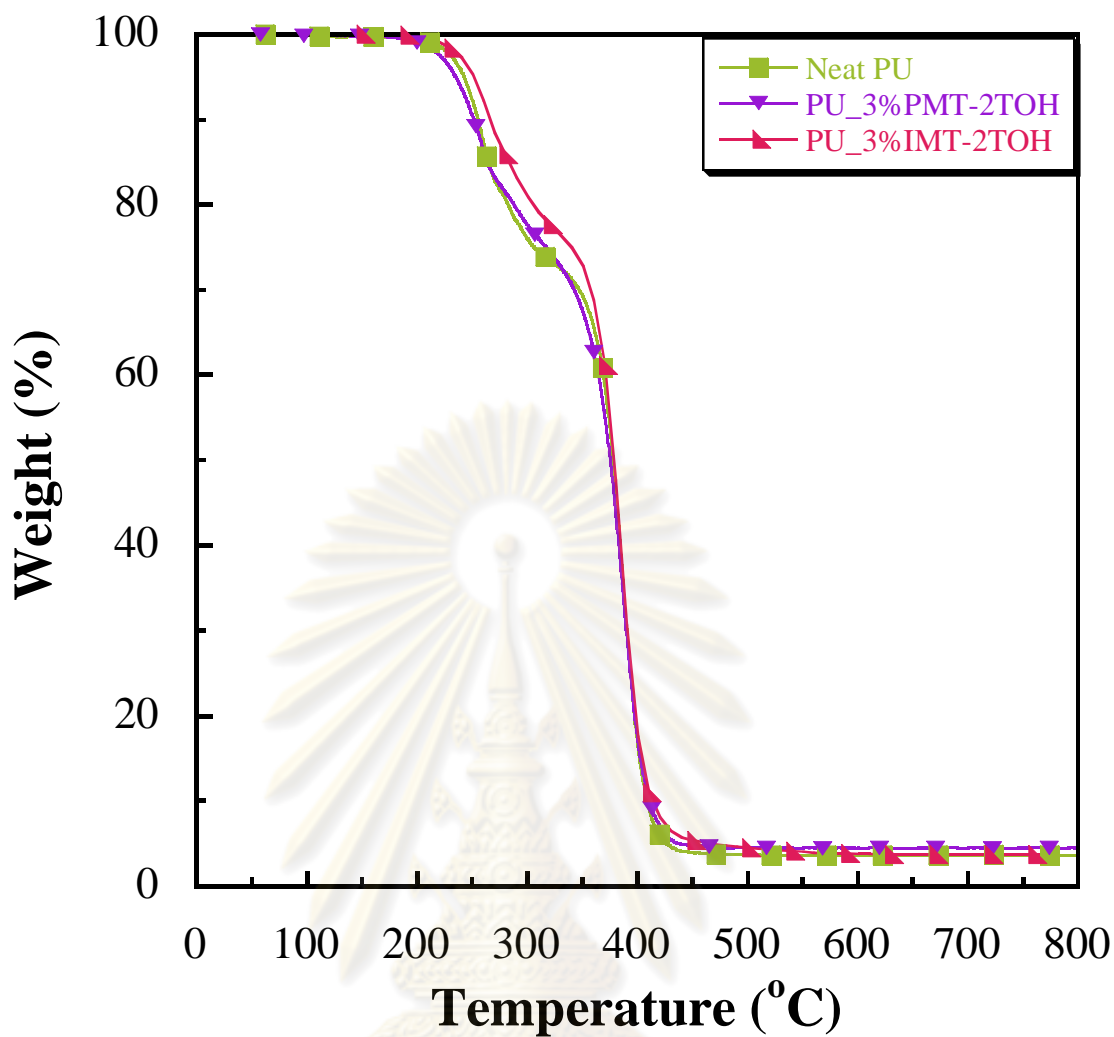


Figure 5.29: Thermal degradation of polyurethane/clay nanocomposite foams compared between using 3 wt% of modified clay premixed with isocyanate, PU_3%IMT-2TOH and 3 wt% of modified clay premixed with polyol, PU_3%PMT-2TOH

5.8.1.3 Effect of clay composition and organoclay loading

The thermal stability of polyurethane and polyurethane/clay nanocomposite foams was investigated by TGA. TGA thermograms of the nanocomposites were shifted toward high temperatures as compared to polyurethane, indicating that addition of clay improved the thermal stability of the system and was concentration dependence. This may be attributed to strong interactions between the organoclay and polyurethane matrix. Thermal degradation of polyurethane/clay nanocomposite foams containing 0, 1, 3, 5, 7 and 10 wt% of MMT-2TOH modified clay premixed with isocyanate are shown in Figure 5.30. All foams are shown in the form of three step degradation stage, hence decomposition temperature reported in this figure presents the temperature corresponding to 5% weight loss of the specimens. It is observed that 3 wt% of modified clay shows the highest decomposition temperatures at 252 °C, which increased 3.7% from neat polyurethane. However, in Figure 5.32 the thermal degradation of polyurethane/clay nanocomposite foams containing 0, 1, 3, 5, 7 and 10 wt% of MMJ-2TOH modified clay premixed with isocyanate cannot be distinguished at 10% weight loss.

The activation energies of degradation of polyurethane/clay nanocomposites were higher than those of neat polyurethane because the silicates served as a thermal barrier for delaying the hard segments from degradation during heating. Nevertheless, the thermal stability of polyurethane/clay nanocomposites decreased as the amount of silicate in polyurethane foam was increased to more than 3 wt%, attributed to a better dispersion of the silicates in the polyurethane at low organoclay loading.

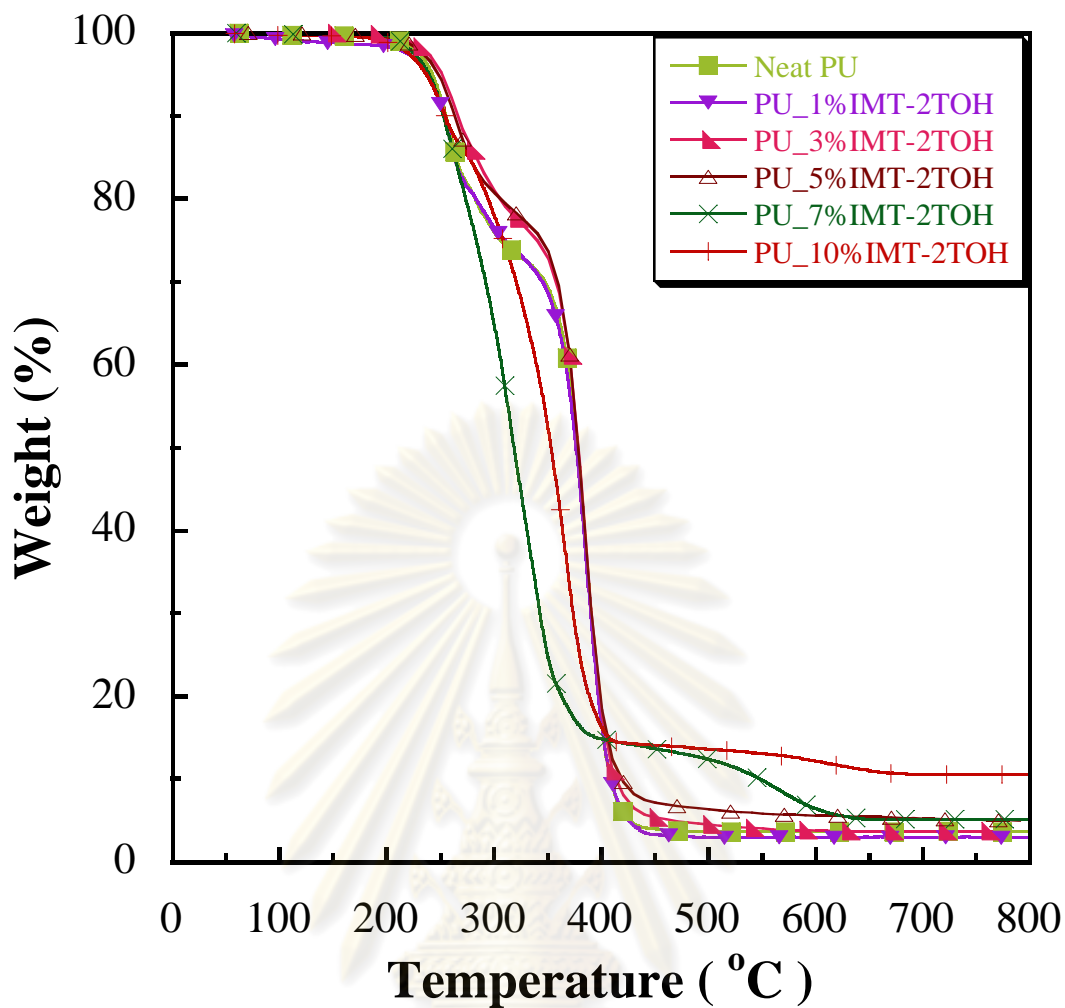


Figure 5.30: Thermal degradation of polyurethane/clay nanocomposite foams containing 0, 1, 3, 5, 7 and 10 wt% of MMT-2TOH modified clay premixed with isocyanate

ศูนย์วิทยทรัพยากร
จุฬาลงกรณ์มหาวิทยาลัย

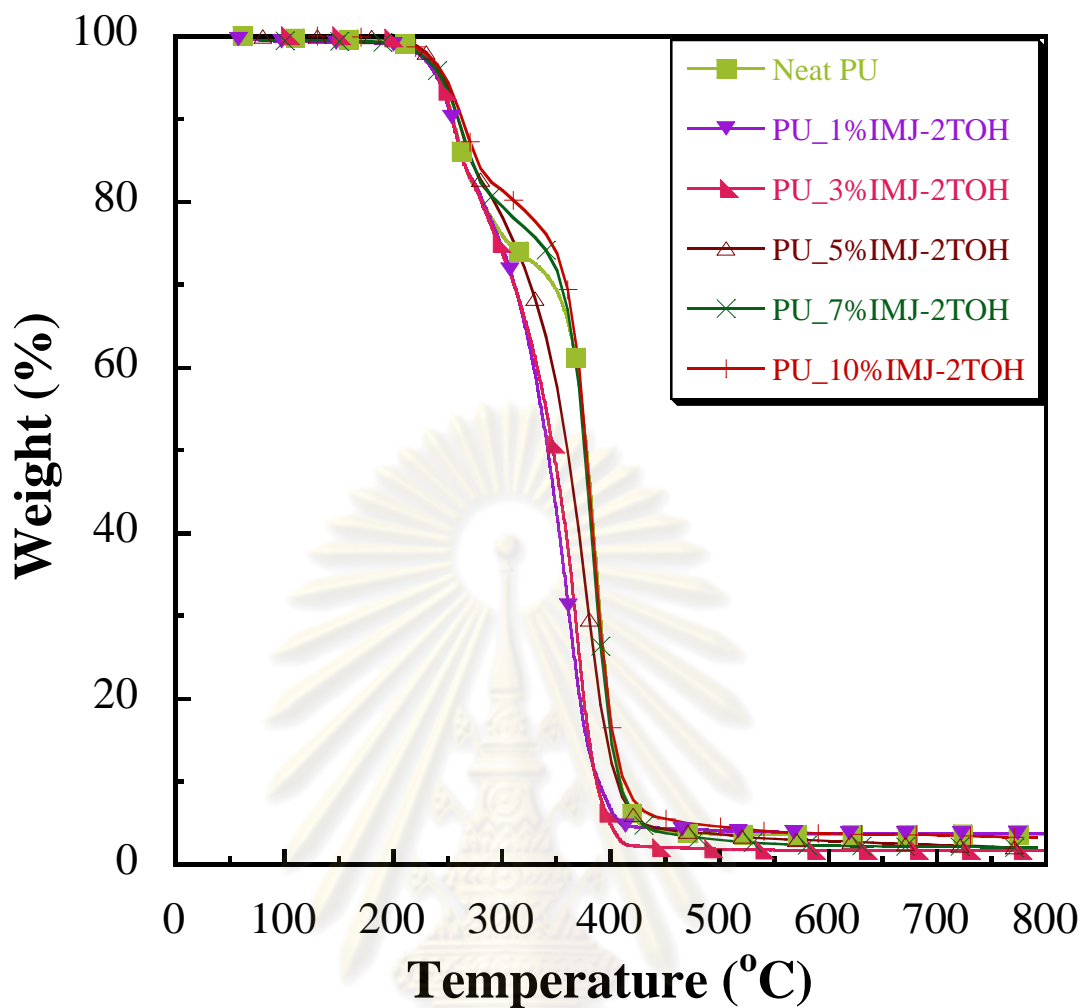


Figure 5.31: Thermal degradation of polyurethane/clay nanocomposite foams containing 0, 1, 3, 5, 7 and 10 wt% of MMJ-2TOH modified clay premixed with isocyanate.

ศูนย์วิทยทรัพยากร
จุฬาลงกรณ์มหาวิทยาลัย

CHAPTER VI

CONCLUSIONS

6.1 Conclusions

- i) Appropriate chemical structure of surfactant on the mechanical properties and degree of clay dispersion in polyurethane/clay nanocomposite foams is octadecylmethyl[polyoxyethylene (15)] ammonium chloride, (2TOH).
- ii) The suitable synthesis route of polyurethane/clay nanocomposite foams is premixed organoclay with isocyanate first.
- iii) MMT clay showed high efficiency in mechanical properties and degree of clay dispersion in polyurethane/clay nanocomposite foams. Although, fined MMJ clay had higher CEC but this type of nanoclay is easy to agglomerate; therefore, the properties of foams decreased.
- iv) Good dispersion of clay is observed at low organoclay loading but the data give no clear relationship between mechanical properties and degree of clay dispersion.

6.2 Recommendations for Further Studies

Reactive foaming of polyurethane nanocomposites is a complicated process where many factors could influence bubble nucleation, bubble growth and coalescence, and in turn the cell morphology. Detailed mechanisms on how nanoparticles influence cell morphology in reactive foaming need further investigation.

REFERENCES

- [1] Yao, K. J.; Song, M.; Hourston, D. J.; and Luo, D. Z. Polymer/layered clay nanocomposites: 2 polyurethane nanocomposites. *Polymer* 43(2002): 1017-1020.
- [2] Song, L., et al. Study on the properties of flame retardant polyurethane/organoclay nanocomposite. *Polymer Degradation and Stability* 87(2005): 111-116.
- [3] Lu, Y. L., et al. Microstructure and properties of highly filled rubber/clay nanocomposites prepared by melt blending. *Composites Science and Technology* 67(2007): 2903-2913.
- [4] Sharif, J.; Dahlan, K. Z. M.; and Yunus, W. Electron beam crosslinking of poly(ethylene-co-vinyl acetate)/clay nanocomposites. *Radiation Physics and Chemistry* 76(2007): 1698-1702.
- [5] Wirpsza, Z. *Polyurethanes Chemistry, Technology and Applications*. Ellis Horwood Limited, 1993.
- [6] Xiong, J. W.; Liu, Y. H.; Yang, X. H.; and Wang, X. L. Thermal and mechanical properties of polyurethane/montmorillonite nanocomposites based on a novel reactive modifier. *Polymer Degradation and Stability* 86(2004): 549-555.
- [7] Rehab, A.; and Salahuddin, N. Nanocomposite materials based on polyurethane intercalated into montmorillonite clay. *Materials Science and Engineering a-Structural Materials Properties Microstructure and Processing* 399(2005): 368-376.
- [8] Cao, X.; Lee, L. J.; Widya, T.; and Macosko, C. Polyurethane/clay nanocomposites foams: processing, structure and properties. *Polymer* 46(2005): 775-783.
- [9] Tantiviwattanawongsa, M. (2006). Effect of organoclay on mechanical and gas barrier properties of nylon 6/clay nanocomposite films. *Chemical Engineering*. Bangkok, Chulalongkorn University. **Master**: 92.
- [10] Eaves, D. *Handbook of Polymer Foams*. Rapra Technology Limited, 2004.
- [11] Deng, R.; Davies, P.; and Bajaj, A. K. Flexible polyurethane foam modelling and identification of viscoelastic parameters for automotive seating applications. *Journal of Sound and Vibration* 262(2003): 391-417.

- [12] Yuan, Y.; and Shutov, F. Foam-in-foam polyurethane composite (Reprinted). *Journal of Cellular Plastics* 38(2002): 497-506.
- [13] Abisaleh, T., et al. *The polyurethanes book*. John Wiley & Sons, Ltd, 2002.
- [14] Woods, G. *The ICI Polyurethanes Book*. 2 nd Ed. John Wiley & Sons, 1990.
- [15] Pentrakoon, D.; and Ellis, J. W. *An Introduction to Plastics Foams*. Chulalongkorn University Press, 2005.
- [16] Klempner, D.; and Frisch, K. C. *Handbook of Polymeric Foams and Foam Technology*. Hanser, 1991.
- [17] Yariv, S.; and Cross, H. *Organo - Clay Complexes and Interactions*. Marcel Dekker, Inc., 2002.
- [18] Wypych, F.; and Satyanarayana, K. G. *Clay Surfaces Fundamentals and Applications*. Interface science and technology, 2004.
- [19] Tjong, S. C. Structural and mechanical properties of polymer nanocomposites. *Materials Science & Engineering R-Reports* 53(2006): 73-197.
- [20] http://www.visionlearning.com/librery/modules_viewer.php.
- [21] <http://www.up.ac.za/themes/theme2/objectives2.html>.
- [22] Pinnavaia, T. J.; and Beall, G. W. Polymer - Clay Nanocomposites. John Wiley & Sons, Ltd, 2000.
- [23] www.scielo.cl/scielo.php.
- [24] Lee, L. J., et al. Polymer nanocomposite foams. *Composites Science and Technology* 65(2005): 2344-2363.
- [25] www.oxford_instruments.com/xrf_principal.gif.
- [26] www.msm.cam.ac.uk/printall.php.
- [27] www.uweb.engr.washington.edu/atr.html.
- [28] Sri-ngo, W. (2008). Effects of calcium carbonate filler on mechanical properties of flexible polyurethane foam. Chemical Engineering. Bangkok, Chulalongkorn. **Master:** 83.
- [29] Pattanayak, A.; and Jana, S. C. Synthesis of thermoplastic polyurethane nanocomposites of reactive nanoclay by bulk polymerization methods. Polymer 46(2005): 3275-3288.
- [30] Chavarria, F.; and Paul, D. R. Morphology and properties of thermoplastic polyurethane nanocomposites: Effect of organoclay structure. Polymer 47(2006): 7760-7773.

- [31] Tortora, M., et al. Structural characterization and transport properties of organically modified montmorillonite/polyurethane nanocomposites. Polymer 43(2002): 6147-6157.
- [32] Pattanayak, A.; and Jana, S. C. Thermoplastic polyurethane nanocomposites of reactive silicate clays: effects of soft segments on properties. Polymer 46(2005): 5183-5193.
- [33] Wang, X. D.;Luo, X.; and Wang, X. F. Study on blends of thermoplastic polyurethane and aliphatic polyester: morphology, rheology, and properties as moisture vapor permeable films. Polymer Testing 24(2005): 18-24.
- [34] Berta, M.;Lindsay, C.;Pans, G.; and Camino, G. Effect of chemical structure on combustion and thermal behaviour of polyurethane elastomer layered silicate nanocomposites. Polymer Degradation and Stability 91(2006): 1179-1191.
- [35] Tien, Y. I.; and Wei, K. H. Hydrogen bonding and mechanical properties in segmented montmorillonite/polyurethane nanocomposites of different hard segment ratios. Polymer 42(2001): 3213-3221.
- [36] Song, M.;Xia, H. S.;Yao, K. J.; and Hourston, D. J. A study on phase morphology and surface properties of polyurethane/organoclay nanocomposite. European Polymer Journal 41(2005): 259-266.
- [37] Javni, I.;Zhang, W.;Karajkov, V.;Petrovic, Z. S.; and Divjakovic, V. Effect of nano- and micro-silica fillers on polyurethane foam properties. Journal of Cellular Plastics 38(2002): 229-239.
- [38] Saha, M. C.;Kabir, M. E.; and Jeelani, S. Enhancement in thermal and mechanical properties of polyurethane foam infused with nanoparticles. Materials Science and Engineering a-Structural Materials Properties Microstructure and Processing 479(2008): 213-222.
- [39] Limpanart, S., et al. Effect of the surfactant coverage on the preparation of polystyrene-clay nanocomposites prepared by melt intercalation. Materials Letters 59(2005): 2292-2295.



APPENDICES

ศูนย์วิทยทรัพยากร
จุฬาลงกรณ์มหาวิทยาลัย

Appendix A

Calculation of surfactant loading

The replacement of surfactant with natural cation in nanoclay was used for organoclay treatment. Surfactant loading was calculated as follows:

$$g_{surf} = \frac{CEC \times conc \times Mw \times kg_{clay}}{\%assay}$$

Where

- g_{surf} = Weight of surfactant (g_{surf})
- CEC = Cation exchange capacity of untreated clay (meq/ g_{clay})
- conc. = Concentration of surfactant ($mmol_{surf}$)
- Mw = Molecular weight of surfactant (g_{surf}/mol_{surf})
- kg_{clay} = Weight of untreated clay (kg_{clay})
- %assay = Effectiveness of surfactant

For example: the preparation of organoclay based on Dimethyl bis (hydrogenated-tallow) ammonium chloride, (2T) which had 585.5 of MW, at stoi ratio of clay and surfactant 1.0 by using 400 g of MMT-clay (CEC of clay = 0.6 meq/g of clay), showing as follow:

$$\begin{aligned} \text{Surfactant loading} &= \frac{0.6 \times 1.0 \times 585.5 \times 0.4}{0.75} \\ &= 187.36 \text{ g} \end{aligned}$$

Appendix B

Calculation of percentage of inorganic content and concentration value in organoclay

The percentage of inorganic content in organoclay was calculated by equation:

$$\% \text{ inorganic content} = \frac{\text{final weight}}{\text{initial weight}} \times 100 \%$$

In this study, we fixed initial weight at 2 g.

The concentration (conc) value of organoclay was determined by equation

$$\text{conc} = \frac{g_{\text{surf}} \times \% \text{ assay}}{\text{CEC} \times \text{MW} \times \text{kg}_{\text{clay}}}$$

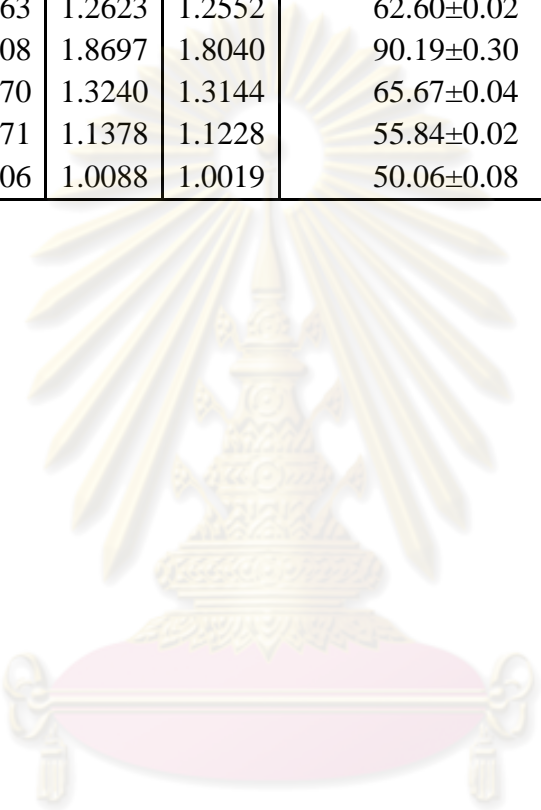
For example: the calculation of MT2T organoclay conc value, which 24.41 g_{surf} *, 75 % assay and 585.5 of MW by using 67.45 g of MMT-clay (CEC of clay = 0.6 meq/ g of clay), showing as follow:

$$\text{conc} = \frac{24.41 \times 0.75}{0.6 \times 585.5 \times 0.06745} = 0.77 \text{ mmol}_{\text{sur}}/\text{g}_{\text{clay}}$$

*Note $g_{\text{surf}} = \text{inorganic of MMT} - \text{inorganic of MT2T} = 91.86 - 67.45 = 24.41$

Table B.1: Inorganic content and percentage of inorganic content of clay and organoclay

Sample	Final weight (g)			Percentage of inorganic content (wt%)	Concentration value (mmol _{sur} /g _{clay})
	1	2	3		
MMT	1.8963	1.9350	1.9202	91.86±0.23	-
MT1T	1.5144	1.5157	1.5145	75.59±0.08	0.52
MT2T	1.3214	1.4515	1.2739	67.45±4.60	0.77
MT2TOH	1.2563	1.2623	1.2552	62.60±0.02	0.74
MMJ	1.8708	1.8697	1.8040	90.19±0.30	-
MJ1T	1.3170	1.3240	1.3144	65.67±0.04	0.60
MJ2T	1.1171	1.1378	1.1228	55.84±0.02	0.88
MJ2TOH	1.0106	1.0088	1.0019	50.06±0.08	0.85



คุนยวทยทรพยากร
จุพาลงกรณมหาวิทยาฬย

Appendix C

Determination of d-spacing of layered silicate of clay

The interlayer spacing of clay and organoclay (or degree of clay dispersion) is calculated by the Bragg's equation. Bragg's law is derived by physicists W.H. Bragg and his son. It was determined the spacing between the planes in the atomic lattice by the following equation:

$$n\lambda = 2d \sin \theta$$

- Where:
- n = Peaks correspond to the {001} basal reflection (n=1)
 - λ = The wavelength of the X-ray radiation used in the diffraction experiment (angstroms), which equals to 1.542 Å when CuK α was used.
 - d = The spacing between the planes in the atomic lattice (Å)
 - θ = The angle between the incident ray and the scattering planes (degrees)

The X-ray diffractometer determine double diffraction angle (2θ). For example, 2θ peak of MTT was 7.21° in which d-spacing of layered clay can be determined as follow:

$$(1)(1.541) = 2d \sin (7.21/2)$$

$$d = 1.22 \text{ nm}$$

Table C.1: Diffraction peak and interlayer spacing of pristine clay and organoclay

Sample	2θ (°)	Interlayer spacing (nm.)
MMT	1.61 (001)	5.49 (001)
	7.21 (001)	1.22 (001)
MT1T	2.17 (001)	4.06 (001)
	3.89 (001)	2.27 (001)
MT2T	2.66 (001)	3.31 (001)
	4.29 (001)	2.06 (001)
MT2TOH	2.50 (001)	3.52 (001)
	5.07 (001)	1.74 (001)
MMJ	7.28 (001)	1.21 (001)
MJ1T	2.41 (001)	3.66 (001)
	4.24 (001)	2.08 (001)
	4.61 (001)	1.92 (001)
MJ2T	2.83 (001)	3.12 (001)
	4.93 (001)	1.79 (001)
	6.85 (001)	1.29 (001)
MJ2TOH	2.58 (001)	3.42 (001)
	5.19 (001)	1.70 (001)

ศูนย์วิทยทรัพยากร
จุฬาลงกรณ์มหาวิทยาลัย

Table C.2: Diffraction peak and interlayer spacing of neat polyurethane foam and polyurethane/clay nanocomposite foams, which contained 3 wt% of different organoclay and different routes of synthesis

Sample	2θ (°)	Interlayer spacing (nm.)
Neat PU	2.59 (001)	3.41 (001)
PU_3%PMT	2.45 (001)	3.60 (001)
	5.56 (001)	1.59 (001)
PU_3%PMT-1T	5.05 (001)	1.75 (001)
	5.67 (001)	1.56 (001)
PU_3%PMT-2T	1.42 (001)	6.23 (001)
	1.99 (001)	4.44 (001)
	4.48 (001)	1.97 (001)
PU_3%PMT-2TOH	2.06 (001)	4.27 (001)
	5.63 (001)	1.57 (001)
	5.92 (001)	1.49 (001)
PU_3%IMT	5.62 (001)	1.57 (001)
	5.97 (001)	1.48 (001)
PU_3%IMT-1T	2.39 (001)	3.69 (001)
PU_3%IMT-2T	2.15 (001)	4.11 (001)
	4.54 (001)	1.94 (001)
PU_3%IMT-2TOH	2.41 (001)	3.66 (001)

Table C.3: Diffraction peak and interlayer spacing of neat polyurethane foam and polyurethane/clay nanocomposite foams, which contained different types of clay and different of organoclay loading

Sample	2θ (°)	Interlayer spacing (nm.)
Neat PU	2.59 (001)	3.41 (001)
PU_1%IMT-2TOH	1.87 (001)	4.72 (001)
PU_3%IMT-2TOH	2.41 (001)	3.66 (001)
PU_5%IMT-2TOH	1.91 (001)	4.61 (001)
PU_7%IMT-2TOH	2.00 (001)	4.42 (001)
	5.77 (001)	1.53 (001)
PU_10%IMT-2TOH	2.07 (001)	4.26 (001)
	6.01 (001)	1.47 (001)
PU_1%IMJ-2TOH	2.26 (001)	3.91 (001)
PU_3%IMJ-2TOH	2.20 (001)	4.00 (001)
	4.50 (001)	1.96 (001)
PU_5%IMJ-2TOH	2.25 (001)	3.93 (001)
	4.60 (001)	1.92 (001)
PU_7%IMJ-2TOH	2.25 (001)	3.92 (001)
	4.53 (001)	1.95 (001)
PU_10%IMJ-2TOH	2.24 (001)	3.95 (001)
	4.54 (001)	1.94 (001)

Appendix D

Data of mechanical properties of flexible polyurethane/clay nanocomposite foams

Table D.1: Hardness of the polyurethane/clay nanocomposite foams

Sample	Hardness (N/cm ²)	SD
Neat PU	0.0334	0.0015
PU_3%PMT	0.0456	0.0009
PU_3%PMT-1T	0.0536	0.0023
PU_3%PMT-2T	0.0412	0.0011
PU_3%PMT-2TOH	0.0484	0.0018
PU_3%IMT	0.0408	0.0022
PU_3%IMT-1T	0.0414	0.0015
PU_3%IMT-2T	0.0466	0.0036
PU_3%IMT-2TOH	0.0328	0.0020
PU_1%IMT-2TOH	0.0361	0.0009
PU_3%IMT-2TOH	0.0296	0.0019
PU_5%IMT-2TOH	0.0339	0.0009
PU_7%IMT-2TOH	0.0258	0.0034
PU_10%IMT-2TOH	0.0285	0.0043
PU_1%IMJ-2TOH	0.0418	0.0032
PU_3%IMJ-2TOH	0.0372	0.0034
PU_5%IMJ-2TOH	0.0291	0.0025
PU_7%IMJ-2TOH	0.0285	0.0033
PU_10%IMJ-2TOH	0.0190	0.0014

Table D.2: Support factor of the polyurethane/clay nanocomposite foams

Sample	Support factor	SD
Neat PU	4.76	0.33
PU_3%PMT	5.56	0.30
PU_3%PMT-1T	5.33	0.34
PU_3%PMT-2T	5.56	0.39
PU_3%PMT-2TOH	5.41	0.36
PU_3%IMT	4.62	0.43
PU_3%IMT-1T	4.83	0.4
PU_3%IMT-2T	4.56	0.46
PU_3%IMT-2TOH	3.76	0.39
PU_1%IMT-2TOH	4.95	0.31
PU_3%IMT-2TOH	4.19	0.36
PU_5%IMT-2TOH	4.74	0.34
PU_7%IMT-2TOH	4.41	0.33
PU_10%IMT-2TOH	4.84	0.32
PU_1%IMJ-2TOH	4.11	0.86
PU_3%IMJ-2TOH	9.72	2.18
PU_5%IMJ-2TOH	6.02	0.88
PU_7%IMJ-2TOH	5.67	0.80
PU_10%IMJ-2TOH	4.76	0.89

ศูนย์วิทยทรัพยากร
จุฬาลงกรณ์มหาวิทยาลัย

Table D.3: Guide factor of the polyurethane/clay nanocomposite foams

Sample	Guide factor	SD
Neat PU	0.26	0.030
PU_3%PMT	0.30	0.038
PU_3%PMT-1T	0.35	0.033
PU_3%PMT-2T	0.30	0.034
PU_3%PMT-2TOH	0.35	0.030
PU_3%IMT	0.27	0.029
PU_3%IMT-1T	0.26	0.021
PU_3%IMT-2T	0.28	0.025
PU_3%IMT-2TOH	0.33	0.024
PU_1%IMT-2TOH	0.32	0.037
PU_3%IMT-2TOH	0.32	0.036
PU_5%IMT-2TOH	0.28	0.032
PU_7%IMT-2TOH	0.24	0.038
PU_10%IMT-2TOH	0.25	0.039
PU_1%IMJ-2TOH	0.31	0.052
PU_3%IMJ-2TOH	0.19	0.059
PU_5%IMJ-2TOH	0.21	0.056
PU_7%IMJ-2TOH	0.21	0.051
PU_10%IMJ-2TOH	0.18	0.053

ศูนย์วิทยทรัพยากร
จุฬาลงกรณ์มหาวิทยาลัย

Table D.4: Compression set value of the polyurethane/clay nanocomposite foams

Sample	Compression set (%)	SD
Neat PU	14.39	2.52
PU_3%PMT	20.31	6.23
PU_3%PMT-1T	27.95	1.77
PU_3%PMT-2T	28.97	5.83
PU_3%PMT-2TOH	20.81	3.00
PU_3%IMT	12.72	0.76
PU_3%IMT-1T	15.54	3.25
PU_3%IMT-2T	13.01	0.18
PU_3%IMT-2TOH	15.36	1.86
PU_1%IMT-2TOH	2.13	0.50
PU_3%IMT-2TOH	1.60	1.68
PU_5%IMT-2TOH	3.92	1.65
PU_7%IMT-2TOH	2.44	1.14
PU_10%IMT-2TOH	0.57	0.85
PU_1%IMJ-2TOH	2.20	1.53
PU_3%IMJ-2TOH	1.53	1.14
PU_5%IMJ-2TOH	0.57	0.41
PU_7%IMJ-2TOH	1.11	0.30
PU_10%IMJ-2TOH	0.64	0.54

ศูนย์วิทยทรัพยากร
จุฬาลงกรณ์มหาวิทยาลัย

Table D.5: Resilience value of the polyurethane/clay nanocomposite foams

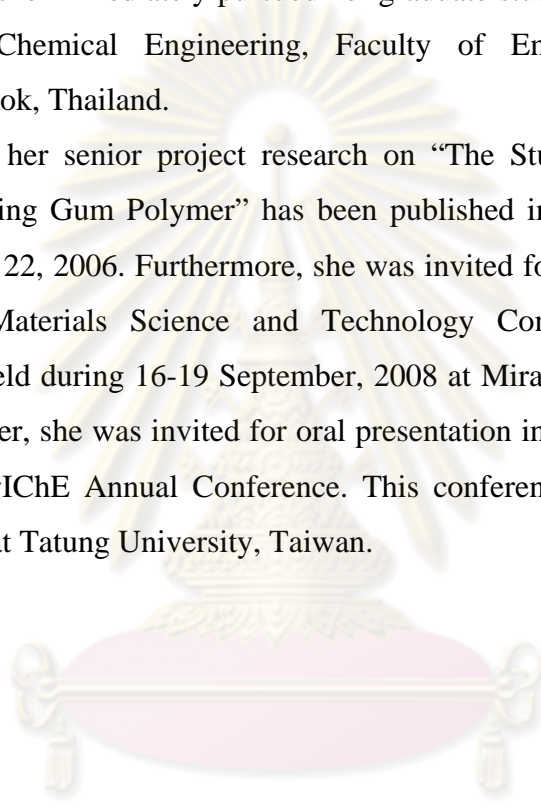
Sample	Resilience (%)	SD
Neat PU	63.56	0.10
PU_3%PMT	62.88	0.16
PU_3%PMT-1T	61.08	0.78
PU_3%PMT-2T	61.64	0.24
PU_3%PMT-2TOH	62.52	0.22
PU_3%IMT	62.36	0.92
PU_3%IMT-1T	63.52	0.15
PU_3%IMT-2T	61.76	0.34
PU_3%IMT-2TOH	63.52	0.12
PU_1%IMT-2TOH	64.12	0.14
PU_3%IMT-2TOH	62.64	0.27
PU_5%IMT-2TOH	56.96	0.70
PU_7%IMT-2TOH	57.40	1.39
PU_10%IMT-2TOH	60.00	0.18
PU_1%IMJ-2TOH	66.48	0.22
PU_3%IMJ-2TOH	62.84	0.84
PU_5%IMJ-2TOH	66.16	0.39
PU_7%IMJ-2TOH	65.08	0.32
PU_10%IMJ-2TOH	65.76	0.34

ศูนย์วิทยทรัพยากร
จุฬาลงกรณ์มหาวิทยาลัย

VITA

Miss. Sevita Inthapichai was born in Bangkok, Thailand on January 24, 1984. She completed senior high school from Triamudomsuksa Pattanakarn School Bangkok, Thailand in 2002. She received Bachelor degree from the Department of Chemical Science, Faculty of Science, Srinakharinwirot University, Bangkok, Thailand in 2006. After graduation, she immediately pursued her graduate study for a Master's Degree at Department of Chemical Engineering, Faculty of Engineering, Chulalongkorn University, Bangkok, Thailand.

In addition, her senior project research on "The Study of Nicotine Releasing Factors for Chewing Gum Polymer" has been published in Srinakharinwirot Science Journal on March 22, 2006. Furthermore, she was invited for oral presentation in "The Fifth Thailand Materials Science and Technology Conference: MSAT-5". This conference was held during 16-19 September, 2008 at Miracle Grand Hotel, Bangkok, Thailand. Moreover, she was invited for oral presentation in 2008 Taiwan/Korea/Japan ChE and 55th TwICHe Annual Conference. This conference was held during 20-22 November, 2008 at Tatung University, Taiwan.



ศูนย์วิจัยทรัพยากร
จุฬาลงกรณ์มหาวิทยาลัย